

https://dspace.org/

Immune escape in HIV-1 subtype C accessory proteins VIF, VPR and VPU

Pereira, Roberto Carlos

2016
http://hdl.handle.net/10539/21419

Downloaded from a DSpace repository. https://dspace.org/

Immune escape in HIV-1 subtype C accessory proteins Vif, Vpr and Vpu

Roberto Carlos Pereira

A dissertation submitted to Faculty of Health Sciences,

University of the Witwatersrand,

in fulfillment of the requirements for the degree of

Master of Science in Medicine

Johannesburg, June 2016

Declaration

I, Roberto Carlos Pereira declare that this dissertation is my own work. It is being submitted for the degree of Master of Science in Medicine in the University of the Witwatersrand, Johannesburg. It has not been submitted before for any degree or examination at this or any other University.

_____

Roberto Carlos Pereira

_____day of_____2016

Abstract

Human Leukocyte Antigen (HLA) class I (HLA-I)-restricted CD8+ cytotoxic T lymphocyte (CTL) responses are major drivers of human immunodeficiency virus type 1 (HIV-1) evolution, resulting in the selection of CTL escape mutants. This is particularly well described for HIV-1 proteins such as Gag, Pol and Nef. For the accessory proteins Vif, Vpr and Vpu though, it is still not clear to what extent HLA-I-mediated responses influence their evolution. Moreover, preliminary data from our laboratory showed that Vpu was the most targeted of the accessory proteins with regards to CD8+ CTL and natural killer (NK) cell responses in a long term non progressor/elite controller cohort. Thus, the overall aims of the study were to describe immune escape in Vif, Vpr and Vpu epitopes from HIV-1 infected patients in South Africa, and to clone, express and purify recombinant Vpu for the ultimate detection of anti-Vpu antibodies in South African patient sera. Longitudinal plasma samples were available for 25 patients from two cohorts (18 from Lung and seven from M002). Viral RNA was extracted and the *vif, vpr* and *vpu* regions were RT-PCR (Reverse transcription polymerase chain reaction) amplified and sequenced. HLA-A, B and C data for Lung cohort individuals were available, thus the HLA-A, B and C alleles were typed and assigned for the M002 cohort individuals. The Vif, Vpr and Vpu amino acid sequences were subsequently extensively analysed for HLA-driven CTL escape mutations. Lastly, three *vpu* sequences, Cons. C, 05ZAFV05 and 05ZAFV15 were selected for codon-optimization (humanized), each cloned into the pcDNA3.1/V5-His mammalian expression vector, and used to optimize expression of recombinant Vpu proteins in HEK 293T cells. The HEK 293T cells were harvested and the Vpu was purified using standard nickel affinity chromatography procedures. Protein expression and purification was monitored by SDS-PAGE, Western blot and dot blot analyses. Overall, longitudinal sequences were obtained from Vif, Vpr and Vpu from eight of the 18 patients in the Lung cohort and all seven patients in the M002 cohort. Of these, HLA-driven immune escape mutations were detected in four patients from the Lung cohort and six from the M002 cohort. Interestingly, for the M002 cohort, some reversions to the baseline sequences were noted over time. None of the identified escape mutations are amongst the best described and most optimal HIV-1 CD8+ CTL epitopes of HIV-1 accessory proteins in the HIV-1 databases. Eight and eleven HLA alleles contributed to immune escape in the Lung and M002 cohort Vif, Vpr and/or Vpu sequences, respectively. Overall, HLA-driven immune pressure in the Vif, Vpr and/or Vpu motifs described here may have contributed to the changes in viral loads seen in these patients over time, and likely impacted

on disease progression, albeit in combination with escape mutations in the more highly targeted HIV-1 proteins, such as Gag, Pol and Nef. Future work looking at longitudinal sequence analysis of the entire HIV-1 proteome in these patients will likely reveal the contributing factors leading to immune escape and ultimately impact disease progression to AIDS. Expression of all three recombinant Vpu proteins in HEK 293T cells was successfully optimized however, as evidenced by SDS-PAGE, Western blot and dot blot analyses, the expression and purification protocol used in this study did not provide sufficient protein yields, nor an optimally purified protein for use in the downstream assays required. Future work will focus on optimization of Vpu expression and purification protocols to aid in the detailed elucidation of the role of Vpu and anti-Vpu immune responses in control of HIV-1 infection.

Acknowledgements

I would like to express my deepest gratitude and sincerest appreciation to everyone that made it possible for me to carry out this project:

To my supervisor, Prof. Maria Papathanasopoulos, a special thank you for your expertise, guidance, understanding and enthusiasm. I'd also like to thank you for the numerous opportunities that you have afforded me, both financial and academic, over the last couple of years which has provided me with an invaluable opportunity to grow as a young researcher. Your friendship and continued encouragement of my scientific endeavors is greatly appreciated.

To my co-supervisor, Prof Caroline Tiemessen, thank you for your technical assistance, and invaluable insight on the more nuanced and challenging aspects of this project. Your friendship and continued encouragement of my scientific endeavors is greatly appreciated.

To my friends and colleagues in the HIV Pathogenesis Research Unit, both past and present, thank you for the continued support throughout the years, it is a pleasure to be around and work with such a special and talented group of people. Special thanks especially go to Nichole, Mark, Irene and Michelle who have mentored and guided me since the beginning, and Dean and Rafeeqah who began this Masters journey with me and kept me smiling until the end.

To my brothers, sister-in-laws, nieces and nephews your love and support has helped me realize this achievement.

To my dear Rachel, your love, understanding and unshaken faith in my abilities helped me push through the most difficult of obstacles.

To my mother and late father, I will forever be grateful for your love and encouragement to pursue academic studies and to always seek to better myself.

To the University of the Witwatersrand for providing me with a Postgraduate Merit Award, and the Poliomyelitis Research Foundation and National Research Foundation for bursary funding.

To the Medical Research Council, Strategic Health Innovations Partnership (SHIP): Elite controllers study (PI: CT Tiemessen) and the HIV Pathogenesis Research Unit for funding of the study.

Contents

Declaration i

Abstract ii

Acknowledgements iv

List of Figures 2

List of Tables 6

List of abbreviations 7

1 Chapter 1 10

1.1 Introduction 10

1.1.1 Disease burden 10

1.1.2 Origins, classification and diversity 10

1.1.3 Viral genome and proteome 12

1.1.4 HIV-1 Tropism 26

1.1.5 Viral Life Cycle 26

1.1.6 The HIV-1 immune response 28

1.2 Rationale for study conducted, aims and objectives 36

2 Chapter 2 38

2.1 Methods 38

2.1.1 Patient cohorts used in this study 38

2.1.2 Extraction, RT-PCR Amplification and Sequencing of HIV-1 *vif, vpr* and *vpu* 39

2.1.3 PCR Amplification and Sequencing of HLA class I Loci 42

2.1.4 Expression and purification of recombinant Vpu protein 44

3 Chapter 3 53

3.1 Results 53

3.1.1 Clinical and demographic data of patients used 53

3.1.2 Viral RNA extraction, RT-PCR amplification and sequencing 56

3.1.3 HLA class I motif analysis 63

3.1.4 Expression and purification of recombinant Vpu protein 67
4 Chapter 4 77
4.1 Discussion 77
4.1.1 RT-PCR and analysis of Vif, Vpr and Vpu functional domains 77
4.1.2 HLA class I background and targeted motifs 79
4.1.3 Expression of recombinant Vpu proteins 85
4.2 Conclusions 88
5 References 90
Appendix A: Bacterial and DNA Work 105
Appendix B: Recombinant Protein Work 106
SDS-PAGE 106
Gel staining and Western blotting 107
Protein purification 107
Appendix C: Manufacturer's protocols 108
Plasmid Extraction/Midi Prep (Qiagen, USA) 108
GeneJet PCR Purification Kit (Thermo Fisher Scientific, USA) 109
Agencourt AMPure XP - PCR Purification 96 well plate (Beckman Coulter, USA) 109
Appendix D: Ethics Approval 110

List of Figures

Figure 3.1: RT-PCR amplification of *vif, vpr* and *vpu* regions (approximately 1,3 kb) of extracted HIV-1 RNA from the Lung cohort (A) and M002 cohort (B) depicted on a 1% agarose gel under UV transillumination. The molecular weight marker (MWM, O'GeneRuler DNA Ladder Mix #SM1173, Thermo Fisher Scientific, USA) was used for sizing (base pairs (bp)) and is depicted on the left. Numbers in brackets represent time points of sample, 0= baseline at 0 months, 1= 1st follow up at 6 months, 2= 2nd follow up at 12 months, 3rd follow up at 18 months and 4= 4th follow up at 24 months (for M002 only). **.....57**

Figure 3.2: Amino acid sequence alignment of Lung Cohort Vif (A), Vpr (B) and Vpu (C) proteins. The *vif*, *vpr* and *vpu* nucleotide sequences were analysed using Sequencher 5.1 and then aligned using Clustal X, and translated into amino acid sequences using GeneDoc Multiple Sequence Aligner. On the left are the patient sequence ID codes and number of the longitudinal sample that the sequence belongs to ie. 0=baseline, 1=follow-up 1 at 6 months, 2=follow up 2 at 12 months, 3=follow up at 18 months and 4=follow up at 24 months. Sequences were compared to a Consensus HIV-1 Subtype C sequence. Dots represent identical residues, variant residues are shown, and dashes indicate insertions/deletions. Highlighted regions represent important functional regions (see key below). The patient numbers depicted correspond to the last three numbers shown in the patient ID column in Table 3.1. **.....58**

Figure 3.3: Amino acid sequence alignment of M002 Cohort Vif (A), Vpr (B) and Vpu (C) proteins. The *vif, vpr* and *vpu* nucleotide sequences were analysed using Sequencher 5.1 and then aligned using Clustal X, and translated into amino acid sequences using GeneDoc Multiple Sequence Aligner. On the left are the patient sequence IDs and number of the longitudinal sample that the sequence belongs to ie. 0=baseline, 1=follow-up 1 at 6 months, 2=follow up 2 at 12 months, 3=follow up at 18 months and 4=follow up at 24 months. Sequences were compared to a Consensus HIV-1 Subtype C sequence. Dots represent identical residues, variant residues are shown, and dashes indicate insertions/deletions. Highlighted regions represent important functional regions (see key below). **.....60**

Figure 3.4: Amino acid alignments of Lung cohort-derived Vif (A), Vpr (B) and Vpu (C) sequences depicting HLA class I motif immune escape. HLA class I targeted motifs which are no longer recognised following a mutation within a key anchor residue are

outlined by red boxes. Key anchor residues are highlighted in magenta with subsequent longitudinal sequence mutations being highlighted in grey. Boxes branching off from the motifs contain the patient HLA class I genes with a representation of their associated target motif which includes key anchors. **.....64**

Figure 3.5: Amino acid alignments of M002 cohort-derived Vif (A), Vpr (B) and Vpu (C) sequences depicting HLA class I motif immune escape. HLA class I targeted motifs which are no longer recognised following a mutation within a key anchor residue are outlined by red boxes. Key anchor residues are highlighted in magenta with subsequent longitudinal sequence mutations being highlighted in grey. Boxes branching off from the motifs contain the patient HLA class I genes with a representation of their associated target motif which includes key anchors. Blue boxes indicate motifs which return following reversion of anchor amino acid mutations. **.....65**

Figure 3.6: Amino acid alignment of Consensus C, 052AFV5, and 052AFV15 Vpu proteins, Three Vpu proteins were chosen for expression and purification in this study. Cons.C is derived from a consenus of HIV-1 subtype C strains with 052AFV5 having a fairly similar sequence compared to Cons. C. 052AFV15 is differentiated from the other two proteins by four amino acid deletions located towards the N-terminus of the protein**. 67**

Figure 3.7: Restriction enzyme digest analysis of plasmid preparations of pcDNA3.1/V5-His-Cons. C, pcDNA3.1/V5-His-FV5 and pcDNA3.1/V5-His-FV25 *vpu* constructs. Undigested single digests to linearise the constructs (using *BglII)* and double digests to excise the 276 bp *vpu* gene from the 5698 bp vector (using *HindIII* and *XhoI*) were run on a 1% agarose gel and visualised using UV transillumination. The arrow on the right indicates the excised *vpu* genes. Undigested *vpu* constructs depict typical banding pattern of plasmid DNA. The molecular weight marker (MWM, O'GeneRuler DNA Ladder Mix #SM1173, Thermo Fisher Scientific, USA) used for sizing is indicated on the left and depicts sizes in base pairs (bp). **.....68**

Figure 3.8: Western blots of whole-cell lysate of transfected HEK 293T cells for detection of polyhistidine-tagged Vpu proteins following tranfection with 5 different transfection reagents. HEK 293T cells were transiently transfected with pcDNA3.1/V5-His-05ZAFV15 and pcDNA3.1/V5-His-Cons. C plasmid constructs (**A**), and pcDNA3.1/V5-His-05ZAFV5 or a 2dCD4 constructs (**B**) utilising the transfection reagents Fugene HD, Lipofectamine XTL/2000, Polyfect and JetPrime. Following transient transfection and 48 hours of protein expression, whole-cell lysate was used for

SDS-PAGE and Western blotting, with a polyhistidine-targeting antibody used for probing. The circle on the left indicates the first instance of Vpu protein expression. Vpu proteins were sized approximately in the estimated 10-12 kDa range (protein molecular weight marker not shown). Untransfected whole-cell lysate was used as a negative control. **Untransfected**= untransfected HEK 293T cell lysate, **Cons. C**= whole cell lysate of cells transfected with pcDNA3.1/V5-His-Cons. C and expressing Cons. C Vpu protein, **05ZAFV5/05ZAFV15**= whole cell lysate of cells transfected with pcDNA3.1/V5-His-FV5/FV15 and expressing 05ZAFV5/FV15 Vpu protein, **1dCD4**=one domain CD4 sizing control, **2dCD4**= whole cell lysate of cells transfected with the 2dCD4 construct. **.....69**

Figure 3.9: Western blot analysis of samples collected during protein purification procedure of the recombinant 05ZAFV5 Vpu protein. Different imidazole wash buffer concentrations and varying numbers of washes were used. The washing procedure in Figure **A** utilised only a 10 mM and 50 mM wash and was therefore less stringent, whilst Figure **B** depicts a more stringent washing procedure with added 20 mM wash buffer step. An anti-polyhistidine antibody was used for probing. **1dCD4**=one domain CD4 sizing control, soluble fraction=protein-containing fraction following centrifugation of whole-cell lysate, **post-harvest**=supernatant following Vpu-bound agarose bead harvest, **10, 20** and **50 mM** = wash buffer imidazole conentrations, **beads**=agarose beads following elution of Vpu protein, **500 mM elute**= eluted protein with 500 mM imidazole wash buffer, **concentrate**= concentrated eluted Vpu protein. **.71**

Figure 3.10: Western blot analysis for detection of recombinant Vpu protein expression in stably transfected HEK 293F cells. Stably transfected HEK 293F cell lines were established and expressed recombinant Vpu proteins (and 2dCD4 as a control) as shown by the arrow. Whole-cell lysate was used for SDS-PAGE and Western blotting, with a polyhistidine-targeting antibody used for probing of 6 × polyhistidine-tagged Vpu proteins. **1dCD4**=one domain CD4 sizing control, **05ZAFV15 Purified**= previously expressed and purified Vpu protein as a control, 2dCD4= whole cell lysate of cells stably transfected with 2dCD4 construct, **Cons. C**= whole cell lysate of cells transfected with pcDNA3.1/V5-His-Cons. C and expressing Cons. C Vpu protein, **05ZAFV5**= whole cell lysate of cells transfected with pcDNA3.1/V5-His-FV5 and expressing 05ZAFV5 Vpu protein, **05ZAFV15**= whole cell lysate of cells transfected with pcDNA3.1/V5-His-FV15 and expressing 05ZAFV15 Vpu protein. **.....72**

Figure 3.11: Western blot analysis for detection of purified recombinant Vpu protein from upscaled expression and purification of stably transfected HEK 293F cells. Cons. C Vpu was purified from upscaled stably transfected HEK 293F cells following previously describe procedures. Even after upscaling production, Cons. C appears to be in a lower concentration as compared to purified 05ZAFV15 Vpu protein even when concentrating down to comparable volumes. Contaminants can also be seen to be increased (indicated by arrow). Anti-polyhistidine antibody was used for probing. **1dCD4**=one domain CD4 sizing control, **05ZAFV15** Purified= previously expressed and purified Vpu protein as a control, **Stable Cons. C Elute**= eluted Cons. C Vpu protein purified from stably transfected HEK 293F cells, **Stable Conc. C Concentrate**= eluted and concentrated Cons. C Vpu protein purified from stably transfected HEK 293F cells. **.....73**

Figure 3.12: Dot blot analysis of recombinant Vpu proteins and appropriate controls. Four separate dot blots were conducted, each probed with either anti-Vpu subtype C rabbit sera, anti-HIV-1 NL4-3 Vpu rabbit sera, HIV-1 negative human sera or anti-polyhistidine antibody and then probed with their respective HRP-linked secondary antibody counterparts (anti-rabbit or anti-human). **DMEM**= Dulbecco's modified eagle medium, **1dCD4**=one domain CD4 sizing control, **2dCD4**= purified 2dCD4 protein. **Cons. C**= purified Vpu protein, **05ZAFV5**= purified Vpu protein. **.....75**

Figure 3.13: Western blots probed with anti-Vpu rabbit sera or anti-polyhistidine antibody. Western blot analyses conducted in conjunction with dot blot analyses. In **A**, the Western blot was probed with Anti-Vpu Rabbit Antiserum against subtype C Vpu. Cons. C Vpu was detected as shown in circle, 05ZAFV5 may have been detected as well as shown in circle but the banding is unclear. 1dCD4 and 2dCD4 were not detected as expected. In **B**, the Western blot was probed with an anti-polyhistidine antibody, all proteins were detected as expected. 1dCD4=one domain CD4 sizing control, 2dCD4=purified 2dCD4 protein, Cons. C= purified Cons. C Vpu protein, 05ZAFV5 = purified 05ZAFV5 Vpu protein. **.....76**

List of Tables

PAGE

Table 1.1: Best described and most optimal HIV-1 CD8+ CTL epitopes of HIV-1 accessory proteins (Llano et al., 2013).....32

Table 3.1: Clinical data of Lung cohort patient samples used in this study. Red highlighted cells in the viral load columns indicate patient samples that could not be RT-PCR amplified and blue letters indicate patient was initiated on antiretroviral therapy. 54

Table 3.2: Clinical data of M002 cohort patient samples used in this study. Red highlighted cells indicate patient samples that could not be RT-PCR amplified.....55

Table 3.3: Number of total amino acid sequence changes in longitudinal samples of Vif, Vpr and Vpu of the Lung and M002 cohorts, as compared to the earliest time point available sequence. 62

List of abbreviations

ADCC	Antibody-dependent cellular cytotoxic responses
ANT	Adenine nucleotide translocator
AIDS	Acquired Immune Deficiency Syndrome
APOBEC3G	Apolipoprotein B mRNA editing enzyme, catalytic polypeptide-like 3G
ATR	Ataxia telangiectasia and Rad3-related protein
BST-2	Bone marrow stromal antigen 2
CCR5	C-C chemokine receptor type 5
CD1d	Cluster of differentiation d receptors
CD4	Cluster of differentiation 4
Cdc	Cyclin-dependent kinase
CNV	Copy number variation
CRF	Circulating recombinant forms
CTLs	Cytotoxic T-lymphocytes
CXCR4	C-X-C chemokine receptor type 4
DCAF1	DDB1- and CUL4-associated factor homolog 1
DMEM	Dulbecco's Modified Eagle Medium
DDB1	DNA damage-binding protein 1
Env	Envelope
ER	Endoplasmic reticulum
ERAD	Endoplasmic reticulum-associated degradation
ESCRT	Endosomal sorting complexes required for transport
Gag	Group-specific antigen

GFP	Green Fluorescent Protein
GPI	Glycosyl-phosphatidylinositol
HIV	Human Immunodeficiency Virus
HLA	Human leukocyte antigen
HEK	Human Embryonic Kidney
HRP	Horse Radish Peroxidase
IFN-γ	Interferon gamma
IκBα	Nuclear factor of kappa light polypeptide gene enhancer in B-cells inhibitor alpha
KIR	Killer-cell immunoglobulin-like receptors
LTNPs	Long term non-progressors
LTR	Long terminal repeat
LB	Lysogeny broth
MHC	Major Histocompatibility Complex
MIP-1ß	Macrophage Inflammatory Proteins
Nef	Negative factor
NF-κB	Nuclear factor kappa-light-chain-enhancer of activated B cells
NK	Natural killer
NLS	Nuclear localisation signal
NMR	Nuclear magnetic resonance
NTB-A	NK-T and -B cell antigen
PEI	Polyethylenimine
PIC	Pre-integration complex
PLK1	Polo-like kinase 1
PTPC	Mitochondrial permeability transition pore complex

RhCMV	Rhesus Cytomegalovirus vectors
RT-PCR	Reverse transcription polymerase chain reaction
SCF	Skp1/Cullin-1/F-Box
SDS-PAGE	Sodium dodecyl sulphate polyacrylamide gel electrophoresis
SIV	Simian Immunodeficiency Virus
SMUG1	Single-Strand-Selective Monofunctional Uracil-DNA Glycosylase 1
SOCS-box	Suppressor of cytokine signalling-box
SSEs	Structure-specific endonucleases
TAP	Transporter associated with antigen processing
Tat	Trans-Activator of Transcription
TCRs	T-cell Receptors
TNF-α	Tumour necrosis factor alpha
UNG	Uracil DNA glycosylase protein
Vif	Viral infectivity factor
Vpr	Viral protein R
Vpu	Viral protein U

Chapter 1

1.1 Introduction

1.1.1 Disease burden

The late 20th Century through to the early 21st Century has seen the rise of the devastating Human Immunodeficiency Virus (HIV) pandemic. Both HIV types 1 and 2 (HIV-1, 2) lead to Acquired Immune Deficiency Syndrome (AIDS) with HIV-1 being responsible for the current pandemic and HIV-2 being mostly isolated to certain regions in west central Africa (Popovic et al., 1984). As of March 2015, nearly 78 million people had contracted the virus, 36.9 million people were living with HIV-1 and almost 39 million people had died from AIDS-related causes (UNAIDS, 2014). A large portion of the burden of the pandemic is carried by Sub-Saharan Africa with an average of 26 million people living with the virus. Since the early-2000's AIDS-related deaths have fallen by around 42% (down to 1,2 million in 2014) and new HIV-1 infections have fallen by 35% (down to 1,8 million in 2014) (UNAIDS, 2014). Although the fall in deaths and new infections is promising, it is still of grave concern that millions are still becoming infected and dying every year at an alarmingly high rate. Vast amounts of resources have also been invested with nearly US$ 21 billion allocated to low and middle income countries alone in 2014 and the number is set to rise to US$ 30 billion annually in the coming years (UNAIDS, 2014). Antiretroviral treatments have proven successful in lowering death rates of HIV-infected individuals, but the key goal moving forward should be the development of efficacious HIV-1 vaccines which offer the best hope to provide protection against acquisition of HIV-1 and change the course of the pandemic. In parallel, the continued study of the virus at the molecular level and its interaction with the host immune system will prove invaluable in illuminating potential new drug and vaccine targets.

1.1.2 Origins, classification and diversity

AIDS (caused by infection with HIV-1, a lentivirus of the family *Retroviridae*), was first described in 1981 with previously healthy homosexual men presenting with *Pneumocystis carinii*, a disease only manifesting in immune weakened patients (Gottlieb et al., 1981, Klatzmann and Gluckman, 1986). The origins of HIV-1 can be traced back much further though and it has been shown that the HIV-1 progenitor was likely a Simian Immunodeficiency Virus (SIV) which crossed over at various time points from wild primates

to human hunters throughout the 20th century. The progenitor of HIV-1 is said to be the strain SIVcpz, found in the chimpanzee subspecies *Pan troglodytes troglodytes*, and which likely crossed over into the human population on three different occasions leading to the three HIV-1 groups, M (responsible for the current HIV-1 pandemic), N and O (Keele et al., 2006). A fourth group has been noted, designated group "P" which is said to originate from the gorilla SIV strain SIVgor (Plantier et al., 2009). HIV-2 originated from a different primate lentivirus found to infect sooty mangabeys and eight distinct groups have been identified, termed groups A to H (Sharp and Hahn, 2011). To add further complexity, group M of HIV-1 can further be divided into nine subtypes and sub-subtypes known as A (sub-subtypes A1, A2, A3, A4), B, C, D, F (sub-subtypes F1, F2), G, H, J, and K which are all phylogenetically-linked strains (Vidal et al., 2000). Subtype C is the predominant subtype found throughout southern Africa and India, and accounts for nearly half of all HIV-1 prevalence worldwide (Van Harmelen et al., 1999, Taylor et al., 2008).

Circulating recombinant forms (CRFs) exist as well, which are HIV strains that are derived from the recombination of two or more different viral subtypes (Taylor et al., 2008). Recombination occurs when an individual is dually infected with different subtypes and then subsequently transfers a recombinant form to another individual. A Common CRF is CRF01_AE which is one of dominate strains affecting the South East Asia region (Ha et al., 2004). New CRF strains are continually appearing in the HIV-1 infected population with at least 72 or more described so far, with CRF65_cpx and CRF76_01B being just two examples of novel CRFs to be discovered between 2014 and 2015 (Feng et al., 2014, Ogawa et al., 2015, LosAlamosNationalLaboratory, 2016).

Driving the diversity of HIV-1 are various factors including the speed at which the viral genome can evolve within the human host due to the error-prone nature of HIV-1 reverse transcriptase, coupled with smaller contributions from RNA polymerase II. HIV-1 reverse transcriptase can easily incorporate and extend nucleotide mispairings due to the lack of 3' to 5' exonucleolytic proofreading capabilities, with errors occurring at a rate of 3.4×10^{-5} per base pair per replication cycle (O'Neil et al., 2002). It has been shown that HIV-1 can evolve at a rate of one million times greater than that of eukaryotic genomes such as that of mammals (Preston et al., 1988). HIV-1 reproduction is also relatively rapid and high-throughput with an average of 52 hours for one generation of virions to complete a life cycle and form the next generation of virions, with 10^{10} virions on average being formed per day

(Ho et al., 1995, Murray et al., 2011). Thus, millions of viral variants/quasispecies can be formed daily within any infected person contributing to the immense diversity seen in HIV-1.

It has been shown that in almost 80% of all infections (by heterosexual transmission) a single founder virus is responsible for establishing an infection in an individual, with a smaller fraction being due to two, or more founder viruses (Salazar-Gonzalez et al., 2009). These founder viruses are by-and-large C-C chemokine receptor type 5 (CCR5) and cluster of differentiation 4 (CD4) dependent as well (Keele et al., 2008). These findings may account for the relatively low transmission risks seen when looking at subjects engaging in heterosexual vaginal intercourse, with risks of infection being shown to be 1 in 1250 (Boily et al., 2009). This is likely due to the protective nature of mucosal barriers coupled with the specificity for co-receptors that a founder virus requires for infection (Baggaley et al., 2010, Keele and Estes, 2011) . Interestingly, as infection progresses the homogeneity of the viral population shifts to many heterogeneous populations/quasispecies, which are isolated in various compartments within the body such as in the pleural tissues, brain, peripheral blood and lymphatic tissues (Wolfs et al., 1992, Poss et al., 1995). Not only does the error-prone reverse transcriptase contribute to this genetic variation, but other factors may contribute such as selective pressures from the immune system or co-infection with other pathogens such as *Mycobacterium tuberculosis* which may encourage further selective pressures from the host immune system by over stimulating the host's immune responses (Collins et al., 2002, Salazar-Gonzalez et al., 2009). Injection drug users have been shown to harbor a highly diverse viral population, with subjects shown to be infected with more than several viruses at any one time due to the lack of a mucosal barrier involvement in the route of transmission (Bar et al., 2010).

1.1.3 Viral genome and proteome

The HIV-1 genome consists of two single-stranded, plus sense-strands of RNA of approximately 9.5 kb length, and which contain 9 open reading frames that can produce at least 16 different proteins (Watts et al., 2009). Housing the viral genome, tight genome-bound nucleocapsid proteins and important replicative enzymes is the viral capsid core which consists of the protein p24 arranged in a conical shape (Briggs et al., 2004). Further surrounding the capsid core is the matrix protein (p17) and host-derived membrane. Embedded within the membrane are the viral envelope spikes responsible for the attachment of virus to host-target cells, consisting of the surface glycoprotein gp120 and the

transmembrane glycoprotein gp41 arranged in a "tripod"-like trimeric formation of heterodimers (Zhu et al., 2006, Zhu et al., 2008).

The HIV-1 genes encode for three broad types of proteins, namely those that are structural, those that are important for enzymatic functioning and regulation, and lastly those that are considered to have accessory functioning (*vif, vpr, vpu* and *nef*) (Watts et al., 2009). *Gag* (Group-specific antigen) encodes for matrix protein (p17), capsid protein (p24), nucleocapsid protein (p7) and p6 protein (Briggs et al., 2004). *Pol* encodes for the important HIV-1 enzymes protease (required for cleavage of Gag and Gag-Pol polyprotein), reverse transcriptase (transcribes the viral RNA genome into cDNA), integrase (inserts viral cDNA into the host cell genome) and RNase H (Watts et al., 2009). *Env* (Envelope) encodes for a signal peptide, and the precursor protein gp160 which is subsequently cleaved by host cellular proteases into the viral surface glycoproteins gp120 and gp41 (Zhu et al., 2006, Kwong et al., 1998). *Tat* (Trans-Activator of Transcription) enhances viral transcription via its interactions with host cellular transcription factors, improving binding of reverse transcriptase to its RNA template and improving regulation of mRNA production (Debaisieux et al., 2012, Lin et al., 2015). *Rev* is a transcriptional trans-activator and plays an important role in viral replication, interacting with the Rev response element which is a highly structured nucleotide sequence within the *env* gene and allows for mRNA transport to the cytoplasm (Malim et al., 1989, Rausch and Le Grice, 2015).

Lastly, there are the accessory genes. Negative factor (*nef)* encodes for a highly multi-functional protein which is important for establishment of a successful infection and said to be one of the key factors to disease progression in HIV-1 patients. Long term non-progressors (LTNPs), patients who are able to maintain CD4 counts greater than 500 cells/mm^3 with a detectable viral load over a prolonged period of time have in some cases been shown to be infected with HIV-1 that has defective and non-functional forms of *nef* (Kirchhoff et al., 1995). Further, attempts at developing a live attenuated vaccine have included studies done in rhesus macaques in which live SIV strains with deleted *nef* genes were utilised, with the monkeys showing no sign of pathogenicity further highlighting the importance of *nef* in the pathogenicity of HIV-1 infection (Daniel et al., 1992). The Nef protein is able to downregulate major histocompatibility complex class I (MHC class I) by promoting degradation of the said protein and increasing survival of infected cells against cytotoxic T-lymphocytes (CTLs) (Collins et al., 1998). Secondly, it is also able to downregulate CD4 on the surface of infected cells which avoids the binding of the Env to CD4 while virions are

budding (Lama et al., 1999). Lastly, Nef is able to facilitate the down or up regulation of T-cell receptor signalling which can aid in HIV-1 replication in CD4+ T-lymphocytes (Baur et al., 1994, Luo and Peterlin, 1997). Other functioning has also been noted over the years including remodelling of the cytoskeleton and manipulation of the cellular vesicular system (Campbell et al., 2004, Mangasarian et al., 1997).

The remaining three accessory proteins, Viral infectivity factor (Vif), viral protein R (Vpr) and viral protein U (Vpu) are the focus of this dissertation, and thus their function is described in more detail below.

1.1.3.1 Vif

1.1.3.1.1 Vif targets APOBEC

Vif encodes a 192-amino acid, ~23 kDa protein that has been implicated in counteracting the anti-viral restriction factor apolipoprotein B mRNA editing enzyme, catalytic polypeptide-like 3G (APOBEC3G) which is part of the APOBEC protein superfamily which are known to be editors of nucleic acids. More specifically, APOBEC proteins have a potent cytidine deaminase activity, deaminating cytosine residues to uracil residues. It was first noted that certain cell lines including the primary HIV-1 target cells, T-cells, expressed genes that would make the cells permissive or non-permissive to production of HIV-1 strains whose *vif* genes were non-functional (Gabuzda et al., 1992). It was later found that a single gene, then dubbed *CEM15*, which was expressed in cell lines that did not normally express the CEM15 protein was responsible for this phenomenon, and Vif was responsible for the downregulation of CEM15 (Sheehy et al., 2002). CEM15 was then shown to be identical to APOBEC3G in both structure and functioning, and thereby the same (Kao et al., 2003). During virion budding from an infected HIV-1-producing cell, APOBEC3G is incorporated into newly formed HIV-1 viral particles which then go on to infect other cell targets. Following attachment and entry of the virus into the target cell, APOBEC3G is released and deaminates the cytosine residues of the first strand of the viral cDNA. Acting as a template for the second strand of viral cDNA, adenine is misincorporated resulting in strand-specific C/G to T/A hypermutations which can affect viral open reading frames or result in incorporation of termination codons (Mangeat et al., 2003, Zhang et al., 2003). It is also proposed that deamination of the viral cDNA cytosine residues results in a DNA excision repair response, resulting in cDNA degradation and failure of integration into the genome of the infected host cell because of previous observations of *vif*-defective viruses being unable to produce full-

length cDNA (Simon and Malim, 1996, Kao et al., 2003). Touching on variation of HIV-1 once more, it has been shown that APOBEC3G or natural variation within Vif drives evolution and diversification of HIV-1. Defective *vif* has been noted in very different patient samples, in both LTNPs and acutely infected patients, and these defective Vif proteins may selectively neutralize or partially neutralize APOBEC3G activity which can result in mutations of HIV-1 at any given time by APOBEC3G, therefore driving HIV-1 diversity within an individual (Simon et al., 2005). This is further shown by evidence of sub-lethal mutagenesis in HIV-1 due to APOBEC3G, in which APOBEC3G manages to mutate HIV-1 without the mutations becoming deleterious to the virus therefore conferring possible favourable mutations (Sadler et al., 2010). Recently it was shown by Squires and colleagues that mutations in epitopes targeted by CD8+ T-cells can result in escape by HIV-1 due to a loss of recognition by the human leukocyte antigens (HLA) class I proteins which present these epitopes to the CD8+ T-cells, therefore the rationale exists that APOBEC is a driver of immune escape mutations and disease progression of HIV-1 (Squires et al., 2015).

1.1.3.1.2 Vif and Ubiquitination

The functioning of Vif is that of an adaptor protein, involved in the ubiquitination of APOBEC3G and its proteolytic degradation by the proteasome (Stanley et al., 2008). Studies utilising immunoprecipitation of recombinant Vif expressed in mammalian cells followed by mass-spectrometry detected various proteins associated with Vif, namely cullin-5 (a scaffold protein), elongins B and C (substrate adaptors), and Rbx1 (catalyst of ubiquitin polymerization) (Yu et al., 2003). Vif binds APOBEC3G and these other associated proteins which form an E3 ubiquitin ligase complex which ubiquitinates APOBEC3G. Also important for this complex formation is CBF-β, a transcription factor required for Vif stability and assembly of the E3 ubiquitin complex (Jager et al., 2012). The structure of Vif is conducive to its functioning with various regions of the protein assigned to different functioning. A suppressor of cytokine signalling-box (SOCS-box) motif is located within Vif which is required for the association with the cullin-5, elongins B and C ubiquitin ligase complex. This conserved domain within Vif specifically binds elongins B, C and cullin-5, and is anywhere from 25 to 40 amino acids long with an N-terminal BC-box region which contains the SLQYLA amino acid motif, and a C-terminal Cullin-box containing a proline-leucine (PPLP) amino acid motif (Mehle et al., 2004, Stanley et al., 2008). A zinc-binding region is located upstream from the SOCS-box containing a histidine and cysteine (HCCH) motif which is able to coordinate a single zinc ion and position hydrophobic residues for binding with cullin-

5 (Mehle et al., 2006). Conserved tryptophan amino acid residues in the N- terminal region of Vif are vital in the interaction of Vif with APOBEC3G and APOBEC3G's suppression (Tian et al., 2006). Residues 33 to 83 in Vif are said to form the vital interface involved in binding of Vif to APOBEC3G, with a mutation specifically of residue 42 or 43 inhibiting the interactions between Vif and APOBEC3G (Mehle et al., 2007). Vif has been shown to oligomerize, with the PPLP motif, HCCH motif and BC box said to be vital for this (Techtmann et al., 2012). Oligomerization has been shown to be critical for Vif functioning and it is likely due to APOBEC3G existing in a high-molecular mass form, with Vif oligomers being able to bind with greater avidity to this high-molecular mass APOBEC3G (Miller et al., 2007, Techtmann et al., 2012).

1.1.3.2 Vpr

1.1.3.2.1 Vpr is expressed during late viral protein expression

Vpr encodes a 96-amino acid, ~14 kDa protein implicated in a plethora of HIV-1 life-cycle related functioning including cell cycle arrest, apoptosis, effects on reverse transcription, import of the viral pre-integration complex (PIC) into the nucleus, and effects on viral and host cell gene expression. Vpr is expressed during late viral protein expression and is relatively conserved among HIV-1, HIV-2 and SIV strains. It is also similar to the HIV-2 and SIV-specific Vpx protein (Collins and Collins, 2014). Virions that are formed from infected cells contain packaged Vpr, with the HIV-1 Gag precursor known as $Pr55^{Gag}$ being essential for this packaging into virions (Selig et al., 1999). More specifically, the p6 domain of $Pr55^{Gag}$ has been shown to be essential as shown by studies where p6 was deleted from HIV-1 and Vpr failed to incorporate into newly formed virions (Bachand et al., 1999). The C-terminus of Vpr was identified early on as vital for incorporation of Vpr and likely interacts with the p6 domain (Bachand et al., 1999). The rationale of this incorporation into virions is that Vpr is an important protein involved in the early stages of viral replication before the formation of new virus (Guenzel et al., 2014).

1.1.3.2.2 Vpr and the PIC

HIV-1 is able to replicate in non-dividing cells such as terminally developed macrophages, a process which is not dependant on mitosis of the infected cell, but relies on various viral components which associate into a PIC for nuclear localization, with Vpr being one of those components (Heinzinger et al., 1994, Eckstein et al., 2001). Other components of the PIC include integrase, matrix protein and the viral cDNA itself (Depienne et al., 2001, Haffar et

al., 2000, Miller et al., 1997). Vpr has been shown to interact with the cellular receptor of nuclear transport α-importin, even though Vpr lacks a typical nuclear localisation signal (NLS) amino acid sequence (Vodicka et al., 1998). It is suggested that a variant pathway for import is used by Vpr with other proteins of the PIC utilising the classical pathway of transport into the nucleus, with the α-importin/vpr interaction being essential . The α-helix domain of the N-terminus of Vpr has been implicated in the interaction with α-importin (Nitahara-Kasahara et al., 2007) In order for integration of the PIC it needs to dock with the nucleoporins of the nuclear pore complex, which associate with matrix protein and integrase (Popov et al., 1998). Vpr has been shown to stabilize this docking with the nucleoporins in an α-importin dependant manner (Popov et al., 1998). The dependence of Vpr solely for the transport of the PIC may not be entirely founded though as it has been shown that two NLS found on the matrix protein are vital for import of the PIC into the nucleus in conjunction with Vpr (Haffar et al., 2000). Vpr has also been found to damage the nuclear envelope by causing herniation and eventual rupture, leading to a mixing of the cytosolic and nuclear regions of the cell. It is hypothesized that these herniations and ruptures could allow for the PIC to be localized into the nucleus in a non-traditional manner (de Noronha et al., 2001)

1.1.3.2.3 Role of Vpr in the cell cycle

Vpr is a well described driver of cell cycle arrest in the G2 phase, but the entire process is not fully understood and there are still many gaps in the understanding of how exactly Vpr does this. The result of cell cycle arrest is an increase in viral production due to the increased expression of the HIV-1 long terminal repeat (LTR) which houses promoter and enhancer regions essential for HIV-1 gene expression (Temin, 1982). The LTR is more active during the G2 phase of the cell cycle resulting in a greater amount of virus from each infected cell. Infected cells which would die after the G2 phase also survive longer *in vivo* as they remain in G2 for longer and subsequently have more time to express HIV-1 proteins (Gori et al., 1998). It was first found that Vpr was responsible for the hyperphosphorylation of the cyclin B-p34^{cdc2} (a cyclin-dependant kinase integral to cell cycle progression) complex which prevents progression of the cell cycle to mitosis (Re et al., 1995). Vpr has also been shown to interact with the kinase domain of Wee1 which is a known regulator of cdc2 and subsequently blocks progression of the cell cycle due to Wee1's increased kinase activity for cdc2. However, this binding interaction has been shown to not be sufficient alone in cell cycle-arrest in G2, therefore a separate mechanism of cell cycle-arrest by Vpr must be at work (Kamata et al., 2008). Other implicated proteins in the arrest of the cell cycle of HIV-1

infected cells that interact with Vpr are 14-3-3 proteins. These key cell cycle regulatory proteins are able to interact with Vpr resulting in the translocation of cdc25C phosphatase to the cytoplasm, which then results in a permanent state of phosphorylation of cdc2, therefore arresting the cell cycle (Kino et al., 2005). Interestingly, cdc25C also interacts with Wee1 which stabilises and enhances its kinase abilities (Wang et al., 2000).

Vpr acts as an adaptor protein in ubiquitination pathways much like the other HIV-1 accessory proteins and this has implications for cell cycle arrest. Through immunoprecipitation, Wen and colleagues showed that Vpr forms an ubiquitin ligase complex consisting of Vpr, DNA damage-binding protein 1 (DDB1), VprBP (also known as DDB1- and CUL4-associated factor homolog 1 (DCAF1)) and cullin4A (Wen et al., 2007). Vpr recruits DCAF1 through its first and third α-helices which then links Vpr to DDB1 (Le Rouzic et al., 2007). The proposed cellular target of ubiquitination that results in G2 arrest is still controversial, but it is predicted that the C-terminus of Vpr contains the target cellular-protein binding domain. A result of this ubiquitin complex formation, and the likely overall mechanism for the arrest of HIV-1 infected cells in G2 is the activation of the ataxia telangiectasia and Rad3-related protein (ATR) DNA repair pathway which senses DNA damage and halts the cell cycle (Zimmerman et al., 2004, Roshal et al., 2003). Evidence for Vpr promoting a stress response within infected cells has been noted by the occurrence of Vpr-dependant nuclear foci which are markers of a DNA stress response, consisting of ATR pathway targets γ-H2AX (a histone type which is greatly phosphorylated in the ATR pathway) and BRCA1 (a DNA repair protein) (Zimmerman et al., 2004). Recently, it has been shown that Vpr interacts with the scaffold protein SLX4 and structure-specific endonucleases (SSEs), MUS81-EME1, which are responsible for processing of Holiday Junctions during DNA repair (Laguette et al., 2014). Vpr is able to interact with the C-terminus of SLX4, the ubiquitin ligase complex of DCAF1-cullin4A-DDB1 and the polo-like kinase 1 (PLK1). PLK1 phosphorylates EME1, whilst MUS81 is ubiquitinated resulting in an untimely activation resulting in cell cycle arrest; this process has now been confirmed with SIV Vpr as well (Laguette et al., 2014, Berger et al., 2015).

A possible consequence of Vpr-induced cell cycle arrest is apoptosis in infected cells therefore possibly contributing to the declining CD4+ T cell counts noted in HIV-1 patients, though much is not understood of the role that Vpr has on apoptosis of HIV-1 infected cells. It was found in one study where caffeine was utilised as an inhibitor of the DNA-damage response in HIV-1 positive test cells that the cell cycle arrest and the DNA-damage response

seems to be vital to Vpr-induced apoptosis (Roshal et al., 2003). The reliance on G2 arrest for apoptosis was further shown in a study where Vpr-activated ATR activity was inhibited in infected cells and the downstream apoptotic protein BAX was prevented from activating (Andersen et al., 2006).

1.1.3.2.4 Vpr has differing effects on mutation rates of HIV-1

The mutation rate of the HIV-1 virus during *in vivo* infection is said to be influenced by Vpr although there is some controversy to its exact role. Vpr has been shown to interact with the uracil DNA glycosylase protein (UNG), with the highly conserved tryptophan at position 54 of Vpr important for this interaction (Mansky et al., 2000, Chen et al., 2004, Bouhamdan et al., 1996). UNG is a protein which is involved in the base excision DNA repair pathway and is able to remove misincorporated uracil residues from DNA or uracil residues that occur from the deamination of cytosine. The human *UNG* gene is spliced into two variants, a mitochondrial or nuclear form, with the nuclear form (UNG2) said to interact with Vpr in the nucleus, and then incorporated into forming virions (Chen et al., 2004). Cells with replicating virus that lack UNG2 have shown many several-fold increases in the mutation rates of the replicating virus, especially non-dividing cells such as macrophages, further highlighting the importance Vpr plays in the viral life cycle of HIV-1-infected non-dividing cells (Chen et al., 2004). Interestingly, non-dividing cells such as macrophages exhibit an intracellular environment which is low in UNG2 and has high levels of free uracil residues (Miller et al., 2000).

In contrast, other studies have shown a different role for UNG2 which may be detrimental to viral production *in vivo*, with UNG2 having been proposed to be a viral-host restriction factor against HIV-1 early replication (Weil et al., 2013). It has been shown that Vpr can actually inhibit rather than promote the incorporation of UNG2 and related enzyme Single-Strand-Selective Monofunctional Uracil-DNA Glycosylase 1 (SMUG1) into forming virions, promoting the ubiquitination of those proteins utilizing the familiar Vpr-associated ubiquitin complex of DCAF1-cullin4A-DDB1 (Schröfelbauer et al., 2007). Excessively high amounts of Vpr have been shown to promote UNG2 degradation and decrease total cellular uracil DNA glycosylase activity in T-lymphocytes (Eldin et al., 2013). It has been argued that due to HIV-1 being single stranded during the period of increased incorporation of uracils due to APOBEC3G activity for example, UNG2 has no template strand with which to repair the negative-sense strand, and even a single excision of a uracil by UNG2 would prevent formation of a plus-sense strand (Schrofelbauer et al., 2005). There may in fact be benefits to

the uracilation of HIV-1 cDNA as it has been shown to inhibit autointegration of the HIV-1 cDNA. Autointegration occurs when integrase activates the ends of newly formed cDNA in preparation for insertion into the host genome, but the ends actually attack the viral cDNA itself resulting in deletions or inversion circles (Yan et al., 2011). Another possible benefit to uracilation of viral DNA is the masking of cytosolic viral cDNA against intracellular innate immune sensors (Yan et al., 2010, Eldin et al., 2013). The effects that Vpr has on viral mutation rates may of course be dynamic, depending on what stage viral replication is at or the uracil content of the infected cell which may explain the mystery surrounding this functioning of Vpr.

1.1.3.3 Vpu

1.1.3.3.1 Vpu Structure

Vpu encodes for a ~81-amino acid, ~9 kDa protein implicated in the degradation of CD4, enhanced release of virions from the infected host cell, modification of immune-regulatory pathways and possible ion channel formation in cellular membranes. The Vpu protein is produced from a bicistronic mRNA encoding both Env and Vpu and is suggestive of the coordinated expression of both (Schwartz et al., 1990). Vpu is a type I membrane protein with a hydrophobic N-terminal transmembrane domain and a hydrophilic C-terminal cytoplasmic portion, with the protein being able to embed itself in both the endoplasmic reticulum (ER) and the cellular surface membrane, and able to oligomerize as well (Maldarelli et al., 1993). The transmembrane domain consists of a single α-helix (α-helix 1) which spans the lipid bi-layer and has been found to be tilted between 15° and 30° (Zhang et al., 2015). The cytoplasmic region consists of two α-helices (α-helices 2 and 3) attached to each other by a short linker sequence known as loop-2, while the transmembrane α-helix 1 is attached to the cytoplasmic α-helix 2 by a linker sequence, loop-1 (Zhang et al., 2015). An EYR amino acid motif which is responsible for salt-bridge formation is found in loop-1 and is responsible for a tilt which aligns the long axis of α-helix 2 parallel with the cellular membrane surface (Lemaitre et al., 2006). A-helix 3 points towards the lipid bilayer, is relatively flexible and charged, and forms a U-shape with α-helix 2 (Wray et al., 1995, Zhang et al., 2015). Loop-2 is the most conserved region of Vpu and has two important serine residues which are phosphorylated by casein kinase II and are vital sites for the functioning of Vpu (Schubert et al., 1994). Interestingly, Vpu from different HIV-1 subtypes shows a high degree of variability, with HIV-1 subtype C containing a unique LRLL amino acid motif for example (McCormick-Davis et al., 2000). The resultant variability may result in slightly

different functioning between subtypes. Variability within trafficking signals is found between the transmembrane region and α-helix 2, and within α-helix 2, with subtype B Vpu being mostly trafficked and retained within the rough ER and Golgi complex, while subtype C Vpu is trafficked to the cellular surface membrane (Pacyniak et al., 2005, Ruiz et al., 2008).

1.1.3.3.2 Targeting CD4

Vpu, like the other HIV-1 accessory proteins Vif and Vpr, can act as an adaptor protein in ubiquitination pathways, degrading vital host cellular restriction factors. One target of this ubiquitination pathway is CD4, which is ubiquitinated on its cytosolic tail on lysine, serine and threonine residues and subsequently processed by the proteasome (Bour et al., 1995). The primary receptor of HIV-1 binding to CD4+ T-cells is the CD4 receptor, which binds to gp120 found on the HIV-1 viral surface. CD4 is manufactured in the ER and subsequently transported via the Golgi complex to the cell surface. In HIV-1 infected cells, CD4 is downregulated due to the gp120 precursor protein, gp160, which binds to CD4 and forms complexes that remain within the ER (Willey et al., 1992). Downregulation of CD4 would seem counterproductive for HIV-1 as it is its target receptor for infection, but downregulation confers various advantages to the HIV-1 virus which actually promotes infection such as an increase of formation of virions due to more freely available Env proteins and a decreased major histocompatibility class II (MHC class II) immune response (Lanzavecchia et al., 1988, Levesque et al., 2003).

It was noted in early studies that the normal intracellular half-life of CD4 drops from 6 hours to 12 minutes in the presence of Vpu (Willey et al., 1992). It was also noted that Vpu is able to bind to CD4 by its cytoplasmic domain which includes α-helix 2 and α-helix 3, with the important serine residues of the inter-helical linker region (serine 52 and 56) not important for the actual binding of Vpu to CD4 (Margottin et al., 1996, Singh et al., 2012). Through co-immunoprecipitation and yeast two hybrid analysis it was found that βTrCP, a cellular ubiquitin ligase, is a binding partner of Vpu, and Vpu has to be phosphorylated in order for this interaction to occur (Margottin et al., 1998, Butticaz et al., 2007). Complexes were shown to form consisting of CD4, Vpu and βTrCP, with Vpu being a linker between CD4 and βTrCP. Further testing showed that the F-box motif of βTrCP interacts with Skp1, which links these protein complexes to the ubiquitin ligase machinery, forming a Skp1/Cullin-1/F-Box (SCF) ubiquitin ligase complex (Margottin et al., 1998, Ramirez et al., 2015).

The functioning of Vpu and its CD4 degradation can be likened to the endoplasmic reticulum-associated degradation (ERAD) pathway which is implicated in the removal of irregular proteins from the ER (Magadán et al., 2010). The functioning of Vpu in regards to CD4 downregulation can essentially be broken down into 2 activities, the retention of CD4 within the ER and CD4's degradation. The transmembrane domain of Vpu is said to interact with the transmembrane domain of CD4 by a highly conserved tryptophan residue surrounded by other clustered residues such as valine and serine within the Vpu transmembrane domain (Magadan and Bonifacino, 2012). The valine and serine residues are said to interact with the ER lipid bilayer itself in order to retain CD4 while the tryptophan residue is said to hold Vpu in its monomeric form, which is its active form (Magadan and Bonifacino, 2012). As mentioned previously, Vpu acts as an adaptor protein in the ubiquitination and subsequent degradation of CD4; this ties into the ERAD pathway as it has been shown after downregulation of certain components of ERAD utilising siRNA that the VCP-UFD1L-NPL4 complex, which is a known component of ERAD, is vital in the Vpu–mediated degradation of CD4. UFD1L binds to the ubiquitin chains found on CD4, while NPL4 stabilizes this interaction. VCP contributes an ATPase activity that provides the energy required for Vpu to remove CD4 from the ER membrane and locate it to the cytoplasm for degradation by the proteasome (Magadán et al., 2010).

1.1.3.3.3 Targeting Tetherin

It was noted early on that Vpu was required for the efficient maturation and release of progeny HIV-1 viral particles from host cells, with viral particles remaining attached to the membranes of infected cells when non-functional *vpu* was introduced into HIV-1 clones (Klimkait et al., 1990). The transmembrane domain of Vpu was shown to be responsible for the release of newly-formed viral particles from an infected cell, but it wasn't until many years later that the mechanism at work was deduced (Tiganos et al., 1998). It was hypothesized that Vpu is able to target a specific host restriction factor which is responsible for the release of virions from the host cellular membrane, with an interferon-dependant protein likely to be responsible, as highlighted in two studies where HIV-1 virions attached to cellular membranes of infected cells were released once the cells were treated with a protease; and where infected HIV-1-infected-fibroblasts, T-cells and primary lymphocytes lacking in Vpu were treated with increasing amounts of interferon and virions were subsequently retained at the cellular surface (Neil et al., 2006, Neil et al., 2007). The responsible protein for restriction of virion release was finally identified as bone marrow

stromal antigen 2 (BST-2) or also known as HM1.24/CD317/tetherin (Neil et al., 2008, Van Damme et al., 2008). Assays utilizing cell lines that express tetherin and that were infected with *vpu*-deficient HIV-1 strains showed a 20 fold increase in virion release inefficiency as compared to cells infected with the *vpu*-positive HIV-1 strains, highlighting the importance of tetherin in viral release (Neil et al., 2008). Interestingly, tetherin had previously been described as a target of Vpu, though in a study looking at Kaposi sarcoma–associated herpesvirus K5 protein and its immune-modulatory functioning (Bartee et al., 2006).

Tetherin is a 30 to 36 kDa type II transmembrane protein, consisting of 180 amino acids (Ishikawa et al., 1995). It consists of a N-terminal cytoplasmic tail, a transmembrane domain and a C-terminal glycosyl-phosphatidylinositol (GPI) anchor which is said to act as a second transmembrane domain (Andrew et al., 2011). An extra-cytosolic domain consisting of ~120 amino acids in a coil coiled structure connects the N- and C-terminals, allows for flexibility of tetherin which is important for its functioning, and bears two N-linked sugars (Andrew et al., 2011). Tetherin has been shown to associate with lipid rafts and is able to cycle between the Golgi network and cellular surface membrane (Kupzig et al., 2003). Active tetherin occurs as a homodimer, with 3 important cysteines forming disulphide bonds between the tetherin homodimers and allowing for considerable flexibility in the otherwise unstable monomeric tetherin coiled coils, and this configuration of homodimeric tetherin is responsible for its virion trapping abilities (Perez-Caballero et al., 2009, Hinz et al., 2010). Tetherin's mechanism of action is said to involve the preferential insertion of the dimeric tetherin GPI anchors (in an "axial" configuration) into the budding virions while maintaining the N-terminal region in the host cell membrane for possible cellular signalling functioning (Venkatesh and Bieniasz, 2013, Perez-Caballero et al., 2009).

Vpu is thought to antagonise tetherin in three probable ways; degradation of tetherin, displacement of tetherin and inhibition of tetherin recycling, with the exact mechanisms of action not completely understood and often times conflicting. The transmembrane domain of Vpu has been shown to be vital in the downregulation of tetherin from the cell surface with both tetherin and the Vpu transmembrane domain directly binding to each other within the cellular membrane, as shown by crosslinking studies; the importance of transmembrane interactions is also illustrated by studies where site-directed mutagenesis of the Vpu transmembrane domain was done which results in a decreased activity of tetherin downregulation (Skasko et al., 2011, McNatt et al., 2013).

Once again Vpu has been shown to act as an adaptor protein in a polyubiquitination pathway, in this case resulting in tetherin degradation instead of CD4. Vpu can co-immunoprecipitate along with tetherin and βTrCP, with the SCF ubiquitin ligase complex likely involved in the proteasomal degradation of tetherin utilising an ERAD-like pathway once again (Mangeat et al., 2009). Other conflicting studies indicate that the interaction of Vpu, tetherin and βTrCP may lead to lysosomal degradation rather than degradation by the proteasome (Iwabu et al., 2009, Douglas et al., 2009). Ubiquitination of a protein is a regulatory mechanism involved in endocytosis and it has been proposed that βTrCP with the SCF ubiquitin ligase complex promotes endocytosis of tetherin, with the Clathrin adaptor protein complex AP-2 (involved in endocytic trafficking) shown to be important in Vpu-induced endocytosis of tetherin (Iwabu et al., 2009).

Vpu can block the recycling and internal cellular transport of tetherin and newly synthesized tetherin, holding it within the Golgi network independent of any ubiquitination pathways (Schmidt et al., 2011). The α-helix 2 of Vpu is also able to displace tetherin from sites of viral assembly, which is a function that is independent of degradation or internalisation of tetherin by Vpu, and a recent study showed that a tryptophan within α-helix 2 is able to anchor the C-terminus to the cellular plasma membrane and enhance tetherin displacement (only subtypes B, D and G seem to have this tryptophan and the importance in subtype C is unknown) (McNatt et al., 2013, Lewinski et al., 2015). It has been proposed that Vpu induces a new tetherin equilibrium at the cell plasma surface, with 60% of initial tetherin levels being enough to promote HIV-1 virion release from the host cell, and this is achieved through a combination of withholding of tetherin in the Golgi network and degrading of tetherin utilising the proteasomal/lysosomal degradation pathways (Dubé et al., 2011).

1.1.3.3.4 Further tasks for Vpu; NF-kB, ADCC, NTB-A and CD1d

Other functioning of Vpu includes its modulation of the immune response, including effects on NF-kB activity and antagonism of antibody-dependent cellular cytotoxic responses (ADCC).

βTrCP is able to bind nuclear factor of kappa light polypeptide gene enhancer in B-cells inhibitor alpha (IκBα), an inhibitor of nuclear factor kappa-light-chain-enhancer of activated B cells (NF-κB) translocation into the cell nucleus, and promote its degradation by the SCF ubiquitin ligase complex resulting in NF-κB activation. NF-κB is a series of transcriptional regulators that are responsible for activation of genes involved in activation of the immune

system (Hiscott et al., 2001) Since Vpu is able to bind to βTrCP and remain in complex steadily within the cell, cytokine-mediated degradation of IκBα is blocked because of decreased binding of βTrCP, resulting in reduced NF-κB activation (Bour et al., 2001). Tetherin itself is a known stimulator of NF-κB activity acting as a sensor of cellular viral infection upon retention of virions at the cellular membrane, and promoting expression of cytokines and an immune response; Vpu downregulates this activity by virtue of its anti-tetherin activity (Tokarev et al., 2013, Galão et al., 2012)

Due to the HIV-1 viral retention at the surface of infected cells by tetherin, infected cells are more susceptible to antibody-dependent cell-mediated cytotoxicity (ADCC) and natural killer (NK) cell-induced death (Alvarez et al., 2014, Arias et al., 2014). The anti-tetherin activity of Vpu therefore is protective against ADCC activity and the untimely death of HIV-1 infected cells. It has been shown that HIV-1 LTNP exhibit high amounts of ADCC activity which is said to be protective against HIV-1, therefore the importance of ADCC and Vpu's effects on it should not be understated (Lambotte et al., 2009, Wren et al., 2013). Vpu itself is shown to be a target of ADCC responses (likely due to it spanning the cellular membrane and being exposed to the extracellular environment) with Wren and colleagues describing three different epitopes targeted by ADCC in seven LTNP patients as compared to non-LTNP who had no responses at all (Wren et al., 2013). ADCC and its role in HIV-1 infection has recently garnered increased interest after the Thai Phase III HIV-1 Vaccine Trial which showed that ADCC may have played a role in the observed levels of protection within that trial (Rerks-Ngarm et al., 2009).

Recently, it was shown that Vpu is able to down regulate NK-T and -B cell antigen (NTB-A), thus protecting infected HIV-1 infected CD4+ T-cells (Shah et al., 2010). NTB-A activation is required along with the NK cell activation receptor, NKG2D, for the degranulation of NK cells resulting in the killing of infected CD4+ T-cells. Vpu was shown to down-regulate the surface levels of NTB-A utilising a mechanism that is distinct from its adaptor protein functioning in the down-regulation of CD4 and tetherin as illustrated in a study in which a mutant Vpu which had its important serine residues 52 and 56 mutated which abrogated Vpu's interaction with βTrCP, and the resultant mutant was still able to down-regulate cell-surface NTB-A (Shah et al., 2010). The transmembrane domain of Vpu was linked to its functioning of down-regulating NTB-A. Vpu is said to prevent the transport of NTB-A through the Golgi apparatus and subsequent glycosylation of NTB-A by post-ER mechanisms (Bolduan et al., 2013).

The cluster of differentiation d receptors (CD1d) are lipid-antigen presenting proteins found on professional antigen presenting cells, monocytes, macrophages, B-cells and activated T-cells which present to natural killer T-cells (Moody, 2006). HIV-1 infects many of these cell types which express CD1d on their surface and it has been shown that Vpu is able to down regulate this surface protein. Moll and colleagues were able to show that more than half of CD1d was down regulated in HIV-1 infected dendritic cells, with Vpu shown to effect the rate of recycling of CD1d by co-localizing with CD1d in the endosomal compartments (Moll et al., 2010).

1.1.4 HIV-1 Tropism

HIV-1 infection involves the binding of gp120 to CD4 on the target cell followed by the attachment to a secondary chemokine co-receptor, mostly being CCR5 for macrophage-tropic HIV-1 or C-X-C chemokine receptor type 4 (CXCR4) for T-cell tropic HIV-1. Some viral strains have been known to use other co-receptors such as CCR3, CCR2b, CCR8, Apj, Strl33 Gpr1, Gpr15, CX3CR1, ChemR23 or RDC1 (Berger et al., 1998, Gorry et al., 2007). Initial founder viruses utilise the CCR5 co-receptor almost exclusively and throughout the early stages of infection, with the virus sometimes evolving towards the use of CXCR4 or the usage of either co-receptor. The importance of CCR5 in early stages of infection is highlighted by the 32 bp deletion of the CCR5 gene resulting in the protective CCR5-Δ32 mutation (Samson et al., 1996). People who are homozygotes for this mutation are almost fully protected against HIV-1 infection and a stem cell transplant for an HIV-1 patient from a homozygote CCR5-Δ32 donor has been shown to result in total control of HIV-1 infection (Hutter et al., 2009, Gorry and Ancuta, 2011).

1.1.5 Viral Life Cycle

HIV-1 enters through the mucosal membranes (when sexually transmitted) where initial infection takes place in the first encountered CD4+ T-cells, followed by re-location of the virus to the gut-associated lymphoid tissues and lymph nodes to establish chronic infection (Ladinsky et al., 2014). The gp120 binds CD4 by its CD4 binding site, which results in a conformational change exposing the co-receptor binding site, with co-receptor binding mediated largely by the gp120 V3 loop (Kwong et al., 1998, Tamamis and Floudas, 2014). Once gp120, CD4 and co-receptor have bound, gp120 undergoes numerous conformational changes, exposing gp41 which is responsible for membrane fusion. A fusion peptide is exposed on gp41 which targets the host cell membrane and bridges the viral and target cell

membranes (Buzon et al., 2010). A pre-hairpin state of gp41 then refolds into a six-helix bundle core structure which then promotes membrane fusion (Chan et al., 1997).

Once fusion occurs, the viral capsid containing the viral genetic material and proteins including the important reverse transcriptase and integrase enters the host cell, and the capsid subsequently uncoats (Klarmann et al., 1993). Reverse transcription of the viral RNA begins when the viral RNA is still within the capsid and subsequently following uncoating the reverse transcription complexes form, which consists of HIV-1 complexes undergoing reverse transcription by reverse transcriptase (Zhu et al., 2004, Lin et al., 2015). Following reverse transcriptase the PIC is formed consisting of double-stranded viral cDNA, integrase, matrix, Vpr, reverse transcriptase and several host-derived factors such as HMG I(Y) protein (Miller et al., 1997). The PIC is transported into the host cell nucleus utilising many different nuclear localisation signals and along the microtubule network, where it is then integrated into active regions of the host cell genome by the integrase enzyme (Farnet and Haseltine, 1990, Schroder et al., 2002). The LTR regions of the integrated proviral DNA mediate the expression of viral RNA destined for packaging into assembling virus as genomic RNA or as RNA transcripts for translation of viral proteins (Butsch and Boris-Lawrie, 2002).

During the late stages of the replication cycle, various precursor proteins are translated and then cleaved by protease into mature viral proteins which will be assembled into a fully formed HIV-1 viral particle. The Gag precursor (also known as $Pr55^{Gag}$) consists of the matrix, capsid, nucleocapsid and p6 domains (Guo et al., 2015). The GagPol precursor (also known as $Pr160^{GagPol}$) contains the aforementioned proteins as well as protease, reverse transcriptase and integrase domains, and occurs due to a frameshift during translation of Gag mRNA (Pettit et al., 2005). HIV-1 Env is translated from the bicistronic mRNA coding for *vpu* and *env* (Schwartz et al., 1990). The precursor Env, gp160, travels through the endoplasmic reticulum and trans-Golgi network as oligomers (Earl et al., 1990). The host protease furin cleaves gp160 into the mature Env proteins gp120 and gp41 which remain non-covalently bound and all the viral proteins and viral genomic RNA assemble under the cell plasma membrane (Hallenberger et al., 1992). The virus takes shape at the plasma membrane utilising the host cell membrane for its viral lipid membrane, within which the viral Env is embedded. Budding and release is managed by the endosomal sorting complexes required for transport (ESCRT) machinery which is hijacked by the virus, with Gag being responsible for the interaction between virus and host ESCRT machinery (Morita et al., 2011).

1.1.6 The HIV-1 immune response

The current immune correlates of protection against HIV-1 are poorly understood. It is likely that they involve a combination of innate and adaptive (cellular and antibody) driven responses which act together synergistically to prevent chronic infection with HIV-1.

1.1.6.1 Immune correlates of protection; T-cell protection

A closer look at one arm, T-cell responses, is warranted in regards to this author's study which deals with human leukocyte antigen (HLA) class I targeted epitopes of the HIV-1 accessory proteins.

1.1.6.1.1 HLA class I and CD8+ T-cell responses

Pivotal to the immune functioning of vertebrates are the MHC cell surface proteins, or also known as HLA in humans. HLA proteins are responsible for presenting amino acid chains from foreign proteins, such as those of pathogens, for recognition by the immune system resulting in an immune response (Doherty and Zinkernagel, 1975). HLA class I proteins are found on all nucleated cells and present intracellular proteins of either host or pathogenic origin that are transported by the transporter associated with antigen processing (TAP) to the endoplasmic reticulum, where the ~8-12 amino acid peptides associate with HLA class I and are transported to the cell surface (Suh et al., 1994). In contrast, HLA class II proteins are found on antigen presenting cells and are involved in humoral immune responses.

HLA class I proteins present epitopes to CD8+ T-cells which can result in a CTL response. Cellular-mediated killing of the presenting cell by the CD8+ T-cell occurs if the epitope presented by the HLA protein is 'non-self'. There are three primary HLA class I molecules namely HLA-A, -B and -C, with thousands of variants occurring for each molecule type (Carlson et al., 2015). This variation in HLA is driven by the need to identify and present a large variety of pathogen-associated epitopes, with infectious pathogens having driven variation over the millennia. HLA residues are polymorphic in their peptide-binding groove which consists of six different binding pockets designated A-F, which determine the size of the epitopes which can fit in and be presented by each HLA protein (van Deutekom and Keşmir, 2015). Specific anchor residues in the 8-12 amino acid peptides bind within these HLA pockets with at least two amino acid residues acting as dominant binding anchors and binding to pockets B and F of HLA class I (dos Santos Francisco et al., 2015). These anchor residues normally occur at the second position and C-terminus of the presented epitope, though this can differ depending on HLA type, and mutations within these anchors can result

in a specific HLA antigen no longer recognizing the epitope (Yusim et al., 2003). Very similar HLA antigens that differ by even a single amino acid residue have the ability to present the same peptide sequences, but each one can recognize the peptides as wholly unique sequences. A study looking at four similar HLA class I antigens illustrates the previous point; HLA class I antigens B*07:02, B*42:01, B*42:02 and B*81:01 present the same peptide sequences derived from p24 and Nef, but induce different escape mutations within these proteins depending on which HLA presents each peptide sequences (Kløverpris et al., 2015). Even T-cell Receptors (TCRs) recognize each of the presented peptide sequences depending on which HLA antigen is presenting the HIV-1 peptide sequence (Kløverpris et al., 2015).

The importance of HLA class I and CD8+ CTL responses in HIV-1 disease progression to AIDS cannot be understated; time and time again HLA class I proteins have been shown to be a potent determinant of HIV-1 disease progression, either detrimental or protective, with many population studies showing this. At play are the selective pressures from HLA proteins on the HIV-1 virus that could select for deleterious or advantageous mutations; it is even hypothesized that the consensus HIV-1 sequence of a population is partly determined by the predominate HLA types of the population (Moore et al., 2002). It has been shown that over time HIV-1 has less epitopes for presentation to HLA antigens than what is expected and that over time the epitope numbers have dropped from SIV strains to current HIV-1 strains and this may indeed be due to immune pressures driving evolution in the HIV-1 virus (Vider-Shalit et al., 2009). CD8+ T-cell responses have been shown to determine the viral set point of HIV-1 infection patients following the initial peak of virus and decrease in CD4+ T-cell numbers during the acute infection phase, followed by possible protection against rapid declines in CD4+ T-cell numbers into the chronic phase of HIV-1 infection (Streeck et al., 2009).

One of the first larger scale population studies looking at HLA class I and HIV-1 involved two male cohorts. It was found that the HLA class I alleles *HLA-B*57, HLA-B*51* and *HLA-A*25* were associated with a slower disease progression to AIDS (Kaslow et al., 1996). Many HLA studies have been undertaken in the subsequent years describing many different alleles associated with HIV-1 disease progression, with HLA-B alleles showing a significant impact on HIV-1 disease progression and its control (Leslie et al., 2010, Kiepiela et al., 2004). Allele *HLA-B*13* has been shown to control viremia in HIV-1 subtype C infected individuals, with a Gag-specific CD8+ T-cell response likely the cause as *HLA-B*13* targets Gag-specific

epitopes which could result in a fitness cost to HIV-1 if escape mutations were likely to occur within those regions (Honeyborne et al., 2007). The well-known and described *HLA-B*57:01* and *B*58:01* HLA class I alleles are shown to be associated with viral restriction in LTNP groups and are said to target reverse transcriptase and Gag-specific epitopes (the most prevalently targeted one dubbed 'TW10'), which are well documented and shown to mutate often during immune escape of HIV-1 in *HLA-B*57:01* individuals, with the T242N mutation often occurring within the TW10 epitope (Migueles et al., 2000, Tang et al., 2002, Altfeld et al., 2003, Leslie et al., 2004). The very same TW10 epitope has been shown to revert back to its wild type sequence once selective pressures of *HLA-B*57:01* and *HLA-B*58:01* have been removed such as infection in a new host who does not possess the *HLA-B*57:01* and *HLA-HLA-B*58:01* genotype; this highlights fitness costs that may be involved in immune escape mutations by HIV-1 (Leslie et al., 2004).

Mutations within HLA-restricted regions of HIV-1 proteins does not always necessarily confer escape though as shown by Migueles and colleagues, who found that mutations within highly targeted HLA class I regions did not always result in loss of CD8+ T-cell recognition (Migueles et al., 2003). *HLA-B*81* has been shown to reduce viral replication of subtype C HIV-1 by targeting Gag, resulting in the escape mutation T186S which is deleterious to viral replication (Wright et al., 2012) . Though the importance of HLA-B alleles has been shown, it is likely not specific HLA-B alleles solely that determine the effectiveness of immune responses and control of HIV-1, and it may be more of an additive effect of the entire HLA repertoire of an individual (Leslie et al., 2010). The well described Rowland-Jones et al study which looked at resistance to HIV-1 infection in sex workers in Nairobi linked resistance in these women to the presence of CTL responses directed against conserved HLA epitopes of HIV-1, and highlights the importance that HLA and HIV-specific CD8+ CTL responses may play in the control of HIV-1 infection (Rowland-Jones et al., 1998).

Not all CD8+ T-cell responses are protective or are associated with decreased viremia during HIV-1 infection. It has been shown that targeting of HIV-1 proteins by CD8+ T-cell responses can be detrimental or protective depending on the HIV-1 protein being targeted, with Gag-specific responses showing the greatest association with lowering of HIV-1 viremia. HIV-1 positive patients have been estimated to reach full-blown AIDS within 2 or 3 years without any Gag-specific responses versus patients who would take up to 10 years to contract AIDS when they showed greater numbers of Gag-specific responses (Kiepiela et al., 2007). Interestingly, CD8+ T-cell responses targeted against other HIV-1 proteins actually

show an increase in overall viremia in the host, including responses against the accessory proteins Vif, Vpr and Vpu and this may be due to the expression timing of each HIV-1 protein during the replication cycle (Kiepiela et al., 2007). Gag is available immediately within an infected cell and can be processed and presented by HLA class I for quick detection by the immune system whereas other proteins require expression first (Kiepiela et al., 2007). This is especially highlighted in a study where the authors were looking at epitope presentation of two HLA class I-restricted epitopes that are associated with protection, KF11 and KK10 of Gag, versus KY9 of Pol and VL9 of Vpr. It was noted that within 3 hours of post-infection of different cell lines that the Gag and Pol epitopes were presented to CD8+ T-cells (with the antigens coming from the infecting virus itself) and the virus was subsequently cleared, whereas presentation of the Vpr antigens took place much later on (Kloverpris et al., 2013).

HLA class I genotypes of course cannot fully account for the CD8+ T-cell responses seen in patients especially in those who are fast progressors or LTNPs; the functionality of the patient's immune system itself including CD8+ T-cell characteristics is important as well, and the mere presence of protective HLA class I alleles does not always result in HIV-1 control nor is it always necessary (Emu et al., 2008). It has been shown that the CD8+ T-cells that have multiple, high-quality responses are the most effective such as CD8+ T-cells of the HIV-1-restrictive allele *HLA-B*27* which targets the KK10 epitope of Gag (Altfeld et al., 2006). LTNP groups are shown to have highly complex and strong CD8+ T-cell responses within the lymphatic tissues of the gastrointestinal tract where primary HIV-1 infection takes place, with responses occurring even without prior exposure to HIV-1 virus indicative of the immediate ability of the cells to confer a protective immune response (Ferre et al., 2009). These effective CD8+ T-cells are shown to secrete high amounts of cytokines such as macrophage inflammatory proteins (MIP-1β), interferon gamma (IFN-γ) and tumour necrosis factor alpha (TNF-α); various clonotypes of effective CD8+ T-cells exist which can recognise the same peptide motifs but have different binding processes; lastly, strong avidity shown by CD8+ T-cells for their target peptides further increases the control of HIV-1 viraemia (Almeida et al., 2007, Betts et al., 2006, Ferre et al., 2009).

What of the HIV-1 accessory proteins Vif, Vpr and Vpu and their interactions with HLA class I alleles? It can be hypothesised that due to their production within the cytoplasm of the host cell, there should be processing and presentation of those proteins by HLA class I antigens and subsequent CTL responses by CD8+ T-cells. Altfeld and colleagues found

through IFN-γ ELISPOT and intracellular flow cytometric analyses that Vpr and Vif are targets of CTL responses with Vpr being one of the most targeted HIV-1 proteins relative to its size (Altfeld et al., 2001). Interestingly Vpu seemed to be recognized infrequently compared to Vif and Vpr. They hypothesized that Vpr may be a common target of CTL responses due to its higher expression levels within the host cell along with Gag which is commonly targeted, or it may be due to the fact that Vpr has a highly conserved amino acid sequence which may result in it being targeted by CTL responses (Altfeld et al., 2001). Nine different epitopes were described by Altfeld et al and the epitopes were subsequently included in the Los Alamos HIV-1 Immunology Database of best-characterized HIV-1 CTL epitopes (Table 1.1) as assembled by Llano and colleagues, as of 2013 (Llano et al., 2013). This list includes only the best described and most optimal epitopes which the authors refer to as the "A-list" of HIV-1 CD8+ epitopes.

Table 1.1: Best described and most optimal HIV-1 CD8+ CTL epitopes of HIV-1 accessory proteins (Llano et al., 2013)

Protein	Amino acid positions	Motif	HLA type
Vif	17-26	RIRTWKSLVK	A*03:01
Vif	28-36	HMYISKKAK	A*03:01
Vif	31-39	ISKKAKGWF	B*57:01
Vif	48-57	HPRVSSEVHI	B*07:02
Vif	57-66	IPLGDAKLII	B*51
Vif	79-87	WHLGHGVSI	B*15:10
Vif	79-87	WHLGQGVSI	B*38:01
Vif	81-89	LGHGVSIEW	B*57:03
Vif	102-111	LADQLIHLHY	B*18:01
Vif	158-168	KTKPPLPSVKK	A*03:01
Vpr	29-37	EAVRHFPRI	B*51
Vpr	30-38	AVRHFPRIW	B*57:01

Vpr	31-39	VRHFPRIWL	B*27
Vpr	34-42	FPRIWLHGL	B*07:02, B*81:01
Vpr	48-57	ETYGDTWTGV	A*68:02
Vpr	52-62	DTWAGVEAIIR	A*68:01
Vpr	59-67	AIIRILQQL	A*02:01
Vpu	5-13	YRLGVGALI	Cw*18
Vpu	29-37	EYRKILRQR	A*33:03

Vpu is infrequently targeted and according to the database assembled by Llano and colleagues only two significant CTL-targeted Vpu epitopes have been described in the literature (Table 1.1). It is surprising that Vpu is so rarely targeted, as Vpr is of a similar amino acid length but is often targeted. The HLA class I allele *HLA-A*33:03* was shown to target the EYRKILRQR motif of Vpu which is in the vicinity of the βTrCP binding domain of Vpu, and interestingly when Addo and colleagues first described this targeted epitope of Vpu it was noted that the subjects involved happened to be LTNPs (Addo et al., 2002a). The lack of apparent CD8+ T-cell targeted epitopes may also be due to the sheer sequence variability that Vpu exhibits, with Vpu having been shown to be one of the most variable of HIV-1 proteins (Yusim et al., 2002). HLA class I targeted epitopes are shown to usually occur around relatively conserved regions of HIV-1 therefore there is a rationale for why Vpu lacks an abundance of these epitopes (Yusim et al., 2002). More recently utilising a 240 member cohort from Japan, it was found that sequence variability in Vpu was likely not driven by HLA class I pressures even when looking at products of all the possible reading frames of *vpu* (Hasan et al., 2012). Interestingly, amino acid residues at position 5 of Vpu which is in the membrane-bound region of Vpu showed the greatest variability of any Vpu amino acid and an association with the *HLA-A*33:03* allele (Hasan et al., 2012).

1.1.6.1.2 Vaccine strategies for inducing protective CD8+ T-cell responses

Over the last three decades, various strategies have been utilised to develop a vaccine to induce protective CD8+ T-cells responses in test subjects, with limited success. Two particular vaccine strategies in recent years however, have shown some promising results.

The macaque model of SIV infection has been an invaluable tool when analysing HIV-1 infection in humans. In 2013, Hansen and colleagues were able to elicit CD8+ T-cell responses utilising SIV-protein expressing Rhesus Cytomegalovirus vectors (RhCMV) (Hansen et al., 2013b). Interestingly, 50% of rhesus macaques who were challenged with pathogenic strains of SIV showed highly favourable SIV control. Unique CD8+ T-cell responses were elicited that were not typical of the rhesus macaque MHC class I allele *HLA-A*01*(Hansen et al., 2013a).

An effective T-cell-based vaccine should theoretically target the conserved regions of HIV-1 as they are common in most strains of HIV-1 and a fitness cost would be associated with any escape mutations within these regions. This was the rationale used by Borthwick and colleagues when developing the HIVconsv immunogen for the HIV-CORE 002 trial, which consisted of the fourteen most conserved protein domains of HIV-1 from Pol, Gag, Vif and Env (Borthwick et al., 2014). A consensus amino acid sequence was utilised to build the immunogen consisting of subtypes A, B, C and D. The plasmid containing the gene coding for HIVconsv was delivered in a chimpanzee adenovirus type 63 followed by a modified vaccinia Ankara boost in a low risk HIV-1 negative group. Interestingly Pol targeting was better than Gag targeting, which has been shown to be the opposite in almost all other cases (Rolland et al., 2008). The CD8+ T-cells elicited were broadly targeting, with ten epitopes on average being recognised by the cells and 40% of these epitopes being novel and not identifiable on the Los Alamos National Laboratory HIV Immunology Database (Borthwick et al., 2014).

1.1.6.2 Killer-cell immunoglobulin-like receptors and the natural killer cells

Killer-cell immunoglobulin-like receptors (KIR) are found on NK cells and a few T-cell subsets, and are encoded by the *KIR* complex located on chromosome 19. They are able to interact with HLA class I antigens and can determine the presence of viral infection of those cells that express lowered levels of HLA class I antigens (Campbell and Purdy, 2011). NK cells detect "missing self" which constitutes the detection of a lack of HLA class I alleles expressed on a cell resulting in the cell being targeted for destruction (Medzhitov and Janeway, 2002). HIV-1 downregulates HLA-A and –B but HLA-C remains relatively intact on the surface of infected cells, which is conducive for HIV-1 immune evasion. This allows the virus to escape the immune system due to a decreased expression of HLA on the surface of the infected cell, but avoid NK-mediated lysis due to "self" antigens such as HLA-C still

being expressed in low quantities on the infected cell surface (Cohen et al., 1999). When abnormal HLA signalling is detected by the KIR receptors such as a decreased expression of a certain HLA class I antigen, NK cells will cause apoptosis of the targeted cell by degranulation of cytolytic granules (Metkar et al., 2002). KIR's are highly polymorphic amongst individuals, with 14 genes and 2 pseudogenes encoding for KIRs, classified according to whether they are inhibitory or activating, and named according to the number of extracellular domains they possess and the length of their cytoplasmic tails. The activation of NK cells is largely determined by the balance of activation or inhibitory signals (Marsh et al., 2003).

NK cells and their KIR proteins are an integral part of the innate immune response and therefore important in the early immune response against pathogens. It has been shown that NK cells and KIR affect the pathogenesis of HIV-1 and can even drive immune escape of HIV-1. Martin and colleagues described an interplay of KIR and HLA class I alleles that was associated with a delayed HIV-1 disease progression. The *KIR* allele, *KIR3DS1,* was shown to be protective when associated with the *HLA-B Bw4-80Ile* allele (codes for a HLA-B molecule with the bw4-associated serological epitope and an isoleucine at position 80) (Martin et al., 2002). A different study relating to the previously mentioned study from Martin and colleagues found that KIR3DS1+ NK cells strongly inhibit HIV-1 replication in HLA-B Bw4-80I+ CD4+ T-cells in an *in vitro* viral inhibition assay, with increasing doses of NK cells inhibiting HIV-1 replication (Alter et al., 2007). This research is further expanded upon in two studies looking at the various effects that combinations of differing *KIR3DL1* allotypes (based on cell-surface expression levels) and *HLA-Bw4* alleles have on HIV-1 disease progression, with *KIR3DL1*h* shown to enhance the protective qualities of the well described protective HLA class I allele *B*57* (Martin et al., 2007, Boulet et al., 2008) .

Copy number variation (CNV) of KIR genes has been found to affect HIV-1 replication. Utilising a genome wide study, 2,102 patients from Europe were analysed and it was shown that greater copy numbers of the *KIR3DL1* gene (when in the presence of *KIR3SL1*) results in lower viral set points and increased overall HIV-1 control (Pelak et al., 2011). The idea of CNV determining viral pathogenesis is further highlighted in a study which looked at CNV in SIV-infected rhesus macaques. The CNV of the macaque-specific *KIR* gene, *KIR3DH*, was analysed. It was found that in rhesus macaques with the MHC class I gene, *Mamu-A*01* and that express restrictive *TRIM5* alleles, peak viral loads were lower as compared to other test groups (Hellmann et al., 2012).

KIR-positive NK cells have also been shown to exhibit immune pressures on HIV-1 which can contribute to evolution and subsequent immune escape of HIV-1, with certain polymorphisms within HIV-1 proteins, such as in Vif and Vpu, being associated with certain KIR genes (Alter et al., 2011). These amino acid polymorphisms within HIV-1 proteins such as Vpu and Vpr, as described by Alter and colleagues, were shown to increase the association of inhibitory KIRs such as KIR2DL2 with HIV-1-infected CD4+ T-cells resulting in a decreased NK cell response against these infected cells (Alter et al., 2011). Recently this HIV-1 immune escape was shown once again in an untreated, large cohort from Southern Africa. Two sequence mutations in p24 Gag of HIV-1 subtype C virus were shown to associate with the combination of *KIR2DL3* and *HLA-C*03:04*. The KIR2DL3 protein was found to have improved binding to HLA-C*03:04 when the mutations in p24 Gag were present resulting in increased inhibitory signals of NK cells (Hölzemer et al., 2015).

1.1.6.3 Antibody responses and Vpu

Antibody responses occur against HIV-1 during the course of infection (Reviewed in Alter and Moody, 2010). Both neutralizing and non-neutralizing antibodies are generated initially against the Env protein, but less information is available for antibodies directed against the accessory proteins..

Reiss and colleagues, utilising an enzyme immunoassay and patient sera from a large patient cohort of men, described early on that antibodies are raised against Vpu at least within the first 12 months of seroconversion (Reiss et al., 1990b, Reiss et al., 1990a). Some years later a different team looked at progression to AIDS and its correlation with anti-Vpu antibody reactivity in 162 patients who were on antiretroviral therapy for 1 year. Interestingly, it was found that there was an association between an increased amount of anti-Vpu antibodies and a slower disease progression (Chen et al., 2003).

A study by Stratov and colleagues confirmed Wren and colleagues findings of anti-Vpu ADCC activity mentioned previously in section 1.1.3.3.4. Stratov and colleagues found that likely-ADCC responses were targeted against a specific motif of Vpu, namely the EMGHHAPWDV epitope (Stratov et al., 2008).

1.2 Rationale for study conducted, aims and objectives

It is clear that the accessory proteins Vif, Vpr and Vpu play a critical role in the pathogenesis of HIV-1 infection. It is also clear that immunogenetic factors can have implications for HIV-

1 infection. South Africa has the highest number of people living with HIV-1 infection worldwide (UNAIDS, 2014), and the predominant circulating HIV-1 subtype is C. There is limited data on viral escape in the context of Vif, Vpr and Vpu and host genotypes of HLA and KIR in our populations most affected by the HIV-1 epidemic. However, there is well described data available for our populations on the representation of HLA alleles (HLA-A, B, C) and HLA allotypes that bind KIR (*HLA-Bw4* allotype variants and HLA-C1 and C2), and for KIR genotypes (Paximadis et al., 2011, Tiemessen et al., 2011). Therefore, it is important to assess this viral-host axis with a focus on variation in the understudied accessory proteins Vif, Vpr and Vpu of HIV-1 subtype C.

Longitudinal plasma samples from two well characterized HIV-1 infected cohorts were available for the purposes of this study. The overall aim of the study was to describe immune escape in Vif, Vpr and Vpu epitopes from HIV-1 infected patients in South Africa. Additionally, preliminary data from the Tiemessen laboratory (unpublished) showed that Vpu was more highly targeted by CD8+ T cells in 14 LTNPs/elite controllers (about 50%), compared to other regulatory regions. Vpu is one of the least targeted HIV-1 proteins, accounting for approximately 10% in subtype C infection (Gray et al., 2009). Furthermore, five of the LTNPs/elite controllers studied had NK cell responses to HIV-1 Vpu peptide pools. As mentioned previously, these NK cell responses, measured in whole blood, have been shown to be mediated by HIV-specific ADCC antibodies (Stratov et al., 2008, Thobakgale et al., 2012), and 3 ADCC epitopes in Vpu were shown to be targeted in Australian LTNPs (n=65) but not in progressors (n=74) (Wren et al., 2013). Thus, based on preliminary data from our laboratory showing that Vpu was the most targeted by CD8+ CTLs and NK cell responses in LTNP patients than the other accessory regions, we cloned and expressed Vpu for the ultimate detection of anti-Vpu antibodies in patient sera from the different cohorts.

The objectives were therefore;

- To sequence the *vif*, *vpr* and *vpu* regions of longitudinal HIV-1 subtype C infected patient samples.
- To analyse HLA-A, B and C specific motifs for escape mutations in the HIV-1 *vif*, *vpr* and *vpu* sequences over time from each patient.
- To design and construct a Vpu mammalian expression vector and to express and purify recombinant Vpu protein.

Chapter 2

2.1 Methods

2.1.1 Patient cohorts used in this study

Plasma and peripheral blood mononuclear cell samples from two different patient cohorts were used for the purposes of this study. Ethical clearance was obtained for Research on Human subjects (Medical) at the University of the Witwatersrand (clearance number M160151; Appendix D).

2.1.1.1 Lung cohort

Samples were obtained from a study called the "Lung Cohort Study" (PI: R.E.Chaisson), the overall aim of which was to establish a clinical database and tissue repository from a clinical cohort of HIV-1 infected South Africans in Soweto (recruited by Dr N. Martinson), in order to longitudinally evaluate lung health. Approximately 750 HIV-1 infected adults were recruited from a period of 2008 to 2013. Baseline and 6-monthly follow up clinical data as well as HLA genotypes were available. For the purpose of this study patient samples were selected based on the following criteria: (i) Evidence of progressive infection (declining CD4 T cell count to <350 cells/µl prior to starting ART; 113 of the total patients had this profile), and (ii) possession of either *HLA-B*58:01* or *HLA-B*58:02* alleles. These *HLA-B* alleles are amongst the most prevalent in our black population and have been associated with viral load set points indicative of slower and more rapid disease progression, respectively (Paximadis et al., 2011, Kiepiela et al., 2004). Of the 113 individuals with progressive CD4 T cell decline, 18 had either of the *HLA-B* alleles (age range 25-47 years); 4 with *HLA-B*58:01* (all female) and 14 with *HLA-B*58:02* (3 male, 11 female). Studying these particular individuals therefore allowed for the evaluation of immune escape mutations in Vpr, Vif and Vpu of individuals with HLA genotypes that otherwise have opposing effects on disease progression, at a time when their clinical progression was comparable (CD4 T cell counts and viral loads at a time point prior to starting antiretroviral therapy were not significantly different; $P>0.05$, and known escape mutations and compensatory mutations in the Gag protein of HIV-1 associated with loss of HIV-1 control in *HLA-B*58:01* have already occurred (Shayne Loubser, unpublished data).

The Lung cohort patient samples used in this study consisted of n=44 longitudinal samples obtained at 6 month intervals from the 18 above mentioned patients.

2.1.1.2 M002 cohort

"M002 cohort" samples were from a subset of high risk antiretroviral drug naïve HIV-1 infected women from the Carletonville area in South Africa collected between 2007 to 2010, and, for the purposes of this study, were selected based on availability of longitudinal plasma samples over a period of 24 months, and had viral loads greater than 10,000 RNA copies/ml at baseline. The original study proposal for the cohort described the women as "…someone who lives in the high transmission areas of the Carletonville District, where the source of income is sex and alcohol. These women have more than one sexual partner and exchange sex for money and/or gifts". There was no significant difference in CD4+ T cell count or viral load between baseline and 18 months in the group of 7 individuals studied (Wilcoxon Rank sums test, $P>0.05$; no viral load was available at 24 months).

The M002 cohort patient samples used in this study consisted of n=28 longitudinal samples obtained at six month intervals from seven patients. The HLA types were unknown (determined during the course of this study).

2.1.2 Extraction, RT-PCR Amplification and Sequencing of HIV-1 *vif, vpr* and *vpu*

Viral RNA was extracted from patient plasma and the *vif, vpr* and *vpu* regions were reverse transcribed and subsequently sequenced.

2.1.2.1 Extraction

Viral RNA was extracted from patient plasma samples utilizing the NucliSENS easyMAG RNA extractor (bioMérieux, France). Briefly, 500 µl of patient plasma was added to 8 well NucliSENS easyMAG disposable cartridges (bioMérieux, France). Following lysis in the RNA extractor, 50 µl of NucliSENS easyMAG magnetic silica beads (bioMérieux, France) were added to each lysed sample and re-suspended. Standard protocol procedures were followed on the NucliSENS easyMAG RNA extractor to extract the viral RNA and RNA was eluted in a final volume of 25 µl.

2.1.2.2 RT-PCR of extracted HIV-1 RNA samples

A 1.6 kb DNA fragment was reverse transcription polymerase chain reaction (RT-PCR) amplified from extracted viral RNA samples which contain the *vif, vpr* and *vpu* genes.

The first round of PCR involved RT-PCR with the Superscript III One step RT-PCR system (Thermo Fisher Scientific, USA). The outer primers (Integrated DNA technologies (IDT), USA) used were Cath1F (5'-GAC AGC AGT ACA AAT GGC AG-3') and Cath2R (5'-GGG

TCT GTG GGT ACA CAG GC-3'). PCR reaction mixes for a single reaction for the RT-PCR were 12.5 µl of 2 × reaction mix, 0.5 µl each of Cath1F and Cath2R primers (at 10 µM), 9 µl of extracted viral RNA, 1.5 µl of 5 mM $MgSO_4$, 0.5 µl of Superscript III reverse transcriptase and 0.5 µl of high quality sterile water, for a total reaction volume of 25 µl.

RT-PCR mixes were placed in the GeneAmp PCR System 2700 (Applied Biosystems, USA) and the following conditions were used; cDNA synthesis at 50ºC for 60 min, initiation at 94ºC for 2 min, followed by 35 cycles of denaturation at 94ºC for 2 min, annealing at 51ºC for 30 s and elongation at 68ºC for 2 min 30 s. Second elongation was 68ºC for 10 min followed by a 4ºC hold.

2.1.2.3 Nested PCR of RT-PCR products

A nested PCR step was done utilizing the 1.6 kb cDNA fragments from the RT-PCR step. Primers from IDT were used and the protocol was as follows:

The nested PCR was conducted utilizing the Platinum Taq DNA Polymerase High Fidelity PCR kit (Thermo Fisher Scientific, USA). The inner primers used for this nested PCR were Cath3F (5'-GGG GTA CAG TGC AGG GGA AAG-3') and Cath4R (5'-GTA CCC CAT AAT AGA CTG TGA CC-3'). PCR reaction mixes for a single reaction for the nested PCR were 0.2 µl of Platinum Taq High Fidelity Polymerase, 1 µl of 10 × High Fidelity PCR buffer, 2 µl of 50 mM $MgSO_4$, 1 µl each of Cath3F and Cath4R (10 µM), 5 µl of cDNA (1.6 kb DNA fragments from RT-PCR step), and 34.8 µl of high quality sterile water; for a total reaction volume of 50 µl.

Nested PCR mixes were placed in the GeneAmp PCR System 2700 for PCR amplification and the following conditions were used; initiation at 94ºC for 2 min, followed by 35 cycles of denaturation at 94ºC for 30 s, annealing at 51ºC for 30 s and elongation at 68ºC for 1 min 30 s. Second elongation was 68ºC for 10 min followed by a 4ºC hold.

Following PCR amplification, PCR products were run on a 1% agarose gel (Appendix A) and visualized under UV trans-illumination. The PCR products were purified in preparation for sequencing utilizing the GeneJet Purification Kit (Thermo Scientific Fisher, USA) and according to the manufacturers protocol (Appendix C).

2.1.2.4 Cycle sequencing of PCR products, Ethanol/EDTA precipitation and genetic analysis

Cycle sequencing of purified *vif, vpr* and *vpu* PCR products was conducted utilising primers (IDT, USA) spanning the ~1.3-kb PCR fragments in both directions. The primers were CBF1 (5'- GAC TAT GGA AAA CAG ATG GC -3'), CBF2 (5'- TGG CAT TTG GGT CAT GGA GTC -3'), CBF3 (5'- ATC TAT GAA ACC TAT GGG GAT AC -3'), CBF4 (5'- ATA GCA ATA GTT GTG TGG -3'), CBR1 (5'- ATG GGA TGT GTA CTT CTG AAC -3'), CBR2 (5'- TCT GGG GCT TGT TCC ATC TAT C -3'), CBR3 (5'- TGC CAT AGG AAA TGC CTA AGC -3') and CBR4 (5'- ATA GAC TGT GAC CCA CAA G -3') . The protocol used was as follows:

The BigDye Terminator v3.1 Cycle Sequencing Kit (Applied Biosystems, USA) was utilized for cycle sequencing reactions and all reactions were performed on 96-well plates. A single cycle sequencing reaction in one well consisted of 1 µl Big Dye Terminator 3.1, 2 µl of 5 × Big Dye Buffer, 5 µl of high quality sterile water, 1 µl of a specific sequencing primer (CBF1, CBF2, CBF3, CBF4, CBR1, CBR2, CBR3 or CBR4 at 3.2 pmol/µl) and 11 µl of diluted PCR product (1:9 dilution in sterile water) for a total reaction volume of 20 µl.

Plates were briefly vortexed and centrifuged and placed in the GeneAmp PCR System 2700 for thermal cycling with the following cycling conditions; initiation at 96ºC for 1 min, followed by 35 cycles of denaturation at 96ºC for 10 s, annealing at 50ºC for 5 s and elongation at 60ºC for 4 min. Second elongation was 72ºC for 10 min followed by a 4ºC hold.

Following thermal cycling, plates were removed and samples purified utilizing an ethanol/EDTA precipitation protocol as follows:

To each well, 5 µl of 125 mM EDTA was added followed by 60 µl of 100% ethanol. The 96 well plates were covered with a rubber membrane and inverted 4 times. Plates were then incubated at room temperature for 15 min. Following incubation the plates were centrifuged at 3000 × g for 30 min. Immediately following centrifugation, the plates were inverted onto disposable paper toweling and centrifuged up to 185 × g and then removed. Following centrifugation, 60 µl of 70% ethanol was added to each well and the plates were centrifuged once again at 1650 × g for 15 min at 4ºC. The plate was inverted onto paper towelling once more and spun up to 185 × g for 1 min. The plates were then briefly left to dry in the dark.

To each reaction well, 12 µl of HiDi Formamide (Thermo Scientific Fisher, USA) was added, and plates were vortexed and centrifuged briefly. Reaction plates were incubated in the GeneAmp PCR System 2700 at 90ºC for 2 min. Plates were cooled at room temperature and subsequently loaded into the 3730xl automated genetic analyzer (Applied Biosystems, USA).

2.1.2.5 Bioinformatic analyses

Generated sequences were analysed and manipulated utilising Sequencher version 5.1 sequence analysis software (Gene Codes Corporation, USA) and GeneDoc Multiple Sequence Alignment Editor (Karl Nicholas, USA). Sequences were aligned using Clustal X (Conway Institute UCD, Republic of Ireland).

2.1.3 PCR Amplification and Sequencing of HLA class I Loci

M002 cohort samples did not have any HLA typing performed on the patient samples. HLA class I genotyping was subsequently done utilising the SBT Resolver HLA kit (Conexio Genomics, Australia) as follows:

2.1.3.1 PCR and agarose gel electrophoresis

High molecular weight genomic DNA obtained from patient samples of the M002 cohort were available, and analyzed using a NanoDrop 2000 UV-Vis Spectrophotometer (Thermo Scientific Fisher, USA) for $OD_{260/280}$>1.8 and concentration range of 20-100 ng/µl. Separate PCR reactions were set up for each HLA locus to be amplified and each individual sample to be tested. PCR reaction master mixes were prepared utilising 16 µl each of proprietary locus-specific PCR mixes (HLA A, B and C) (Conexio Genomics, Australia) and 1 µl of GoTaq Hot Start Polymerase (Promega, USA). Seventeen micro litres of the master mix was dispensed into each reaction well along with 3 µl of sample DNA. Reaction wells were vortexed and centrifuged briefly, and reaction wells were placed into the Geneamp PCR System 9700 (Applied Biosystems, USA). Thermal cycling conditions were as follows; initiation at 95ºC for 10 min, followed by 33 cycles of denaturation at 96ºC for 20 s, annealing at 60ºC for 30 s and elongation at 72ºC for 3 min followed by a 4ºC hold.

Confirmation of amplification of sample reactions was done by loading 2 µl of PCR product with 5 µl of loading buffer on a 1% agarose gel (Appendix A) for electrophoresis, and visualized under UV trans-illumination.

PCR products were purified before cycle sequencing utilising the Agencourt AMPure XP magnetic bead purification kit according to manufacturer's instructions (Beckman Coulter, USA) (Appendix C).

2.1.3.2 Sequencing Reaction

Cycle sequencing of PCR products from patient samples utilised proprietary primers derived from the SBT Resolver HLA kit and were as follows; for HLA-A sequencing they were AEX1F, AEX1R, AEX2F, AEX2R, AEX3F, AEX3R, AEX4F, AEX4R; for HLA-B they were BEX1F, BEX2F, BEX2R, BEX3F, BEX3R, BEX4F; and for HLA-C they were CEX1F, CEX1R, CEX2F, CEX2R, CEX3F, CEX3R, CEX4F, CEX4R, CEX5F, CEX5R, CEX6F, CEX6R and CEX7F.

Sequencing primer mix was prepared utilising 2 µl of sequencing primer (concentration not provided), 11.5 µl of high quality sterile water, 1 µl of BigDye Terminator v3.1 Ready Reaction Mix (Applied Biosystems, USA) and 5 × Sequencing Reaction Buffer (Applied Biosystems, USA) per sample. Total reaction mix (18 µl per sample) was loaded into each appropriate reaction well and 2 µl of purified PCR product was then added accordingly. Reaction wells were sealed, mixed and centrifuged briefly and then loaded into the GeneaAmp PCR System 9700. Thermal cycling conditions were as follows; initiation at 95ºC for 10 min, followed by 33 cycles of denaturation at 96ºC for 10 s, annealing at 50ºC for 5 s and elongation at 60ºC for 2 min followed by a 4ºC hold.

2.1.3.3 Purification of Sequencing Reaction Products and denaturation for capillary electrophoresis

Reaction wells were centrifuged briefly to ensure contents were all at the bottom of reaction wells. To each well, 5 µl of 125 mM EDTA (pH 8.0) was added. Sixty microlitres of 100% ethanol was then added to each reaction well and the wells were vortexed briefly. The sample reactions were centrifuged at 2000 × g for 45 minutes. Immediately after centrifugation the supernatant was discarded by inverting reaction plates onto paper towelling. The inverted plates were then centrifuged at 350 g for 1 minute to remove residual supernatant. Sixty microlitres of 80% ethanol was then added to each reaction well and vortexed briefly. Samples were once again centrifuged at 2000 × g for 5 minutes. Sample plates were then inverted onto paper towelling once again and centrifuged at 350 g for 1 minute. Samples were resealed and stored in the dark at – 20ºC until required (not longer than 24 hours).

To each reaction well 12 µl of HiDi Formamide (Thermo Scientific Fisher, USA) was added, and plates were vortexed and centrifuged briefly. Reaction plates were incubated in GeneAmp PCR System 9700 at 98ºC for 5 min. Plates were cooled at room temperature and subsequently loaded into the ABI 3100 automated genetic analyzer (Applied Biosystems, USA).

2.1.3.4 Designation of HLA genotype

HLA sequencing data from patients was analysed utilising the Assign SBT Sequence Analysis Software made specifically for use with the SBT Resolver HLA kit (Conexio, Australia). Analysis was done in conjunction with a study by Paximadis and colleagues utilised as a reference for the most common alleles in the South African population (Paximadis et al., 2011).

2.1.3.5 HLA class I motif scan

Vif, Vpr and Vpu amino acid sequences obtained from patients from the Lung and M002 cohorts following genomic sequencing and bioinformatics analysis were analyzed utilizing the Los Alamos HIV HLA Anchor Residue Motifs Online Scanner (Los Alamos, USA). The scanner allows for detection of HLA anchor residue motifs within protein sequences for specified HLA genotypes. The motif scanner uses various sources from which it finds motifs such as the SYFPEITHI Database of MHC Ligands available at http://www.syfpeithi.de/. Motifs of 9 amino acids are stored within the database by default but residues of lengths 8, 10 and 11 are computed in real time.

2.1.4 Expression and purification of recombinant Vpu protein

2.1.4.1 Design of Vpu expressing recombinant plasmids

We have previously described the genotypic characterisation of *vif, vpr* and *vpu* from 20 primary HIV-1 isolates available in our laboratory (Bell et al., 2007). The Vpu N-terminal domain of seventeen of the twenty isolates had a 5 amino acid insertion, while one isolate (05ZAFV15) had one amino acid insertion. Three different *vpu* sequences were thus selected (consensus of subtype C (Cons. C), 05ZAFV5 and 05ZAFV15), codon optimized for mammalian expression, synthesized by GeneArt (Thermo Scientific Fisher, Germany), and cloned into the pcDNA3.1/V5-His plasmid vector containing a 6 × polyhistidine-tag (Invitrogen, USA).

2.1.4.2 Transformation of recombinant plasmids into chemically competent Escherichia (E.) coli DH5a for plasmid preparation

The plasmid vectors containing the three different *vpu* sequences were diluted in 50 µl of high quality sterile water each to a concentration of 0,1 µg/µl. From these stocks, chemically competent *E. coli* DH5α (Appendix A) were transformed with these plasmids utilising standard protocols. Briefly, 1 µl of plasmid DNA was added to 30 µl aliquots of chemically competent *E .coli* DH5α cells. Samples were incubated on ice for 20 minutes and then heat shocked for 2 minutes at 42°C. Samples were then incubated on ice for a further 2-5 minutes, and 10 µl of each construct-transformed cell sample was plated on lysogeny broth (LB) ampicillin-positive (Appendix A) agar plates and incubated overnight at 37°C.

2.1.4.3 Plasmid preparations

One colony from each overnight plate (mentioned previously) was picked and inoculated into 100 ml of ampicillin positive LB medium (Appendix A) in 500 ml sterile flasks. Samples were incubated overnight in a shaking incubator at 37°C. A plasmid extraction was then conducted on the samples utilising a plasmid midi preparation kit (Qiagen, USA) according to manufacturer's instructions (Appendix C). Spectrophotometry and agarose gel (1% agarose, Appendix A) electrophoresis was utilised to assess plasmid concentration and purity. DNA bands were visualised under UV trans-illumination and samples were stored at -20°C until required.

2.1.4.4 Restriction enzyme digests

In order to confirm the identity of the purified *vpu*-containing plasmids a restriction enzyme digest was conducted. Single and double enzyme digests were conducted as follows; for the single digest reactions consisted of 1 µg of plasmid DNA, 1 µl of *BglII,* 2 µl of 10 × FastDigest buffer (Thermo Scientific Fisher, USA) all topped up to 20 µl with high quality sterile water. Double digests consisted of 1 µg of plasmid DNA, 1 µl each of *HindIII/XhoI,* 2 µl of 10 × FastDigest buffer all topped up to 20 µl with high quality sterile water. Two hundred nanograms of restriction digest product was loaded onto a 1% agarose gel for electrophoresis. DNA bands were visualised under UV trans-illumination.

2.1.4.5 Recombinant Vpu protein expression

2.1.4.5.1 Mammalian Cell culture

Various mammalian cell lines, Human Embryonic Kidney (HEK) 293 cells and their derivatives HEK 293T and HEK 293F (available in our laboratory), were maintained and

utilised throughout the duration of recombinant Vpu protein expression experiments. All cell counts were performed utilizing the Countess II FL Automated Cell Counter (Life Technologies, USA).

HEK 293 and 293T cells are adherent and were maintained in T25 cm^2 flasks (Nunc, Denmark) in 10 ml of Dulbecco's Modified Eagle's Medium (DMEM) (Sigma-Aldrich, USA with added 10% bovine serum albumin and 100 × Glutamax (Life Technologies, USA)), and subcultured every 3-4 days or at 90% cell confluency. Briefly, to subculture the cells, depleted DMEM was poured off and cells were gently washed with 5 ml of 1 × phosphate buffered saline (PBS) (Sigma-Aldrich, USA). Two millilitres of Trypsin-EDTA (0,25%) (Thermo Fisher Scientific, USA) was added to the flasks to detach cells; after 30 seconds Trypsin-EDTA was poured off and the cells were incubated at 37°C for 2 minutes. Cells were then re-suspended in DMEM and split 1:10.

HEK 293F cells are suspension cells and were maintained in 125 ml Erlenmeyer Flasks (Corning, USA). Cells were subcultured at 0.1-0.2 × 10^6 viable cells/ml per flask in a volume of 25 ml of Freestyle 293 Expression Media (Life Technologies, USA) and allowed to grow to a cell density of 3 × 10^6 cells/ml before subculturing.

2.1.4.5.2 Optimization of Transfection

Various cell lines (HEK 293, 293T and 293F), cell counts, and transfection reagents were tested in order to find optimal conditions for highest transfection efficiency before up-scaling expression of recombinant Vpu proteins.

First rounds of transfections involved testing of different transfection reagents, polyethylenimine (PEI, Polysciences, USA) and jetPrime (Polyplus-transfection SA, France), and the two adherent HEK cell lines, 293 and 293T. Cells were transfected with a Green Fluorescent Protein (GFP) control construct (available in our laboratory), in order to give a visual indication of the transfection efficiency of the reagents tested.

Manufacturer's protocols were followed for both reagents. The day before transfection 350 000 or 450 000 HEK 293 or 293T cells were seeded per well of a 6 well plate (Nunc, Denmark) so that on the day of transfection cell confluency would be between 60-90%.

For jetPrime transfections a 1:2 DNA to jetPrime reagent ratio was used; 2 µg of DNA was mixed with 200 µl of jetPrime buffer and briefly vortexed and spun down. Four microlitres of jetPrime was added, vortexed and spun down once again and the transfection mix was added

to a well. For PEI transfections a 1:3 DNA to PEI reagent ratio was used; 9 µg of PEI was added to a total volume of 150 µl of Opti-MEM (Life Technologies, USA). Three micrograms of DNA was added to a total volume of 150 µl of Opti-MEM. Diluted PEI and DNA were added together and incubated at room temperature for 30 min. Transfection mix was then added to each well. After addition of transfection mixes to the 6 well plates, they were incubated at 37°C with 5% CO_2 for 48 hours.

Second rounds of transfection optimization experiments involved testing transfection and expression of the actual Vpu protein constructs, testing of additional transfection reagents such as 293Fectin (Thermo Fisher Scientific, USA), Fugene HD Transfection Reagent (Promega, USA), Lipofectamine 2000 (Thermo Fisher Scientific, USA), Lipofectamine XTL (Thermo Fisher Scientific, USA), Polyfect (Qiagen, Germany) and an additional HEK cell line, 293F.

Six well plates were prepared with 293 and 293T cells the day before transfection and transfection protocols for PEI and jetPrime were followed as previously mentioned, with the addition of 293Fectin transfections. The 293Fectin transfections utilised a 1:2 DNA to 293Fectin reagent ratio; 5 µg of DNA was diluted in Opti-MEM to a total volume of 250 µl. Fifteen microlitres of 293Fectin was diluted in Opti-MEM to a volume of 250 µl. After a 5 minute incubation, diluted DNA and 293Fectin was added together and incubated at room temperature for 20-30 minutes. Transfection mix was added to a well and the 6 well plate was incubated at 37°C with 5% CO_2 for 48 hours.

For the Fugene HD, Lipofectamine 2000, Lipofectamine XTL and Polyfect transfections a 24 well plate was set up the day before seeded with 100 000 HEK 293T cells per well in 500 µl of DMEM for a confluency on day of transfection of 90%. The various Vpu constructs or a two-domain CD4 construct (2dCD4) used as a positive control (available in our laboratory) were transfected into HEK 293T cells.

For Fugene HD transfections a 1:3 ratio of DNA to transfection reagent was utilised; 1.1 µg of DNA was diluted in Opti-MEM to a volume of 52 µl. To the diluted DNA 3.3 µl of Fugene HD was added and mixture pipetted 15 times. The transfection mix was incubated for 10 minutes at room temperature before adding 25 µl to each well of a 24 well plate. The plates were incubated at 37°C with 5% CO_2 for 48 hours.

For Lipofectamine XTL and 2000 transfections a 1:2.4 ratio of DNA to transfection reagent was utilised with each reaction mix enough for a duplicate transfection of two wells of a 24 well plate; 3 µl of Lipofectamine XTL or 2000 was added to 50 µl of Opti-MEM. To 62.5 µl of Opti-MEM 1.25 µg of DNA was added, and both DNA and transfection reagent mixtures were added together and incubated at room temperature for 5 minutes. To each well of a 24 well plate 50 µl of the transfection mix was added. The plates were incubated at 37°C with 5% CO_2 for 48 hours.

For Polyfect transfections a 1:10 ratio of DNA to transfection reagent was utilised with each reaction mix enough for a duplicate transfection of two wells of a 24 well plate; 0.8 µg of DNA was added to 40 µl of Opti-MEM, mixed and spun down. To this DNA solution 8 µl of Polyfect reagent was added and pipetted up and down 5 times. The transfection mix was incubated at room temperature for 10 minutes and then 120 µl of cell growth media was added to the reaction and mixed together. The mix was split in half and added to each well of a 24 well plate. The plates were incubated at 37°C with 5% CO_2 for 48 hours.

Transfection and expression of Vpu proteins was also tested in suspension culture using HEK 293F cells. Thirty millilitres of Freestyle 293 Expression Media was seeded at 6-7 × 10^5 cells/ml the day before transfections for a final transfection cell density of 1 × 10^6 cells/ml on day of transfection. Transfection protocols for PEI, 293Fectin, jetPrime and Lipofectamine 2000 were used as previously mentioned and scaled up accordingly, and to manufacturers recommendations.

2.1.4.5.3 Establishment of stable cell line

Stably transfected cell lines were established for each of the three Vpu constructs and the 2dCD4 control construct. Briefly, HEK 293F cells were seeded in T75 cm^2 flasks (Nunc, Denmark) at 1 x 10^6 cells per flask with 10 ml of Freestyle 293 Expression Media. JetPrime transfection reagent was utilised for transfection of the Vpu constructs and 2dCD4 control construct utilising previously described protocols and scaled accordingly to manufacturers recommendations. Cells were incubated at 37°C with 5% CO_2 for 48 hours. Following 48 hours post-transfection the antibiotic G418 (Sigma-Aldrich, USA) at a concentration of 50 mg/ml was introduced to transfected cells for a final concentration of 350 µg/ml, and this was added twice weekly. Cells were observed for 2 to 3 weeks and maintained weekly with fresh Freestyle 293 Expression Media and incubated at 37°C with 5% CO_2, until antibiotic resistant colonies began to form. Samples for Western blot analysis were taken after 3 weeks to check for stable

expression of transfected constructs. Following confirmation of stable cell line establishment, stably transfected HEK 293F cells were expanded into 250 ml and 500 ml Erlenmeyer flasks as needed in 1/5th the flask volume of Freestyle 293 Expression Media containing G418 (final concentration of 350 μg/ml), at 0.5 x 10^6 cells/ml and grown to 3 x 10^6 cells/ml before subculturing.

2.1.4.5.4 Protein purification

Cells were harvested forty eight hours post-transient transfections of HEK293T, or when confluent for the stably transfected 293F cells and processed utilizing a Ni^{2+}-affinity chromatography protocol to purify the various 6 × polyhistidine-tagged recombinant Vpu proteins. The purification protocol was adapted from Lv and colleagues who also expressed and purified a 6 × polyhistidine-tagged Vpu protein (Lv et al., 2013).

HEK 293T cells were harvested in 1 × PBS and pelleted at 800 × g for 10 min, and HEK 293F cells were pelleted straight from their expression media at 800 × g for 10 min. The remainder of the purification protocol applies to both 293F and 293T cells. Following centrifugation, the cell pellet was re-suspended in cell lysis buffer (Appendix B) equating to 1/10th of the original media volume along with 25 × cOmplete protease inhibitor cocktail (Roche, Switzerland). The cell lysate was sonicated on ice three times for 30 s each round with an amplitude of 80%, pulse on of 1 s and pulse off of 0.5 s (Sonoplus, Germany). Following sonication, samples were centrifuged at 16 000 × g for 30 min at 4°C. The soluble cellular fraction was then added to 1 ml of agarose resin prepared with $NiSO_4$ (Appendix B) and left to stir gently overnight at 4°C.

A purification protocol was then followed utilising standard nickel affinity chromatography procedures as follows: the prepared agarose resin that was left binding overnight to the His-tagged Vpu proteins of the cellular soluble fractions was harvested by centrifugation at 1800 × g for 3 min. Following collection of the agarose resin, a series of washes was conducted by centrifugation at 1800 × g for 2 minutes at 4°C utilising imidazole-containing wash buffers (Appendix B). Washes were done at 10 bed volumes and once for each increasing imidazole concentration (10, 20, 35 and 50mM), or optimised as required. The protein was eluted with 10 bed volumes of wash buffer containing 500 mM imidazole and concentrated using Centricon Ultra Filtration Tubes NMWL-10 KDa (Millipore, USA). The purified protein was aliquoted, snap frozen with liquid nitrogen and stored at -80°C.

2.1.4.5.5 SDS-PAGE and Western blot

For analysis of recombinant Vpu protein expression and optimisation, Sodium dodecyl sulphate polyacrylamide gel electrophoresis (SDS-PAGE) and Western blotting techniques were utilized.

Fifty microlitre samples from different stages of the expression and purification steps of recombinant Vpu proteins were collected and analysed. SDS-PAGE monomer concentrations used were either 12.5% or 15% depending on desired resolution (Appendix B). After resolving an SDS-PAGE gel, Western blots were conducted by stacking a gel between 6 pieces of blotting paper and a poly-C nitrocellulose membrane (Amersham Bio Sciences, England) that was briefly soaked in Western blot transfer buffer (Appendix B), and then run for 30 min at 15 V in a Trans Blot SD Semi Dry transfer cell (BioRad, USA). The nitrocellulose membrane was washed twice for 5 minutes each time in 1 × Tween-Tris Buffered Saline (T-TBS, Appendix B) and then blocked for 1 hour (or overnight at 4°C) in 1 × T-TBS containing 10 mg/ml of bovine serum albumin (BSA, Sigma-Aldrich, USA). The membrane was then washed twice again in 1 × T-TBS and then probed for 45 min with a Penta·His Horse Radish Peroxidase (HRP) Conjugate antibody (Qiagen, USA) diluted 1:2000 in a Penta·His specific blocking reagent (Qiagen, USA). Following probing, the membrane was washed three times for 10 minutes each in 1 × T-TBS. SuperSignal West Femto Maximum Sensitivity Substrate (Thermo Scientific,USA) reagents in a 1:1 volume ratio was added to the membrane. Luminescence was visualized under a photographic hood on Chemi-Hi Sensitivity mode (BioRad, USA).

2.1.4.6 Dot blot and Western blot analysis

Dot blot and Western blot analysis were conducted in order to set up a proof-of-concept for detection of anti-Vpu antibodies in HIV-1 infected patient sera.

The Schleicher & Schuell Minifold II slot-blotter (GE Healthcare, UK) was assembled as per manufacturer's instructions with blotting paper pre-soaked in 1 × TBS (Appendix B) and a single piece of 1 × TBS pre-soaked poly-C nitrocellulose membrane cut to apparatus size. Dot blot mixes were made up for each protein to be suspended on the poly-C nitrocellulose membrane and these included a one domain CD4 (1dCD4) positive control, purified 2dCD4, purified recombinant Vpu proteins and a DMEM control. Reaction mixes consisted of 5 µl of each protein of interest diluted in 95 µl of 1 × TBS for a total of 100 µl to be loaded per well per dot blot. The 1dCD4 protein was diluted to a known concentration of 1 ng/µl in 1 × TBS

and 100 µl containing 100 ng of 1dCD4 was loaded per well per dot blot. Samples were loaded and spotted onto poly-C nitrocellulose membrane. Membrane strips were cut and blocked overnight in 1 × T-TBS containing 0.05mg/ml of fat-free milk powder (BioRad, USA). The membrane strips were each washed twice in 1 × T-TBS and then probed for 45 min with either the Penta·His HRP Conjugate antibody previously mentioned and diluted 1:2000, Anti-Vpu Rabbit Antiserum against subtype C Vpu (NIH AIDS Reagent Program, USA) diluted 1:5000, Anti-HIV-1 NL4-3 Vpu Polyclonal Rabbit Antiserum (NIH AIDS Reagent Program, USA) diluted 1:5000 or HIV-1-negative Human Sera (Sigma-Aldrich, USA) diluted 1:5000.

Following probing, the Penta·His HRP Conjugate antibody-probed membrane was washed three times for 10 minutes each in 1 × T-TBS. SuperSignal West Femto Maximum Sensitivity Substrate (Thermo Scientific, USA) reagents in a 1:1 volume ratio was added to the membrane.

The membranes probed with the Anti-Vpu Rabbit Antiserum against subtype C Vpu and Anti-HIV-1 NL4-3 Vpu Polyclonal Rabbit Antiserum were then washed twice each in 1 × T-TBS, and each membrane was then probed by an anti-rabbit Amersham ECL HRP Conjugated Antibody (GE Healthcare, UK) in a 1:5000 dilution for 45 minutes. Following this second probing step, the membranes were washed three times for 10 minutes each in 1 × T-TBS. SuperSignal West Femto Maximum Sensitivity Substrate (Thermo Scientific, USA) reagents in a 1:1 volume ratio were added to the membrane.

Additonally, the membrane probed with the HIV-1-negative Human Sera was washed twice in 1 × T-TBS, and then probed by an anti-human Amersham ECL HRP Conjugated Antibody (GE Healthcare, UK) in a 1:5000 dilution for 45 minutes. Following this second probing step, the membrane was washed three times for 10 minutes each in 1 × T-TBS. SuperSignal West Femto Maximum Sensitivity Substrate (Thermo Scientific, USA) reagents in a 1:1 volume ratio were added to the membrane.

Luminescence for all blots was visualized under a photographic hood on Chemi-Hi Sensitivity mode (BioRad, USA).

Western blots were conducted in conjunction with dot blots utilising 20 µl samples of the 1dCD4 positive control, purified 2dCD4, purified Vpu proteins, and utilizing 15% SDS-

PAGE monomer concentrations. Western blots were conducted and the antibody probing procedure followed that of the previously described dot blot probing procedures.

Chapter 3

3.1 Results

3.1.1 Clinical and demographic data of patients used

Lung and M002 cohorts and their CD4+ T cell counts and viral loads taken longitudinally (at six month intervals) are shown in **Table 3.1** and **Table 3.2**, respectively. CD4 T cell counts were all <500 cells/mm^3 for the Lung and M002 cohort patients, with the exception of one patient (M002-423) that was able to maintain a CD4+ T cell count of over 500 cells/mm^3 over time. Nine of the Lung cohort patients were initiated on antiretroviral drug therapy during the course of the trial, and the time of initiation is shown in blue numerical values in the viral load column of **Table 3.1**. For six of the nine Lung cohort patients on treatment, viral loads were <50 RNA copies/ml, two were <500 RNA copies/ml, whereas one patient (170246) did not control viral replication. The Lung cohort age range had a median of 37.5 years while the median CD4 T cell count at commencement of the study was 246 cells/mm^3. The M002 cohort ages were unavailable while the median CD4 T cell count at commencement of the study was 343 cells/mm^3. Overall, 44 Lung cohort and 28 M002 longitudinal samples were available for analysis.

Lung cohort HLA genotypes were available at commencement of this author's study, including typing for both alleles of HLA A, B and C (**Table 3.1**). M002 patient HLA data were not available and subsequently M002 HLA genotyping was conducted. The HLA background (HLA-A, -B and -C) of the seven patients in the M002 cohort were all successfully determined, and are shown in **Table 3.2**. When interpreting the genotyping results, alleles were assigned based on how common they were in the South African population according to Paximadis and colleagues (Paximadis et al., 2011).

Table 3.1: Clinical data of Lung cohort patient samples used in this study. Red highlighted cells in the viral load columns indicate patient samples that could not be RT-PCR amplified and blue letters indicate patient was initiated on antiretroviral therapy.

Patient ID	Gender	Age (in years)	CD4 T cell counts (cells/mm^3)			Viral Load (RNA copies/ml)			Human Leukocyte Antigen (HLA) Genotype						Longitudinal samples available	Longitudional Samples Sequenced
			BASELINE	6 MONTHS	12 MONTHS	BASELINE	6 MONTHS	12 MONTHS	HLA-A, ALLELE 1	HLA-A, ALLELE 2	HLA-B, ALLELE 1	HLA-B, ALLELE 2	HLA-C, ALLELE 1	HLA-C, ALLELE 2		
LC170005	M	36	208	165	122	14652	9871	459	02:01:01G	66:01:01G	15:03:01G	58:02:00	04:01:01G	06:02:01G	2	2
LC 170007	F	38	254	286	222	5867	23963	10246	02:05:01G	30:02:01G	45:01:01G	58:02:00	06:02:01G	16:01:01	3	3
LC 170093	F	40	268	NA	243	30038	NA	67829	23:01:01G	68:01:01G	44:03:02	58:02:00	06:02:01G	07:01:01G	3	2
LC 170204	F	37	252	156	421	7045	2611	49	03:01:01G	68:01:01G	45:01:01G	58:02:00	06:02:01G	16:01:01	2	0
LC 170225	F	41	241	203	200	5055	11813	10442	02:05:01G	30:02:01G	08:01:01G	58:01:01G	07:01:01G	07:01:01G	2	2
LC 170246	F	45	259	47	32	532	481473	209138	23:01:01G	29:02:01G	44:03:02	58:02:00	06:02:01G	07:01:01G	2	1
LC 170274	F	37	226	154	449	6963	19760	49	68:01:01G	68:02:01G	15:10:01	58:02:00	03:04:02	06:02:01G	2	1
LC 170284	F	38	154	134	295	29023	21389	49	02:05:01G	29:02:01G	15:03:01G	58:01:01G	02:10	07:01:01G	2	2
LC 170294	F	47	243	162	270	10872	10321	49	03:01:01G	30:02:01G	39:10:00	58:02:00	06:02:01G	12:03:01G	2	1
LC 170328	M	40	NA	6	3	NA	127803	196678	03:01:01G	36:01:00	53:01:01	58:02:00	04:01:01G	06:02:01G	3	3
LC 170360	F	34	239	133	144	49344	7889	82	29:02:01G	66:01:01G	58:01:01G	58:01:01G	02:10	03:02:01G	2	0
LC 170423	F	42	324	178	253	8688	49	139	02:01:01G	66:01:01G	53:01:01	58:02:00	04:01:01G	06:02:01G	3	0
LC 170430	M	36	246	216	91	16890	7063	4575	29:02:01G	30:02:01G	44:03:02	58:02:00	06:02:01G	07:01:01G	3	0
LC 170472	F	25	245	273	157	85150	250823	119792	29:02:01G	80:01:00	44:03:02	58:02:00	06:02:01G	07:01:01G	3	2
LC 170553	F	32	207	191	200	1231	2476	5330	30:01:01G	30:02:01G	42:01:01	58:02:00	06:02:01G	17:01:01G	3	0
LC 170562	F	34	273	310	258	881	728	833	02:01:01G	68:02:01G	15:10:01	58:01:01G	03:02:01G	08:04	2	0
LC 170700	F	43	307	247	246	255	1255	3228	02:05:01G	23:01:01G	15:10:01	58:01:01G	07:01:01G	16:01:01	3	2
LC 170755	F	37	351	299	382	206	979	49	02:01:01G	68:01:01G	42:01:01	58:02:00	06:02:01G	17:01:01G	2	0
															Total=44	Total=21

M: Male; F: Female; NA: Not available

Table 3.2: Clinical data of M002 cohort patient samples used in this study. Red highlighted cells indicate patient samples that could not be RT-PCR amplified. Antiretroviral therapy information of patients was unavailable

Patient ID	Gender	Age	CD4 T cell counts (cells/mm^3)					Viral Load (RNA copies/ml)					Human Leukocyte Antigen (HLA) Genotype						Longitudinal samples available	Longitudional Samples Sequenced
			BASELINE	6 MONTHS	12 MONTHS	18 MONTHS	24 MONTHS	BASELINE	6 MONTHS	12 MONTHS	18 MONTHS	24 MONTHS	HLA-A, ALLELE 1	HLA-A, ALLELE 2	HLA-B, ALLELE 1	HLA-B, ALLELE 2	HLA-C, ALLELE 1	HLA-C, ALLELE 2		
M002-006	F	NA	219	182	173	209	NA	101000	NA	NA	251000	NA	A*23:01	A*26:01	B*14:02	B*51:01	C*07:01	C*08:02	4	3
M002-020	F	NA	343	350	331	411	NA	10700	NA	NA	9330	NA	A*30:01	A*30:09	B*08:01	B*42:01	C*02:05	C*17:01	2	2
M002-025	F	NA	364	324	345	418	NA	98000	NA	NA	53300	NA	A*02:01	A*23:01	B*44:03	B*58:02	C*07:01	C*07:06	4	4
M002-422	F	NA	273	270	221	242	NA	146000	NA	NA	407000	NA	A*02:01	A*23:01	B*15:01	B*58:02	C*04:01	C*06:02	4	3
M002-423	F	NA	643	453	608	613	NA	49700	NA	NA	70900	NA	A*03:01	A*30:02	B*07:02	B*57:03	C*07:02	C*18:01	5	5
M002-424	F	NA	292	112	137	162	NA	50000	NA	NA	77500	NA	A*26:05	A*30:17	B*39:10	B*42:01	C*03:04	C*12:03	4	4
M002-722	F	NA	478	404	446	447	NA	171000	NA	NA	79200	NA	A*02:01	A*03:01	B*44:03	B*58:02	C*06:02	C*07:01	5	4
																			Total=28	Total=26

F: Female; NA: Not available

3.1.2 Viral RNA extraction, RT-PCR amplification and sequencing

Viral RNA was extracted from the 72 patient samples from both the Lung and M002 cohorts and then used for RT-PCR amplification of the *vif, vpr* and *vpu* regions (**Figure 3.1**). Overall, 21 and 26 (n=47) samples amplified for the Lung and M002 cohorts, respectively, with the expected PCR products of approximately 1.3 kb. Despite repeated RNA extraction and RT-PCR attempts, no additional amplicons were obtained. Samples that did not amplify are depicted in the viral load columns **Table 3.1** and **Table 3.2** in red and corresponding to the particular sample's time point. This may have been attributed to sample degradation due to poor storage conditions, or low viral loads below the limits of detection for the RT-PCR assay used with at least 4 of the unsequenced samples containing low viral loads.

The amplicons were cleaned, and used in the subsequent sequencing reactions. All 47 samples were successfully sequenced. The amino acid sequence alignments of the longitudinal sequences for Vif, Vpr and Vpu of Lung and M002 patients are shown in **Figure 3.2** and **Figure 3.3**, respectively. For the Lung cohort, only eight of the 18 patient sequences had at least two sequences from different time points available (three samples only had single sequences available), and only two of these patients, 225 and 700, had the HLA-B *B*58:01* allele associated with slower disease progression (**Table 3.1**). Sequential sequences from all seven patients from the M002 cohort were obtained in order to compare Vif, Vpr and Vpu amino acid changes changes over time. Interestingly, three of the seven M002 patients, 025, 422 and 722, had the *HLA-B*58:02* allele associated with faster disease progression (**Table 3.2**).

The Vif functional domains (highlighted) appear to be highly conserved for all patients, with the exception of the nuclear localization inhibitory site (**Figure 3.2 and 3.3**). Similarly, for Vpu, functional domains (highlighted) appear to be highly conserved for all patients, with the exception of the casein kinase II site (**Figure 3.2 and 3.3**). Additionally, the total number of amino acid changes in each protein as compared to the earliest time point sequenced is shown in **Table 3.3**. Sequence IDs are presented as 'xxx-vif/vpr/vpu-y' where xxx is the patient ID, vif/vpr/vpu represents one of the three accessory proteins Vif, Vpr or Vpu and y is representative of the time point of the samples. 0= baseline at 0 months, 1= 1st follow up at 6 months, 2= 2nd follow up at 12 months and 3rd follow up at 18 months. The change in amino acids for Vif, Vpr and Vpu from the Lung cohort ranges from 0 to 33, 1 to 8 and 0 to 29, respectively, and for the M002 cohort it is 0 to10, 0 to 4 and 0 to 8 (**Figures 3.2 and 3.3** and **Table 3.3**).

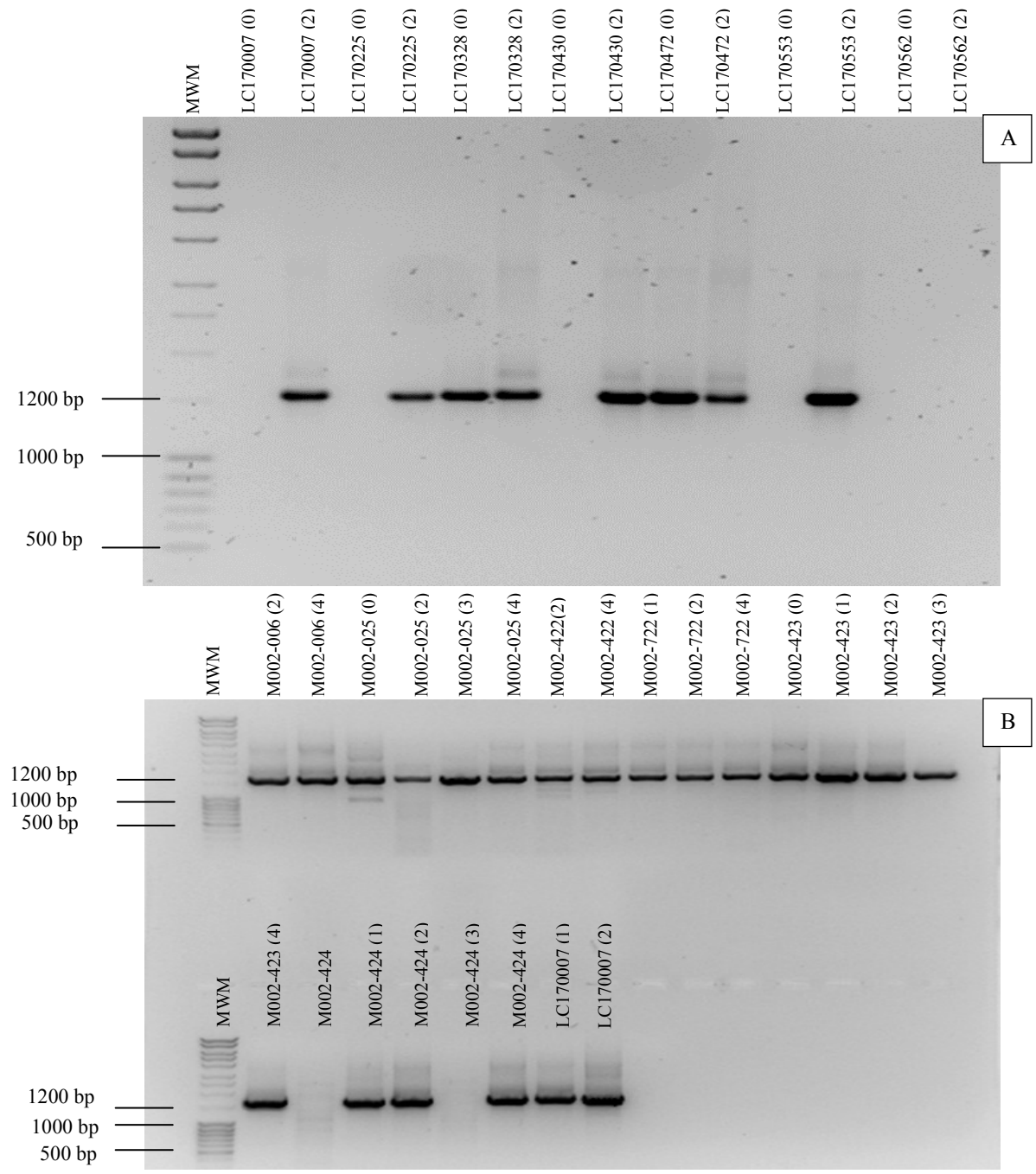


Figure 3.1: RT-PCR amplification of *vif, vpr* and *vpu* regions (approximately 1,3 kb) of extracted HIV-1 RNA from the Lung cohort (A) and M002 cohort (B) depicted on a 1% agarose gel under UV transillumination. The molecular weight marker (MWM, O'GeneRuler DNA Ladder Mix #SM1173, Thermo Fisher Scientific, USA) was used for sizing (base pairs (bp)) and is depicted on the left. Numbers in brackets represent time points of sample, 0= baseline at 0 months, 1= 1st follow up at 6 months, 2= 2nd follow up at 12 months, 3rd follow up at 18 months and 4= 4th follow up at 24 months (for M002 only).

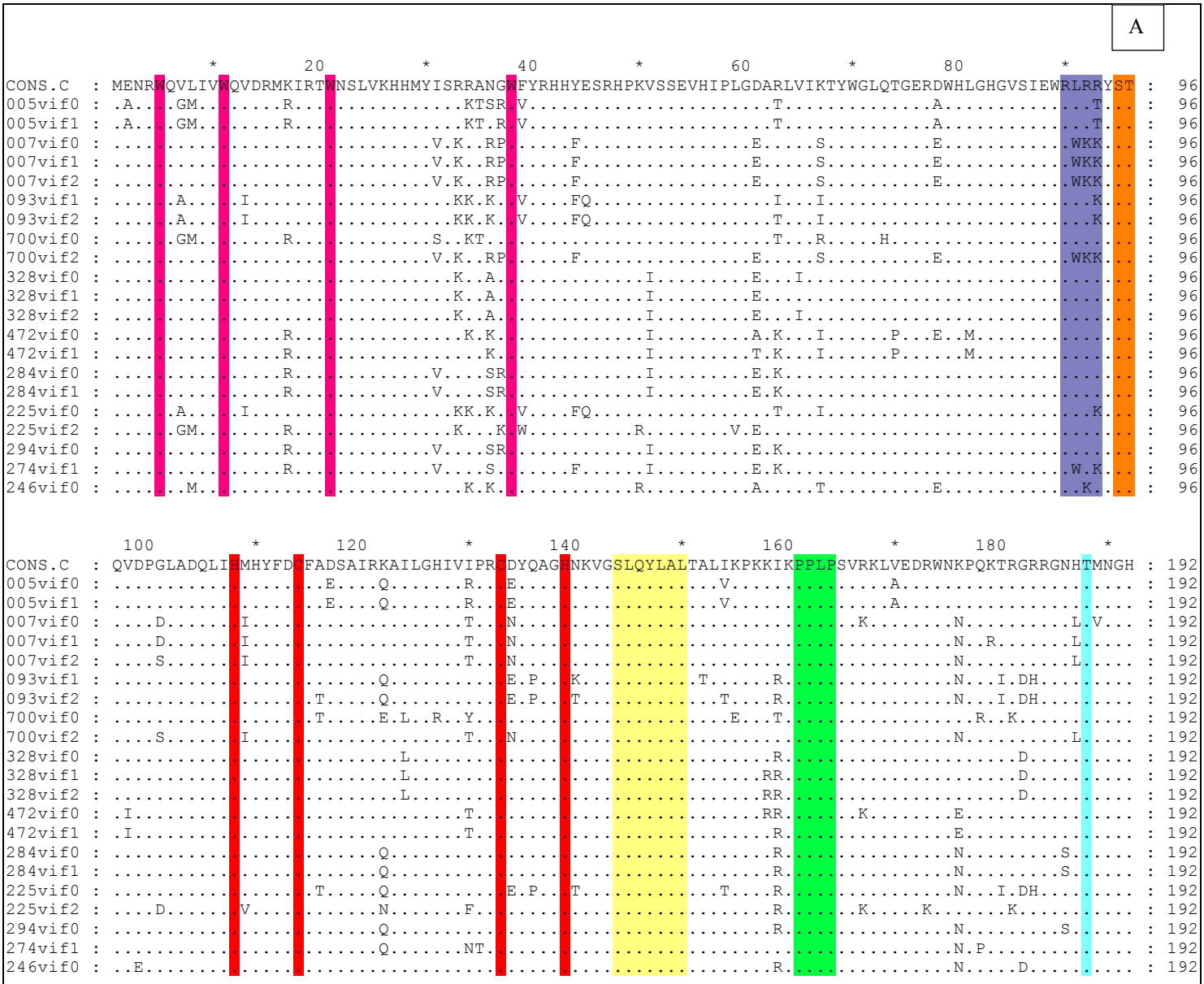


Figure 3.2: Amino acid sequence alignment of Lung Cohort Vif (A), Vpr (B) and Vpu (C) proteins. The *vif*, *vpr* and *vpu* nucleotide sequences were analysed using Sequencher 5.1 and then aligned using Clustal X, and translated into amino acid sequences using GeneDoc Multiple Sequence Aligner. On the left are the patient sequence ID codes and number of the longitudinal sample that the sequence belongs to ie. 0=baseline, 1=follow-up 1 at 6 months, 2=follow up 2 at 12 months, 3=follow up at 18 months. Sequences were compared to a Consensus HIV-1 Subtype C sequence. Dots represent identical residues, variant residues are shown, and dashes indicate insertions/deletions. Highlighted regions represent important functional regions (see key below). The patient numbers depicted correspond to the last three numbers shown in the patient ID column in **Table 3.1**.

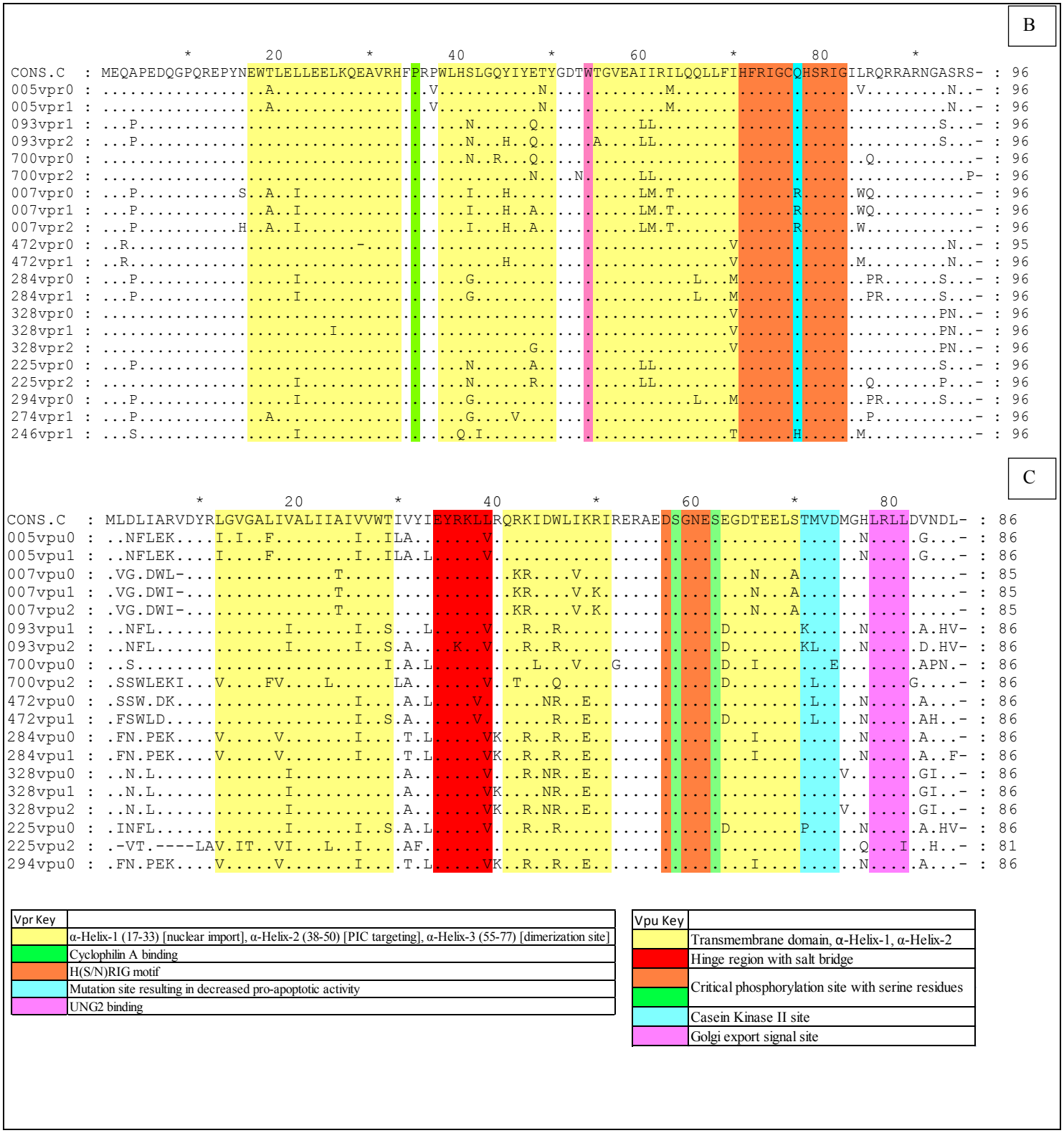


Figure 3.2: (cont)

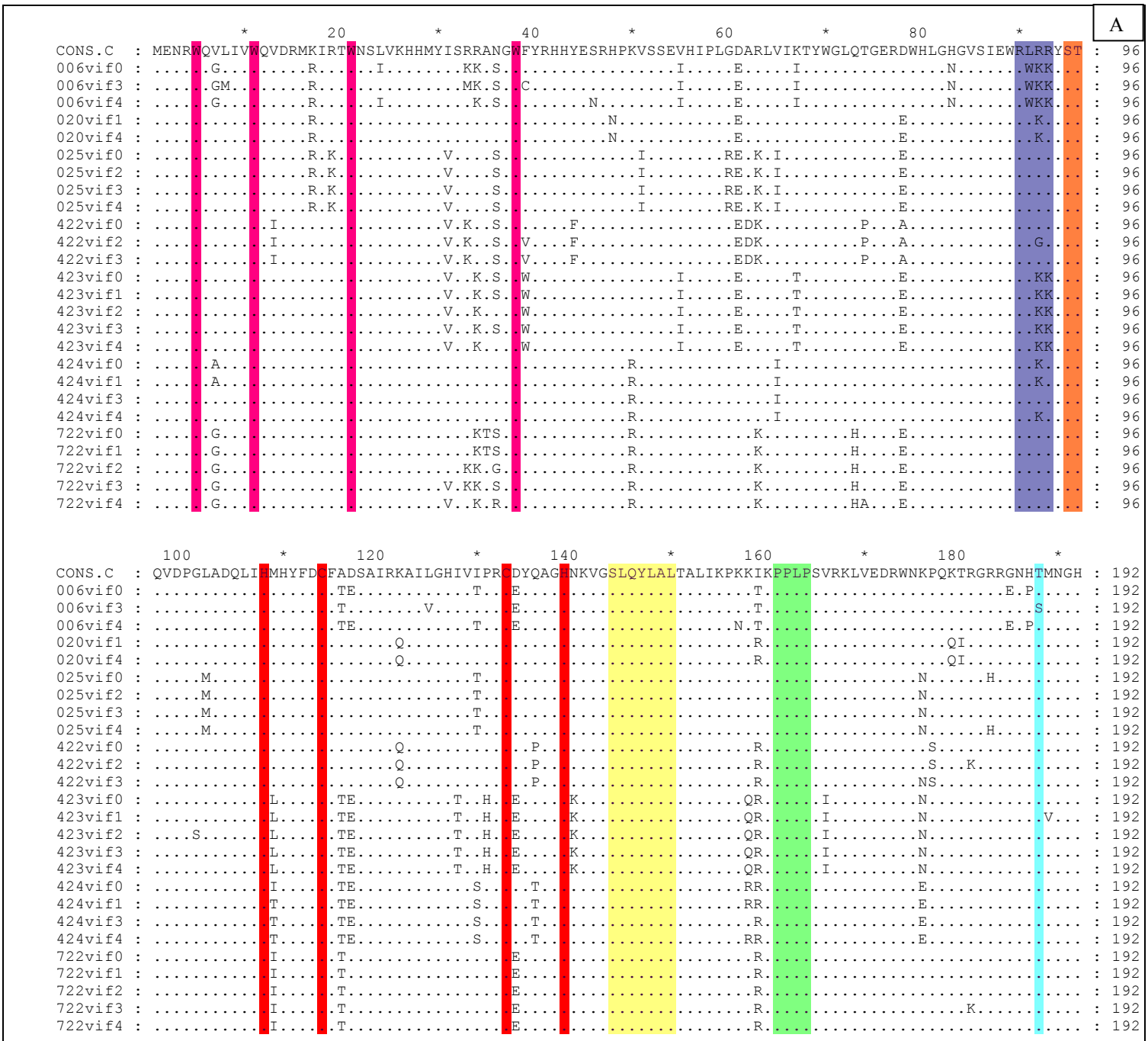


Figure 3.3: Amino acid sequence alignment of M002 Cohort Vif (A), Vpr (B) and Vpu (C) proteins. The *vif, vpr* and *vpu* nucleotide sequences were analysed using Sequencher 5.1 and then aligned using Clustal X, and translated into amino acid sequences using GeneDoc Multiple Sequence Aligner. On the left are the patient sequence IDs and number of the longitudinal sample that the sequence belongs to ie. 0=baseline, 1=follow-up 1 at 6 months, 2=follow up 2 at 12 months, 3=follow up at 18 months and 4=follow up at 24 months. Sequences were compared to a Consensus HIV-1 Subtype C sequence. Dots represent identical residues, variant residues are shown, and dashes indicate insertions/deletions. Highlighted regions represent important functional regions (see key below).

Vif Key	
	Tryptophans important for recognition of APOBEC3G
	Nuclear localisation inhibitory site
	Phosphorylation site
	HCCH zinc binding motif essential for Cullin 5 binding
	BC Box region for Elongin C binding
	Vif dimerization site and part of SOCS-box
	Phosphorylation site

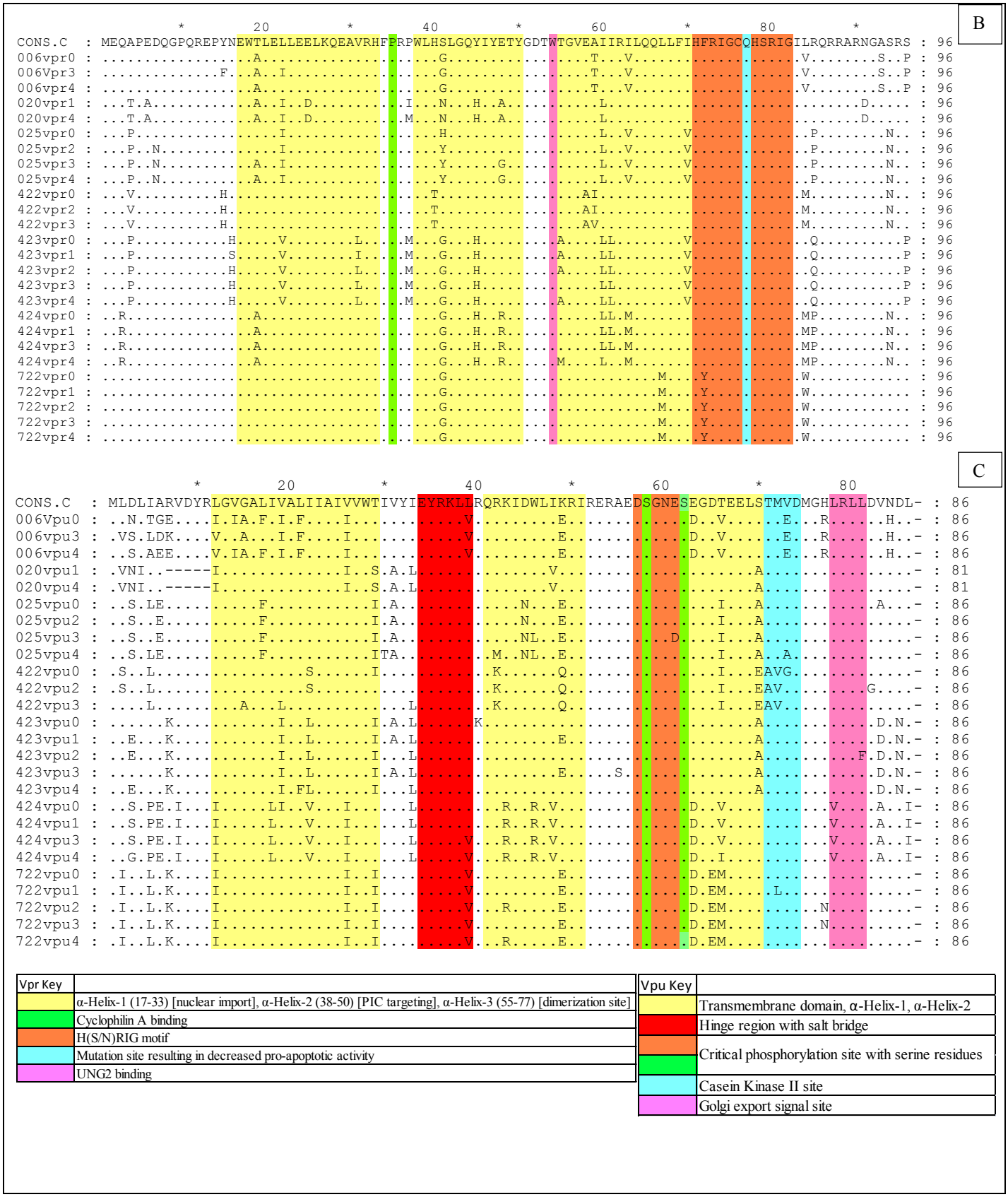


Figure 3.3: (cont)

Table 3.3: Number of total amino acid sequence changes in longitudinal samples of Vif, Vpr and Vpu of the Lung and M002 cohorts, as compared to the earliest time point available sequence.

Cohort	Patient ID sequence	Number of amino acid changes compared to earliest available sequence	Cohort	Patient ID sequence	Number of amino acid changes compared to earliest available sequence
Lung Cohort	005vif1	1	M002Cohort	006vif3	10
	007vif1	3		006vif4	3
	007vif2	3		020vif4	0
	093vif2	5		025vif2	1
	700vif2	32		025vif3	1
	328vif1	2		025vif4	0
	328vif2	0		422vif2	3
	472vif1	5		422vif3	2
	284vif1	0		423vif1	1
	225vif2	32		423vif2	2
				423vif3	0
	005vpr1	1		423vif4	1
	093vpr2	2		424vif1	0
	700vpr2	8		424vif3	3
	007vpr1	2		424vif4	1
	007vpr2	3		722vif1	0
	472vpr1	3		722vif2	3
	328vpr1	1		722vif3	4
	328vpr2	1		722vif4	4
	225vpr 2	5			
				006vpr3	2
	005vpu1	2		006vpr4	0
	007vpu1	1		020vpr4	1
	007vpu2	1		025vpr2	2
	472vpu1	7		025vpr3	4
	284vpu1	1		025vpr4	4
	328vpu1	3		422vpr2	0
	328vpu2	1		422vpr3	1
	225vpu2	29		423vpr1	1
				423vpr2	0
				423vpr3	1
				423vpr4	0
				424vpr1	0
				424vpr3	0
				424vpr4	2
				722vpr1	0
				722vpr2	0
				722vpr3	0
				722vpr4	0
				006vpu3	8
				006vpu4	4
				020vpu4	0
				025vpu2	2
				025vpu3	4
				025vpu4	5
				422vpu2	3
				422vpu3	6
				423vpu1	3
				423vpu2	4
				423vpu3	3
				423vpu4	4
				424vpu1	1
				424vpu3	2
				424vpu4	4
				722vpu1	1
				722vpu2	2
				722vpu3	1
				722vpu4	1

3.1.3 HLA class I motif analysis

Vif, Vpr and Vpu amino acid sequences derived from the Lung and M002 cohorts were analysed for HLA class I related immune escape. The sequences were analysed using the Los Alamos HIV Binding Motif Scanner which scans HIV-1 amino acid sequences for HLA class I anchor residues based on the infected patient's HLA genotype. The potential epitopes are then outputted. **Figure 3.4** and **Figure 3.5** depict Vif, Vpr and Vpu sequences which exhibit possible HLA class I escape due to motifs no longer being recognised by their targeting HLA. Magenta highlighted residues represent the anchor residues which subsequently mutate over time from one longitudinal sample to the next (grey indicates the mutated anchor residue). The HLA class I targeted motif which the anchor residues belong to are boxed in red and the motif is then no longer recognised in the following longitudinal samples with the grey mutated residues.

Also represented in blue boxes are the motifs which re-appear after a certain period of time and are recognised again by its targeting HLA protein due to the reversion of the mutated anchor residues. The patient HLA class I gene and a visual representation of the motif that it targets are depicted in the red boxes surrounding the aligned sequences. The anchor residues are shown in the square brackets with the preferred but not dominant amino acids in the anchor positions being shown in parentheses. Only 9 amino acid-long motifs were represented as that is the size of motifs stored in the database, but where a unique 8, 10, or 11 motif was calculated by the scanner it is also shown.

Immune escape mutations were detected in only a few patients. For the Lung cohort, HIV-1 sequences from patient 093 (*B*58:02)* exhibited immune escape in all three accessory proteins sequenced (**Figure 3.4**). Patient 225 (*B*58:01)* exhibited immune escape in Vif and Vpr, whereas mutations in Vpr and Vpu were detected in patient 472 (*B*58:02)*. Lastly, escape mutations were detected in the Vif from patient 007 (*B*58:02).*

For the M002 cohort, immune escape mutations as well as "back-mutations" or reversions were detected. HIV-1 sequences from patient 423 (*B*57:03*) showed escape mutations in Vif, Vpr and Vpu (**Figure 3.5**). Patients 006 (*B*51:01*) and 422 (*B*58:02*) had escape mutations in Vif and Vpu, whereas patient 424 and 722 had escape mutations in Vif only, and patient 025 exhibited immune escape mutations in Vpu.

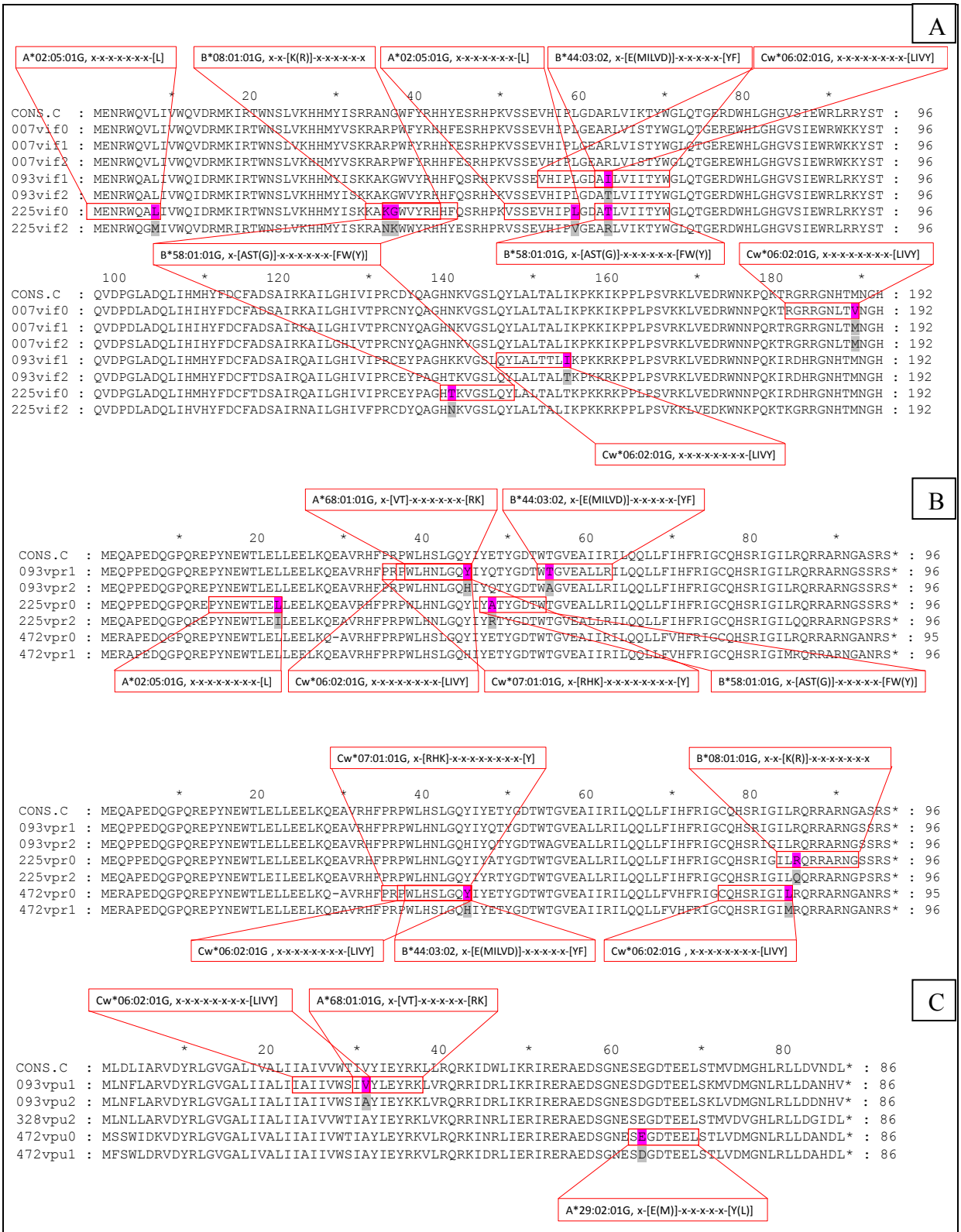


Figure 3.4: Amino acid alignments of Lung cohort-derived Vif (A), Vpr (B) and Vpu (C) sequences depicting HLA class I motif immune escape. HLA class I targeted motifs which are no longer recognised following a mutation within a key anchor residue are outlined by red boxes. Key anchor residues are highlighted in magenta with subsequent longitudinal sequence mutations being highlighted in grey. Boxes branching off from the motifs contain the patient HLA class I genes with a representation of their associated target motif which includes key anchors.

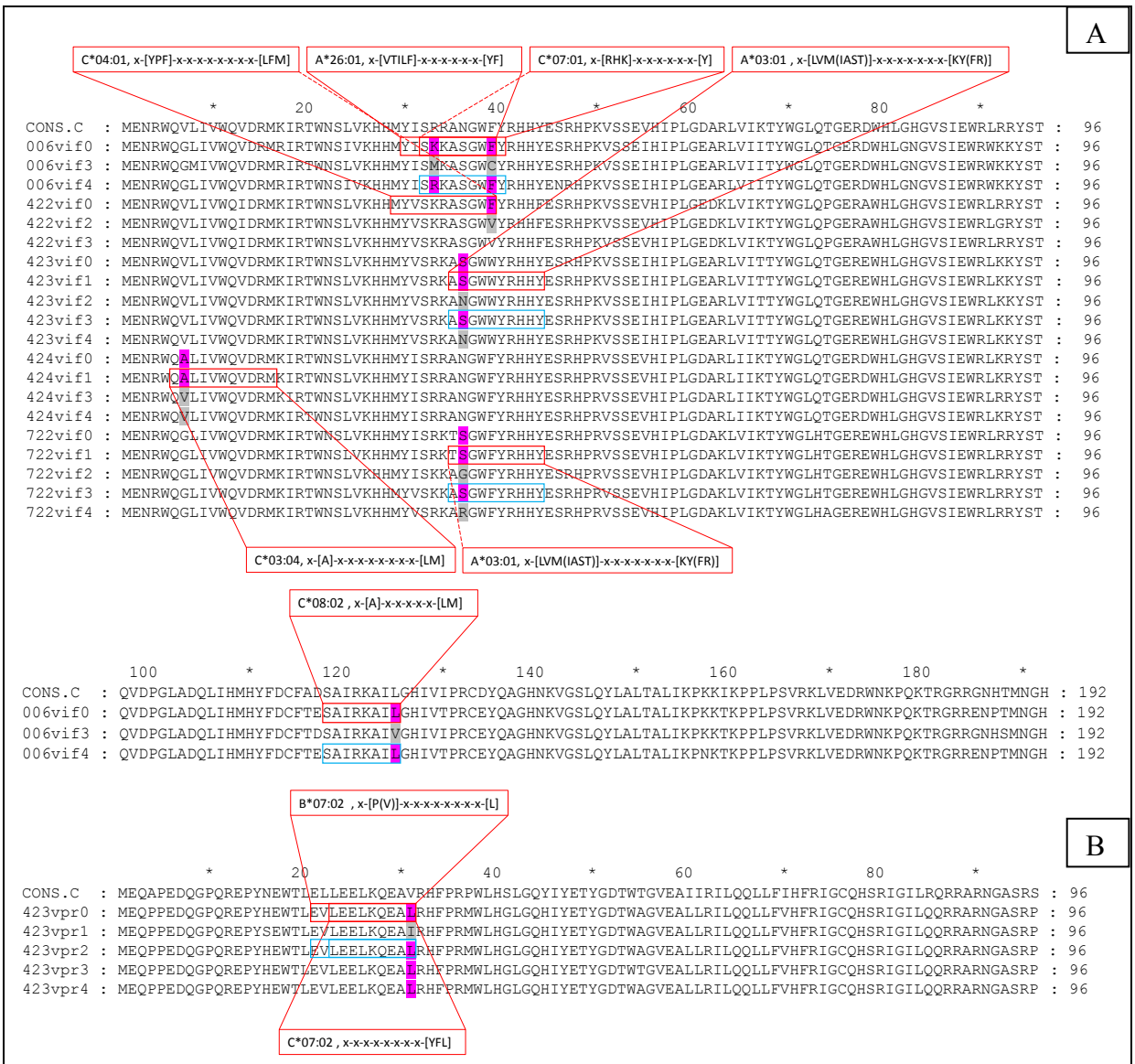


Figure 3.5: Amino acid alignments of M002 cohort-derived Vif (A), Vpr (B) and Vpu (C) sequences depicting HLA class I motif immune escape. HLA class I targeted motifs which are no longer recognised following a mutation within a key anchor residue are outlined by red boxes. Key anchor residues are highlighted in magenta with subsequent longitudinal sequence mutations being highlighted in grey. Boxes branching off from the motifs contain the patient HLA class I genes with a representation of their associated target motif which includes key anchors. Blue boxes indicate motifs which return following reversion of anchor amino acid mutations.

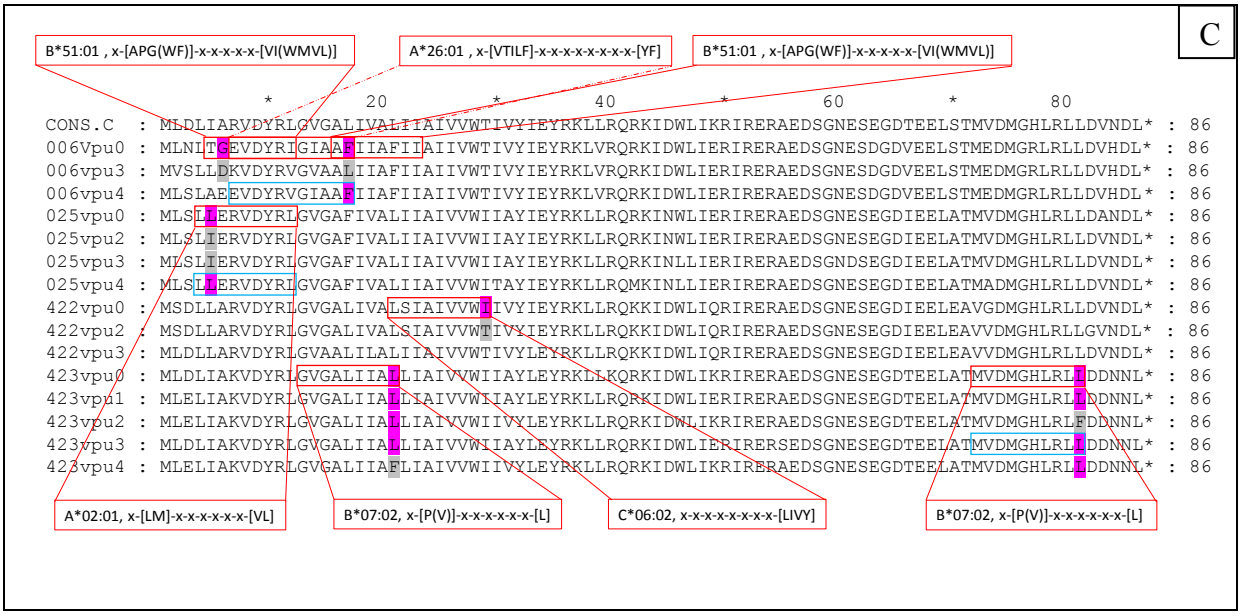


Figure 3.5: (cont)

3.1.4 Expression and purification of recombinant Vpu protein

3.1.4.1 Plasmid preparation and restriction digest of constructs

Three recombinant plasmid vectors containing the *vpu* genes of interest (obtained from GeneArt) were transformed into *E. coli* DH5α and a large scale plasmid isolation protocol was subsequently conducted. **Figure 3.6** depicts an amino acid sequence alignment of the Vpu protein translations for the three *vpu* constructs. Spectrophotometer readings indicated plasmid preparation yields of 131,65 µg of pcDNA3.1/V5-His-Cons. C, 170 µg of pcDNA3.1/V5-His-FV5 and 120,85 µg of pcDNA3.1/V5-His-FV15 all re-suspended in 250 µl of sterile water. Identity of purified plasmids was confirmed using restriction digest analysis as seen in **Figure 3.7**.

```
                  *        20        *        40        *        60        *        80
Cons.C   : MLDLIARVDYRLGVGALIVALIIAIVVWTIVYIEYRKLLRQRKIDWLIKRIRERAEDSGNESEGDTEELSTMVDMGHLRLLDVNDL : 86
05ZAFV5  : .V..L.............L.......I....A.......V...R..R..R.....................L....P.....AA.. : 86
05ZAFV15 : .-VTL---..NITIA.FV.......I....A.......RK.....R..E...................A......Q......... : 82
```

Figure 3.6: Amino acid alignment of Consensus C, 052AFV5, and 052AFV15 Vpu proteins, Three Vpu proteins were chosen for expression and purification in this study. Cons.C is derived from a consenus of HIV-1 subtype C strains with 052AFV5 having a fairly similar sequence compared to Cons. C. 052AFV15 is differentiated from the other two proteins by four amino acid deletions located towards the N-terminus of the protein**.**

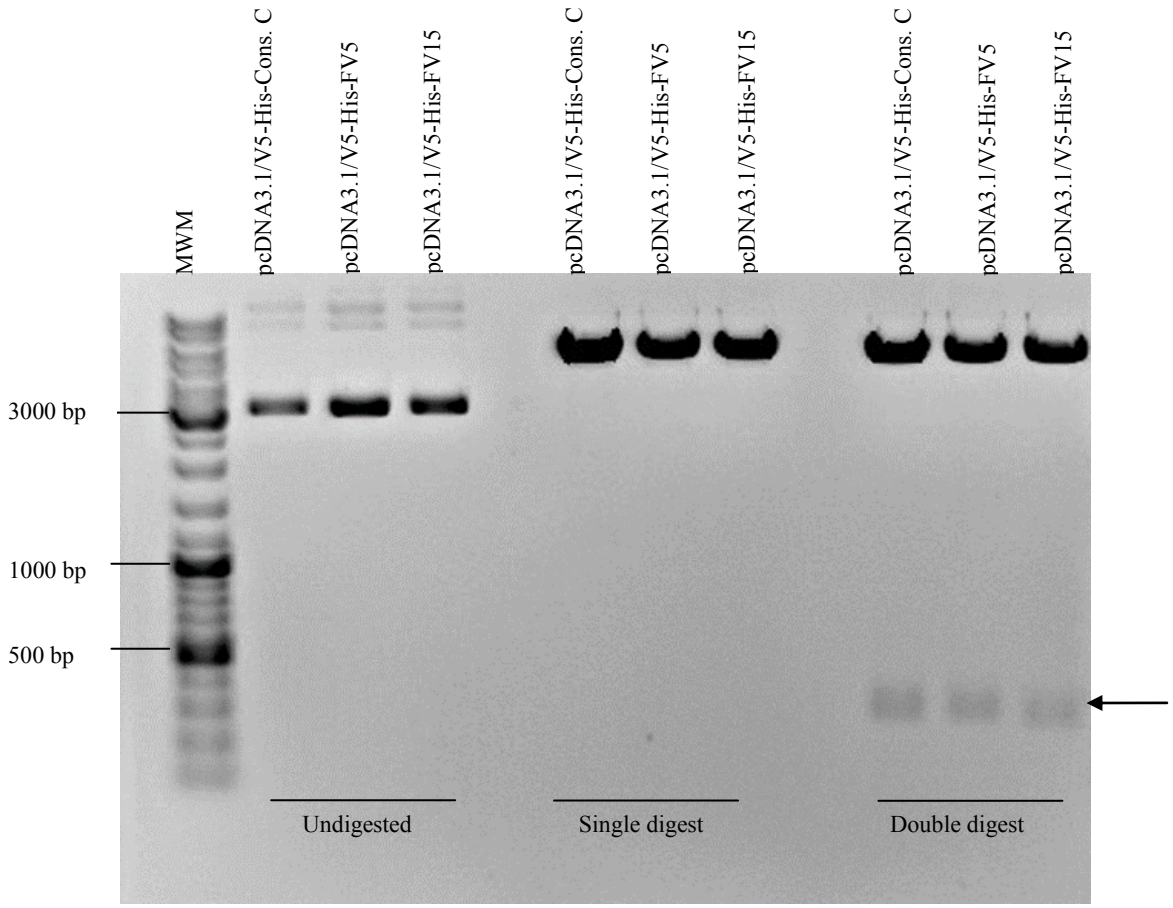


Figure 3.7: Restriction enzyme digest analysis of plasmid preparations of pcDNA3.1/V5-His-Cons. C, pcDNA3.1/V5-His-FV5 and pcDNA3.1/V5-His-FV25 *vpu* constructs. Undigested single digests to linearise the constructs (using *BglII)* and double digests to excise the 276 bp *vpu* gene from the 5698 bp vector (using *HindIII* and *XhoI*) were run on a 1% agarose gel and visualised using UV transillumination. The arrow on the right indicates the excised *vpu* genes. Undigested *vpu* constructs depict typical banding pattern of plasmid DNA. The molecular weight marker (MWM, O'GeneRuler DNA Ladder Mix #SM1173, Thermo Fisher Scientific, USA) used for sizing is indicated on the left and depicts sizes in base pairs (bp).

3.1.4.2 Optimization of Vpu expression

Small scale transfections of the *vpu* constructs were performed in order to test transfection reagents, varying transfection conditions and overall expression levels of the Vpu proteins. The Western blot shown in **Figure 3.8 (A)** depicts the first confirmation of expression of Vpu proteins using the JetPrime transfection reagent, with expression of Cons. C and 05ZAFV15. It also confirms expression levels, identity and correct sizing of the Vpu proteins.

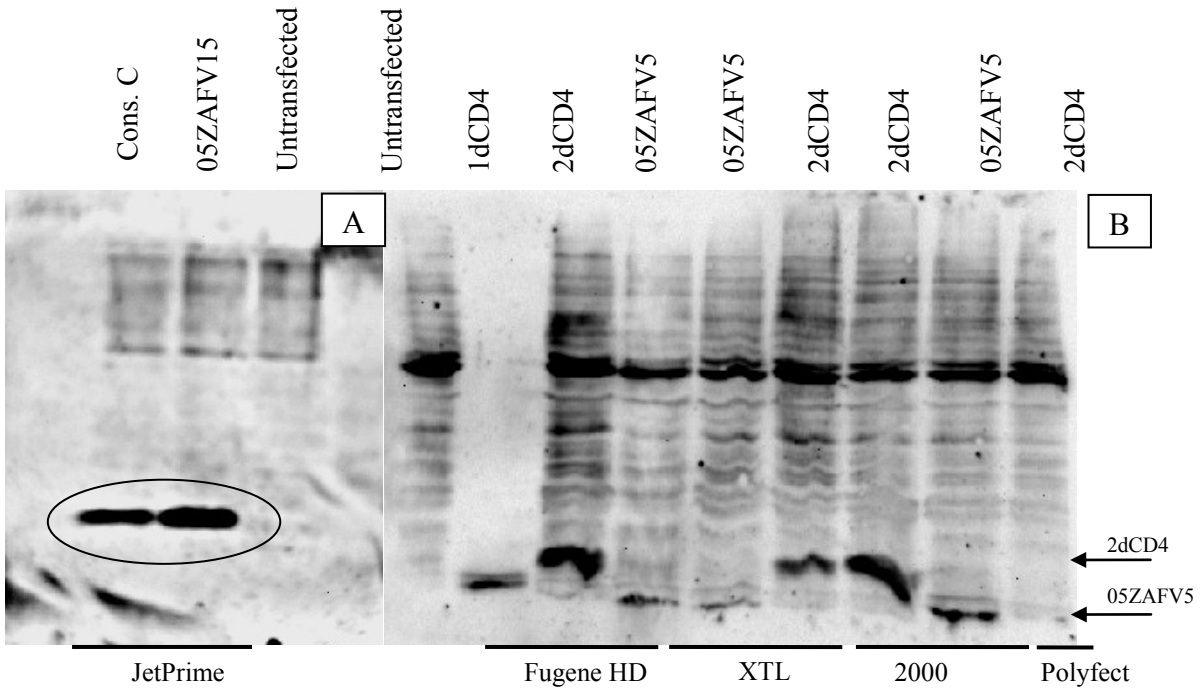


Figure 3.8: Western blots of whole-cell lysate of transfected HEK 293T cells for detection of polyhistidine-tagged Vpu proteins following tranfection with 5 different transfection reagents. HEK 293T cells were transiently transfected with pcDNA3.1/V5-His-05ZAFV15 and pcDNA3.1/V5-His-Cons. C plasmid constructs (**A**), and pcDNA3.1/V5-His-05ZAFV5 or a 2dCD4 constructs (**B**) utilising the transfection reagents Fugene HD, Lipofectamine XTL/2000, Polyfect and JetPrime. Following transient transfection and 48 hours of protein expression, whole-cell lysate was used for SDS-PAGE and Western blotting, with a polyhistidine-targeting antibody used for probing. The circle on the left indicates the first instance of Vpu protein expression. Vpu proteins were sized approximately in the estimated 10-12 kDa range (protein molecular weight marker not shown). Untransfected whole-cell lysate was used as a negative control. **Untransfected**= untransfected HEK 293T cell lysate, **Cons. C**= whole cell lysate of cells transfected with pcDNA3.1/V5-His-Cons. C and expressing Cons. C Vpu protein, **05ZAFV5/05ZAFV15**= whole cell lysate of cells transfected with pcDNA3.1/V5-His-FV5/FV15 and expressing 05ZAFV5/FV15 Vpu protein, **1dCD4**=one domain CD4 sizing control, **2dCD4**= whole cell lysate of cells transfected with the 2dCD4 construct.

JetPrime transfection reagent was decided upon as the principal transfection reagent following comparisons of 5 different transfection reagents as seen in **Figure 3.8 (B)** due to its ease of use and consistent reproducibility of results. **Figure 3.8 (B)** also confirms sizing of the recombinant Vpu proteins (~10.8 kDa) when compared to both expressed recombinant 2dCD4 and purified 1dCD4 sizing controls. Optimal transfection conditions for all 3

constructs utilised 1:2 DNA to JetPrime ratio and harvesting of HEK 293T cells 48 hours post-transfection.

Following optimization of expression of the three recombinant Vpu proteins, the Vpu purification protocol was tested and optimized. Overall, the protocol which was adapted from Lv and colleagues (Lv et al., 2013) was generally unsuccessful due to issues with contaminant proteins and low protein yields. **Figure 3.9** depicts the purification process of recombinant Vpu protein using different imidazole wash buffer concentrations. A ~50 kDa sized protein was consistently seen throughout the entire expression and purification process on all Western blots (**Figures 3.8 to 3.12**) and could not be removed completely even when utilizing variable imidazole washing concentrations, though increasing wash volumes and the introduction of a 20 mM washing step did improve overall purity slightly. The protein seemed to be inherent to the HEK 293T cell lines as the protein was present even in untransfected whole-cell lysate. The protein was also likely polyhistidine rich due to its detection by an anti-polyhistidine antibody in all Western blot analyses.

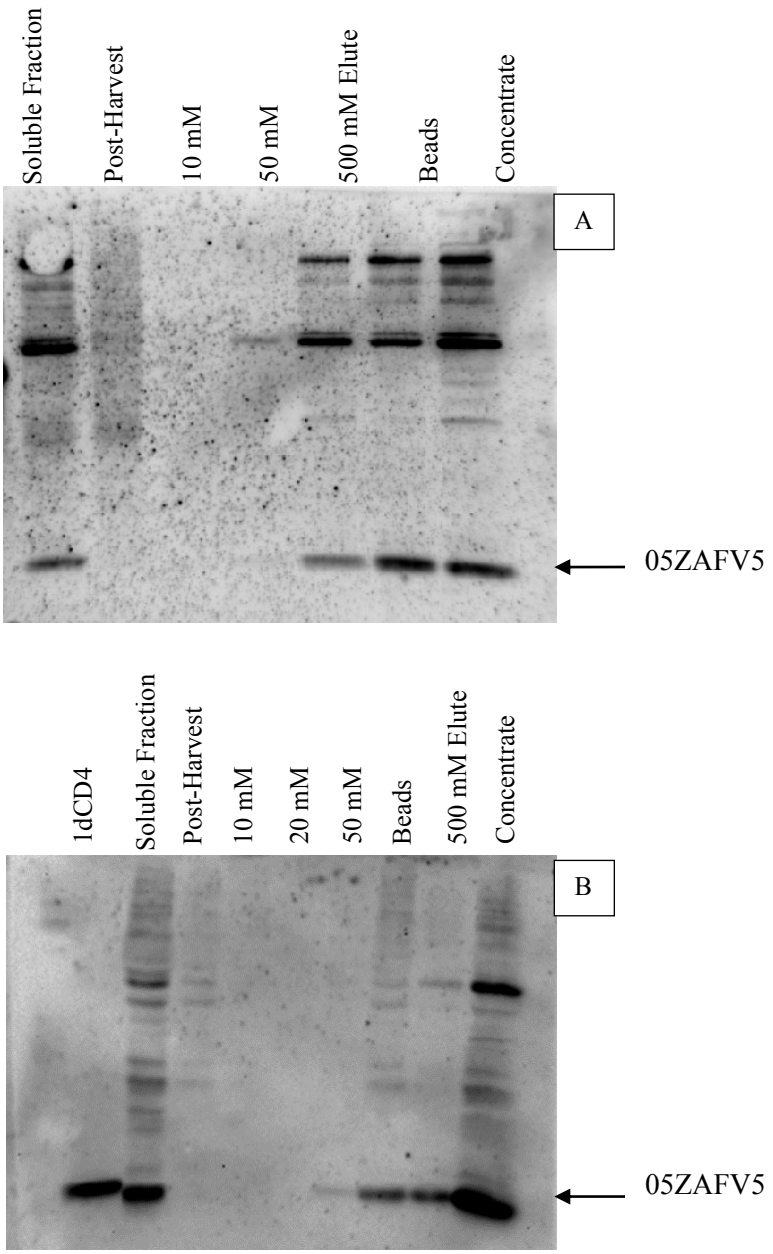


Figure 3.9: Western blot analysis of samples collected during protein purification procedure of the recombinant 05ZAFV5 Vpu protein. Different imidazole wash buffer concentrations and varying numbers of washes were used. The washing procedure in Figure **A** utilised only a 10 mM and 50 mM wash and was therefore less stringent, whilst Figure **B** depicts a more stringent washing procedure with added 20 mM wash buffer step. An anti-polyhistidine antibody was used for probing. **1dCD4**=one domain CD4 sizing control, soluble fraction=protein-containing fraction following centrifugation of whole-cell lysate, **post-harvest**=supernatant following Vpu-bound agarose bead harvest, **10, 20** and **50 mM** = wash buffer imidazole concentrations, **beads**=agarose beads following elution of Vpu protein, **500 mM elute**= eluted protein with 500 mM imidazole wash buffer, **concentrate**= concentrated eluted Vpu protein.

Protein yields were problematic throughout the entirety of the expression and purification process of the Vpu proteins. In order to try overcome this, stably transfected cell lines were established and then up scaled in order to increase protein yields. **Figure 3.10** depicts a Western blot probed with anti-polyhistidine antibody with samples from stably transfected

HEK 293F cells, all successfully expressing recombinant Vpu proteins and the 2dCD4 control.

Even after upscaling protein expression and purification, yields of Vpu proteins did not increase as compared to previous expression and purification runs of the Vpu proteins as seen in **Figure 3.11**. The Vpu proteins were still not visible on Coomassie-stained SDS-PAGE gels (not shown) and the signal intensity on Western blots was decreased as compared to previously expressed Vpu proteins, with the ~50 kDa protein contaminant which was seen throughout the entire protein expression and purification process appearing to be increased in its concentration.

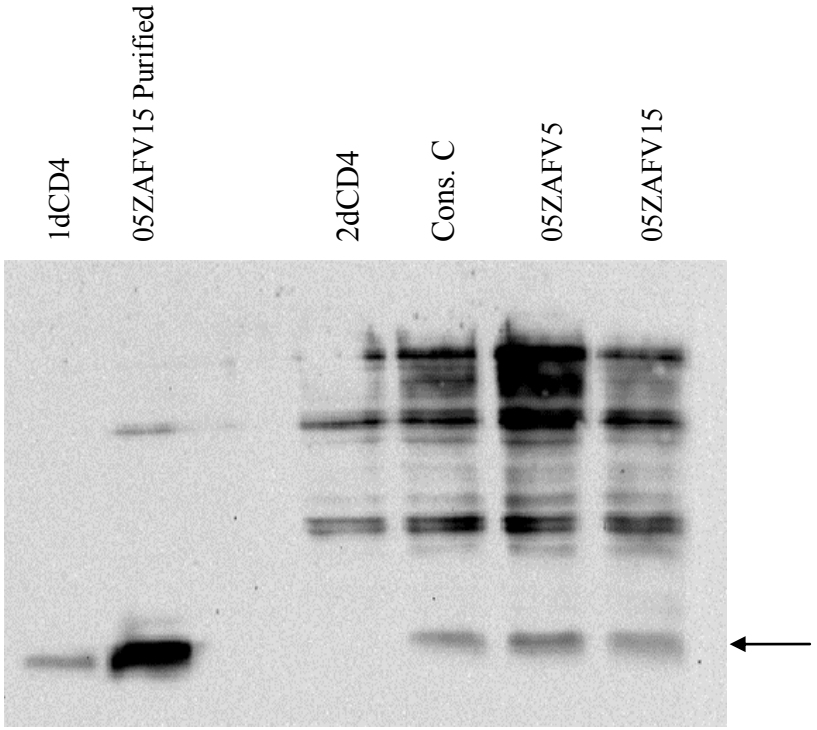


Figure 3.10: Western blot analysis for detection of recombinant Vpu protein expression in stably transfected HEK 293F cells. Stably transfected HEK 293F cell lines were established and expressed recombinant Vpu proteins (and 2dCD4 as a control) as shown by the arrow. Whole-cell lysate was used for SDS-PAGE and Western blotting, with a polyhistidine-targeting antibody used for probing of 6 × polyhistidine-tagged Vpu proteins. **1dCD4**=one domain CD4 sizing control, **05ZAFV15 Purified**= previously expressed and purified Vpu protein as a control, 2dCD4= whole cell lysate of cells stably transfected with 2dCD4 construct, **Cons. C**= whole cell lysate of cells transfected with pcDNA3.1/V5-His-Cons. C and expressing Cons. C Vpu protein, **05ZAFV5**= whole cell lysate of cells transfected with pcDNA3.1/V5-His-FV5 and expressing 05ZAFV5 Vpu protein, **05ZAFV15**= whole cell lysate of cells transfected with pcDNA3.1/V5-His-FV15 and expressing 05ZAFV15 Vpu protein.

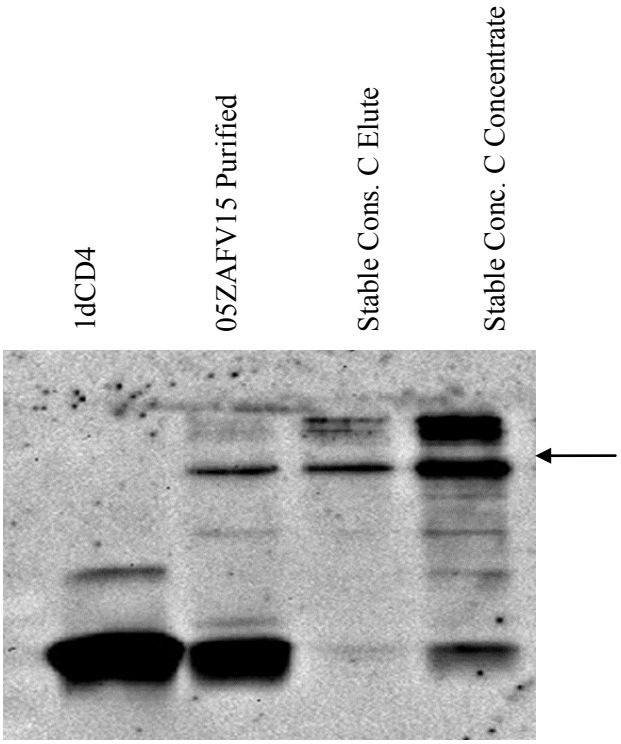


Figure 3.11: Western blot analysis for detection of purified recombinant Vpu protein from upscaled expression and purification of stably transfected HEK 293F cells. Cons. C Vpu was purified from upscaled stably transfected HEK 293F cells following previously describe procedures. Even after upscaling production, Cons. C appears to be in a lower concentration as compared to purified 05ZAFV15 Vpu protein even when concentrating down to comparable volumes. Contaminants can also be seen to be increased (indicated by arrow). Anti-polyhistidine antibody was used for probing. **1dCD4**=one domain CD4 sizing control, **05ZAFV15** Purified= previously expressed and purified Vpu protein as a control, **Stable Cons. C Elute**= eluted Cons. C Vpu protein purified from stably transfected HEK 293F cells, **Stable Conc. C Concentrate**= eluted and concentrated Cons. C Vpu protein purified from stably transfected HEK 293F cells.

3.1.4.3 Dot blot and Western blot analyses

Due to the difficulties in purifying sufficient quantities of recombinant Vpu for setting up ELISAs, dot blot analysis was conducted as a proof-of-concept for detection of anti-Vpu antibodies in HIV-1 positive patient sera as seen in **Figure 3.12.**

Overall, dot blot analysis was unsuccessful due to non-specific binding of the sera tested. In the case of the dot blots probed with both rabbit anti-Vpu sera, the rabbit sera bound to purified Vpu proteins Cons. C and 05ZAFV5 as expected, but also bound to purified 2dCD4 control protein, and the DMEM-only control. Similarly for proteins probed with the anti-polyhistidine antibody or negative patient sera, binding occurred with all blots (DMEM, 1dCD4, 2dCD4, Cons. C and 05ZAFV5).

Western blot analysis was subsequently performed on the same samples to separate out and visualize which proteins the antibodies were binding to in a non-specific manner. Antibodies bound to expected targets as seen in **Figure 3.13**, with **Figure 3.13.A** showing Anti-Vpu rabbit antiserum against subtype C Vpu binding to Vpu proteins but not the CD4 controls whereas in **Figure 3.13.B** the poly-histidine antibody bound to all poly-histagged Vpu and CD4 proteins as expected.

Thus, due to the discrepancies seen between the dot blot and Western blot analyses, it was evident that the purity of the recombinant Vpu protein obtained during the course of this study was not appropriate for setting up a reproducible assay for detection of anti-Vpu antibodies in HIV-1 positive patient sera.

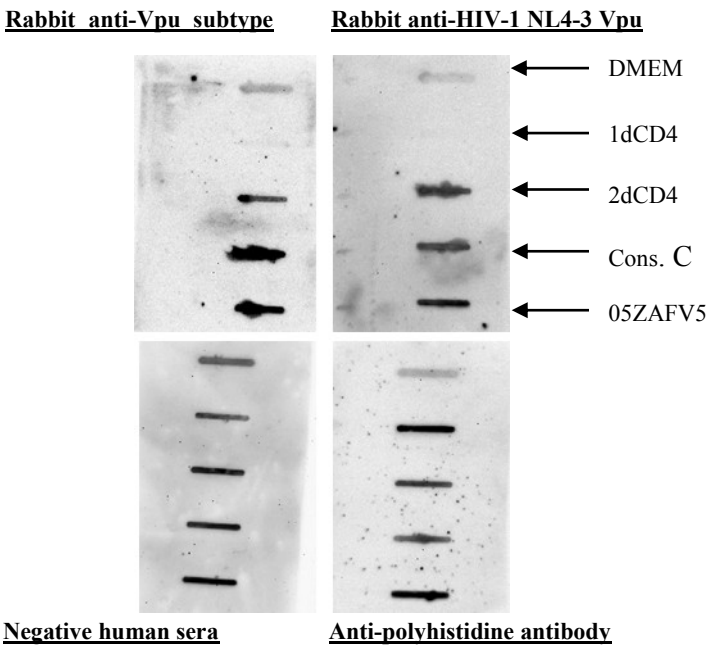


Figure 3.12: Dot blot analysis of recombinant Vpu proteins and appropriate controls. Four separate dot blots were conducted; each probed with either anti-Vpu subtype C rabbit sera, anti-HIV-1 NL4-3 Vpu rabbit sera, HIV-1 negative human sera or anti-polyhistidine antibody and then probed with their respective HRP-linked secondary antibody counterparts (anti-rabbit or anti-human). **DMEM**= Dulbecco's modified eagle medium, **1dCD4**=one domain CD4 sizing control, **2dCD4**= purified 2dCD4 protein. **Cons. C**= purified Vpu protein, **05ZAFV5**= purified Vpu protein.

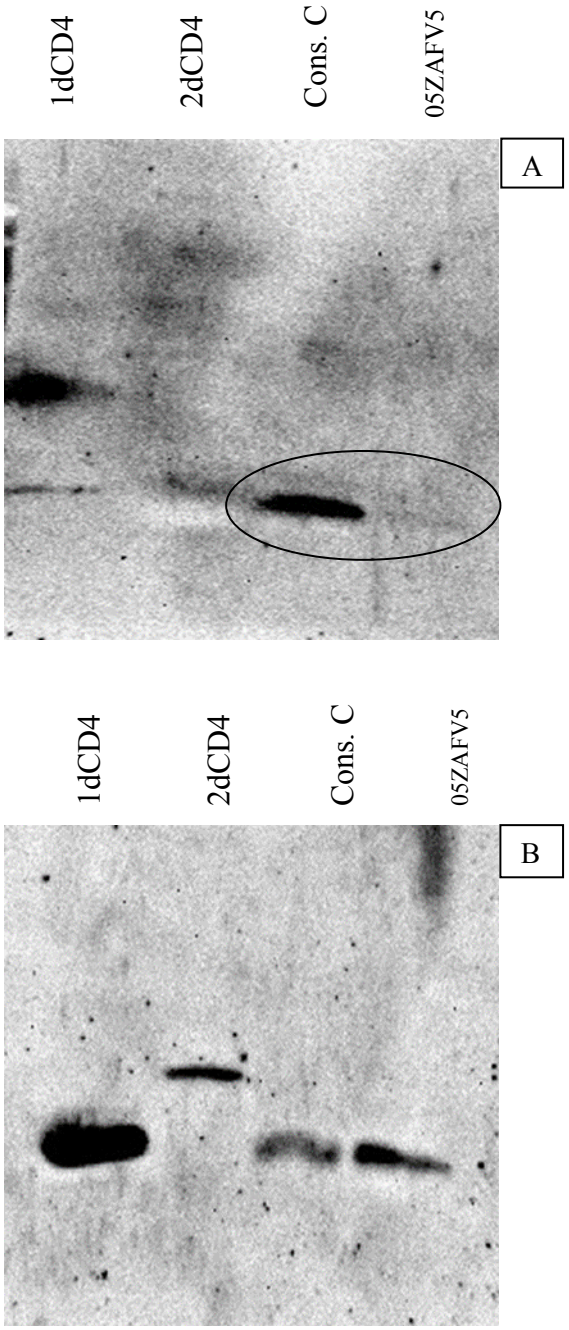


Figure 3.13: Western blots probed with anti-Vpu rabbit sera or anti-polyhistidine antibody. Western blot analyses conducted in conjunction with dot blot analyses. In **A**, the Western blot was probed with Anti-Vpu Rabbit Antiserum against subtype C Vpu. Cons. C Vpu was detected as shown in circle, 05ZAFV5 may have been detected as well as shown in circle but the banding is unclear. 1dCD4 and 2dCD4 were not detected as expected. In **B**, the Western blot was probed with an anti-polyhistidine antibody, all proteins were detected as expected. **1dCD4**=one domain CD4 sizing control, **2dCD4**=purified 2dCD4 protein, **Cons. C**= purified Cons. C Vpu protein, **05ZAFV5** = purified 05ZAFV5 Vpu protein.

Chapter 4

4.1 Discussion

HIV-1 specific CD8+ CTL responses eliminate virus-infected cells by recognizing virus-derived epitopes presented by HLA class I molecules on the surface of the infected cell. The HLA-restricted CTL response plays a major role in the immune control of HIV-1 infection, and is a major mechanism whereby HIV-1 evades the immune response by selecting HLA-restricted CTL escape mutations that allow the virus to evade immune recognition. In this study, immune escape in understudied Vif, Vpr and Vpu epitopes from two cohorts of HIV-1 infected patients in South Africa were analysed in order to further understand the role that HLA class I immune pressure has on HIV-1 immune escape in accessory proteins over time. The longitudinal Lung cohort samples (n=18) were selected to allow for the evaluation of immune escape mutations in Vif, Vpr and Vpu in the context of *HLA-B* alleles associated with slower or more rapid disease progression at a time when their clinical progression was comparable (that is, their CD4+ T cell count and viral loads were not significantly different between the *HLA-B*58:01* and *HLA-B*58:02* individuals). At least 50% of the Lung cohort patients were initiated on antiretroviral drug therapy during the follow-up period. By contrast, the M002 cohort samples (n=7) were from antiretroviral drug naïve patients with consistently high viral loads throughout their follow-up period.

4.1.1 RT-PCR and analysis of Vif, Vpr and Vpu functional domains

Of the 44 available Lung cohort samples, only 21 were successfully RT-PCR amplified and sequenced. This included eight patients with longitudinal sequence data, and three patients with sequence from a single time point only (these were not analysed further). It is possible that the patient samples were not processed and stored optimally prior to being sent to our laboratory. Additionally, long term freezer storage, and potential freeze-thaw cycles can affect RNA quality and concentration, therefore it is not unexpected that some samples were unable to be amplified by PCR (Ginocchio et al., 1997). The low viral loads (<50 RNA copies/ml) in four of the Lung cohort patients who were on antiretroviral therapy at the time also likely attributed to their unsuccessful amplification. Of the 28 available M002 samples, 26 (from all seven patients) were successfully RT-PCR amplified and sequenced. Thus, longitudinal sequence data was available from 15 patients between the two cohorts.

Analysis of longitudinal HIV-1 sequences from the same patient offers the opportunity to observe any changes that occur due to immune pressure in the HIV-1 genome over time. Substitutions, insertions, deletions and frame-shifts can take place conferring possible immune escape mutations. Of importance for this study are the functional regions of the Vif, Vpr and Vpu regions and possible mutations within those regions.

Longitudinal amino acid sequence analysis of the functional regions of HIV-1 Vif from both the Lung and M002 cohorts revealed that many of the important functional regions of Vif such as the SOCS-box region and N-terminal tryptophans are relatively conserved (**Figures 3.2A** and **3.3A**). Mutations within these regions would be disruptive and likely impact on viral fitness rather than confer an immune escape advantage for HIV-1. This is shown by Stanley and colleagues who described the importance of the SOCS-box region of Vif with mutations within the ^{144}SLQYLA^{149} and ^{161}PPLP^{164} motifs disrupting the interactions between Vif and APOBEC3G which would not be favourable for viral fitness (Stanley et al., 2008). Tian and colleagues also showed that any mutations within the N-terminal tryptophans would interfere with Vif binding to APOBEC3G/F (Tian et al., 2006). Also conserved throughout all the Vif sequences is the important zinc-ion binding motif ^{108}H^{114}C^{133}C^{139}H which is essential for Elongin C binding. The nuclear localization inhibitory site of Vif (RKKR for HIV-1 subtype B and the arginine-rich ^{90}RLRR^{93} for HIV-1 subtype C) (Farrow et al., 2005) of several of the patient sequences showed the most diversity. This region has been implicated in rendering Vif non-functional by causing Vif to localize to the nucleus rather than the cytoplasm where Vif carries out its APOBEC3G downregulatory functioning. In the case of HIV-1 subtype B, a change of RKKR to KKRK renders Vif nonfunctional. However, comparison of the sequences for the nuclear localization inhibitory site obtained in this study with other HIV-1 subtype C sequences deposited in the Los Alamos database confirmed this region is highly variable, and the polymorphisms described here are not novel.

With regards to amino acid sequence changes in the HIV-1 Vpr functional regions, the ^{71}H(S/N)RIG^{75} motif in patient 722 from the M002 cohort (**Figure 3.3B**) was HYRIG. H(S/N)RIG is implicated in apoptosis of infected HIV-1 cells with the H(S/N)RIG motif binding adenine nucleotide translocator (ANT) which is a component of the mitochondrial permeability transition pore complex (PTPC) (Macreadie et al., 1996, Jacotot et al., 2001). A mutation within this region (R77Q) was noted by Lum and colleagues and it was found that a large percentage of LTNPs carry this mutation which is said to decrease the apoptotic effects

of Vpr (Lum et al., 2003). Interestingly, HIV-1 subtype C carries a glutamine at position 77 in its wild-type form therefore it is possible that the apoptotic functioning of subtype C Vpr is different from subtype B, with other authors noting that the R77Q mutation is subtype dependant (Fischer et al., 2004, Jacotot et al., 2001). Thus an additional polymorphism, such as the ^{72}Y described here may have an impact on HIV-1 subtype C Vpr mediated apoptosis. Although rare, the ^{72}Y was detected in other non-C subtype Vpr sequences in the Los Alamos database.

The functional domains within the Lung and M002 HIV-1 Vpu sequences were relatively conserved, in particular, the essential serine residues (located at positions 58 and 62 for subtype C) which are phosphorylated by casein kinase II and are vital sites for interaction of Vpu with βTrCP, and thus the functioning of Vpu (**Figures 3.2C and 3.3 C**). Variability was noted in a potential casein kinase II site consisting of the residues ^{71}TMVD^{74}, downstream from the conserved serine residues. Bell and colleagues hypothesised that the potential casein kinase II phosphorylation site, TMVD, may be involved in a particular subtype C-specific intracellular trafficking pattern (Bell et al., 2007). The amino acid variability noted in the hinge region of Vpu has been reported in other HIV-1 subtype C sequences in the Los Alamos website. Interestingly, the putative Golgi export signal ^{78}LRLL^{81} is generally highly conserved amongst HIV-1 subtype C sequences. Thus the variation in this motif noted in Lung cohort patient 225 (twelve months; **Figure 3.2C**), and M002 patients 423 and 424 (**Figure 3.3C**) may impact on Vpu localization to the plasma membrane, and subsequently Vpu function in these patients.

4.1.2 HLA class I background and targeted motifs

It is interesting to consider the implications of HLA class I genotypes of the chosen Lung and M002 patients. The 18 longitudinal Lung cohort samples were selected on the basis of their *HLA-B*58:01* (n=4) and *HLA-B*58:02* (n=14) background. *HLA-B*58:01* has been associated with protective outcomes in disease progression and is closely related to the protective *HLA-B*57:01*, differentiated by a few amino acid differences within the B pocket resulting in similar anchor residues for binding motifs (Goulder et al., 1996). Variation within the Gag epitope TSTLQEQIAW or otherwise known as TW10 was described in a study of 311 subjects and associated with the *HLA-*B58:01* genotype (Leslie et al., 2004). It was noted that the variation within TW10 was in fact the result of escape mutations with a decreased recognition by *B*58:01*. The mutations that result due to immune pressure from

*B*58:01* impart a fitness cost on HIV-1. The T242N mutation which arises in the TW10 epitope is highly predictable and reduces viral replicative capacity due to a loss of stabilisation within the p24 Gag capsid protein (Martinez-Picado et al., 2006). The balance between immune pressure and immune escape during HIV-1 infection is integral to the progression of disease and can result in positive or negative outcomes for the patient in question. Reversion of escape mutations can occur once the immune pressure of a said HLA allele is lifted, such as in *B*58:01*, with Leslie and colleagues describing a case of mother-to child-transmission in which a *B*58:01*-negative child was infected with an HIV-1 strain carrying a *B*58:01* induced mutation followed by a complete loss of the transmitted mutation after 5 years (Leslie et al., 2004).

In contrast to *HLA-B*58:01* HIV-1 positive patients, patients with the *HLA-B*58:02* allele/s normally exhibit a poor prognosis, yet the two HLA antigens differ by only three amino acids (Kiepiela et al., 2004). Ngumbela and colleagues looked at a cohort of over 1000 people and found consistent high viral loads and decreased CD4+ T cell counts for patients with the *HLA-B*58:02* allele, and those that were homozygous for the allele exhibited even further decreases in viral loads and CD4+ T cell counts (Ngumbela et al., 2008). Additionally, it was shown that a lack of immune pressure is applied by *HLA-B*58:02* on its targeted HIV-1 epitope as compared to *HLA-B*58:01,* indicative of its ineffectiveness at controlling disease progression. Leslie and colleagues addressed the effects that combinations of protective and deleterious HLA types would have on an individual, which included examination of the *HLA-B*58:02* allele. It was found that HLA alleles act in an additive fashion (Leslie et al., 2010). Patients that had only protective alleles had significantly lower viral loads and higher CD4+ T cell counts as compared to those individuals that possessed a combination of protective and deleterious alleles. It can be hypothesized that a single HLA allele does not completely dominate an immune response, but rather acts in an additive fashion (Leslie et al., 2010).

Vif, Vpr and Vpu sequence data were obtained for two of the *HLA-B*58:01* individuals and six of the *HLA-B*58:02* individuals. These alleles are very common within the black South African population with frequencies of ~8% and ~9% respectively (Paximadis et al., 2011). These 2 HLA genotypes also have seemingly opposing effects on disease progression. *HLA-B*58:01* is associated with protective outcomes in disease progression while *HLA-B*58:02* is associated with deleterious outcomes (Kiepiela et al., 2004, Leslie et al., 2004). The HLA genotypes were determined and successfully assigned for the M002 cohort. Interestingly,

three of the M002 cohort patients were heterozygous for *HLA-B*58:02* (025, 422, 722; **Table 3.2**).

Overall, HLA-driven escape mutations in Vif, Vpr and/or Vpu were identified in four and six of the Lung and M002 patients, respectively (**Figures 3.4 and 3.5**). Interestingly, none of the identified escape mutations are amongst the best described and most optimal HIV-1 CD8+ CTL epitopes of HIV-1 accessory proteins in the databases (**Table 1.1**). There were eight HLA alleles that contributed to immune escape in the Lung cohort Vif, Vpr and/or Vpu sequences. The specific population allele frequencies of *HLA-A*02:05*, *HLA-A*29:02, HLA-A*68:01, HLA-B*08:01, HLA-B*44:03, HLA-B*58:01, HLA-C*06:02, HLA-C*07:01* in these populations are 6.78%, 6.28%, 3.27%, 6.39%, 5.64%, 8.14%, 14.94% and 7.59% respectively (Paximadis et al., 2011). For the M002 cohort, there were 11 HLA alleles that contributed to immune escape in the Vif, Vpr and/or Vpu sequences. The specific population allele frequencies of *HLA-A*02:01, HLA-A*03:01, HLA-A*26:01, HLA-B*07:02, HLA-B*51:01, HLA-C*03:04, HLA-C*04:01, HLA-C*06:02, HLA-C*07:01, HLA-C*07:02* and *HLA-C*08:02* were 8.29%, 6.53%, 0.75%, 4.58%, 1.02%, 5.06%, 11.9%, 14.94%, 7.59%, 5.82% and 2.28%, respectively (Paximadis et al., 2011).

When looking at the Los Alamos HIV Database list of Best-defined CTL/CD8+ Epitopes specifically for Vif, Vpr and Vpu, there are only two cohort HLA alleles associated with Vif – *HLA-A*03:01* (Addo et al., 2002b) and *HLA-B*07:02* (Altfeld et al., 2001) and one HLA allele associated with Vpr, *HLA-B*07:02* (Cardinaud et al., 2009). Although six of the nine identified HLA alleles in the Lung cohort individuals, and five of the 11 identified HLA alleles in the M002 cohort individuals are described in the database, this is in the context of other HIV-1 proteins such as Gag, Pol, Nef and gp160 (Martin et al., 2014, Sabbaj et al., 2003, Borghans et al., 2007, Rachinger et al., 2008, Geldmacher et al., 2007).

Of the individuals that showed escape mutations in HIV-1 Vif, Vpr and/or Vpu from the Lung cohort (**Figure 3.4**), one was *HLA-B58:01* and three were *HLA-B58:02*. The HIV-1 Vif from patient 007 showed an escape mutation from *HLA-C*06:02* driven immune pressure at position 189, from a valine to a methionine at 6 months, which persisted, as seen in the 12 month sequence. Interestingly, the viral loads increased from 5,867 RNA copies/ml in the baseline sample to 23,963 RNA copies/ml at 6 months, likely attributed to immune escape (in Vif and possibly other HIV-1 proteins) impacting on viral replication.

Longitudinal sequence analysis of HIV-1 from Lung cohort patient 093 revealed HLA-driven escape mutations in Vif, Vpr and Vpu. Two mutations at Vif positions 63 (I to T) and 154 (I to T) in 093 sequences (detected at 12 months) attributed to escape from *HLA-B*44:03*/*HLA-C*06:02* and *HLA-C*06:02*, respectively. Similarly, two escape mutations in Vpr from *HLA-A*68:01* and *HLA-B*44:03* at 12 months were noted. Lastly, one mutation in Vpu at position 31 detected at 12 months resulted in escape from *HLA-A*68:01* and *HLA-C*06:02*. Viral loads increased from 30,038 RNA copies/ml to 67,829 RNA copies/ml at 12 months, likely attributed to HLA-driven immune escape mechanisms. *HLA-B*44:03* found in patient 093 has previously been shown to promote transient escape mutations within Gag and Nef during the early phase of HIV-1 infection (Martin et al., 2014).

Interestingly, HIV-1 Vif sequences from Lung cohort patient 225 revealed mutations in five positions, which allowed for escape from *HLA-A*02:05*, *HLA-B*58:01,* and *HLA-B*08:01* driven immune pressure at 12 months. Additionally, three Vpr mutations driven by *HLA-A*02:05*, *HLA-B*58:01,* and *HLA-B*08:01* were detected. Viral loads in this patient increased from baseline (5,055 RNA copies/ml) to 12 months (10,442 RNA copies/ml). *HLA-A*02:05* has previously been shown to target gp41, whilst *HLA-B*08:01* has been shown to be associated with slower disease progression and is said to target the p24 protein (Sabbaj et al., 2003, Borghans et al., 2007). It is intriguing to note that although *HLA-B*58:01* is considered a protective allele, particularly in the context of Gag, it appears to drive escape mutations in Vif and Vpr in this patient. It will be worthwhile evaluating the full impact of this on disease progression.

Lastly, HLA-driven escape mutations for *HLA-A*29:02*, *HLA-B*44:03* and *HLA-C*06:02* in Vpr (n=2) and Vpu (n=1) were identified in Lung cohort patient 472 at the 6 month timepoint. As expected, viral loads in this patient increased from 85,150 RNA copies/ml to 250,823 RNA copies/ml at 6 months, likely attributed to the immune escape mutations. *HLA-A*29:02* has previously been shown to target Gag, but no known deleterious or protective effects on disease progression have been shown (Rachinger et al., 2008).

For the M002 cohort (**Figure 3.5**), several immune escape and reversion mutations were detected in the longitudinal samples of six of the seven patients analysed. It is interesting to note that reversion mutations occured within the M002 cohort and considering the importance

of the protein regions in question, it can be hypothesised that these mutations may have imparted a fitness cost resulting in reversion.

Virus from patient 006 had detectable mutations at positions 33 and 39 in Vif driven by *HLA-A*26:01* or *HLA-C*07:01* immune pressure and at position 125 (*HLA-C*08:02)* at 6 months, but these had reverted back to the baseline sequence by 12 months. The epitope at positions 33 and 39 where this reversion occurs overlaps with an important tryptophan at position 38 required for APOBEC3G binding (Mehle et al., 2007). The other reversion which occurs at position 125 is within the vicinity of the HCCH zinc binding motif essential for Vif-Cullin5 binding (Mehle et al., 2006). Vpu (*HLA-B*51:01*; *HLA-A*26:01*) escape at positions 6 and 17 occurred at 18 months, but reverted back at 24 months. This mutation is in the important transmembrane domain of Vpu and required for functionality in restricting tetherin (Van Damme et al., 2008, Candler et al., 2005). Viral load in this patient increased from baseline to 18 months, but unfortunately no viral load was available for the 24 months sample. It is possible that viral load may have dropped due to the reversion mutations noted here, and the patient regaining immune control of viral replication.

The HIV-1 Vpu sequences in patient 025 (*HLA-A*02:01*) showed one escape mutation at position 5 which was detected at 12 months, and persisted until reversion was detected in the 24th month sample. Interestingly, viral loads dropped between baseline and 18 months in this patient.

Sequence analysis of Vif from patient 422 revealed one escape mutation in Vif, driven by *HLA-C*04:01* pressure detected in the 12 months sample, which persisted up to 18 months. Similarly, one mutation in Vpu driven by *HLA-C*06:02* pressure at 12 months persisted in the 18 month sample analysed. Viral loads in this patient increased from baseline (146,000 RNA copies/ml) to 18 months (407,000 RNA copies/ml), likely attributed, in part, to these immune escape mutations.

HLA-driven immune escape mutations in patient 423 showed a complex profile, with one mutation in Vif detected at 12 months, reverting back to baseline at 18 months, and then back mutating at 24 months (driven by *HLA-A*03:01*). The Vpr sequences revealed a mutation at position 31 at 6 months (driven by *HLA-B*07:02* or *HLA-C*07:02*), which reverted back to the baseline sequence by 12 months, and remained stable up to 24 months.

What is interesting about this particular mutation is that it occurs within α-helix-1 which is important for Vpr nuclear import by binding of α-importin, and the related epitope overlaps amino acid residues known to regulate Vpr binding to α-importin with mutations within this region shown to be deleterious to Vpr functioning when mutated (Nitahara-Kasahara et al., 2007, Kamata and Aida, 2000). Two mutations in Vpu, one at position 21 (recognised by *HLA-B*07:02*) was detected in the 24 months sample, and the second, at position 81 (recognised by *HLA-B*07:02*) was detected at 12 months, reverted back to baseline at 18 months and remained stable up to 24 months. The second mutation at residue 81 and related epitope in question forms part of, and overlaps the unique HIV-1 subtype C motif LRLL, which may have possible Golgi signal functionality (Bell et al., 2007). Viral loads increased from 49,700 RNA copies/ml (baseline) to 70,900 RNA copies/ml at 18 months. *HLA-B*07:02* is shown to target a single Vif and Vpr epitope, according to the Los Alamos Best-defined CTL/CD8+ Epitope list. This was one of two only cohort-related HLA alleles associated with Vif and Vpr. It has been shown that *HLA-B*07:02* is associated with lower mean viral loads in HIV-1 infected patients coupled with an increase in recognition of a Gag epitope and is possibly considered a protective allele (Geldmacher et al., 2007). In contrast, Kloverpris and colleagues noted that *HLA-B*07:02* was associated with increased disease progression in HIV-1 subtype B infected individuals, but for HIV-1 subtype C infected individuals, it was not associated with increased disease progression, and an increase in Gag-specific responses was shown (Kloverpris et al., 2014). Altfeld and colleagues described a common *HLA-B*07:02*-restricted Vpr epitope, ^{34}FPRIWLHGL^{42}, in the context of CTL responses in the HIV-1 accessory proteins with *HLA-B*07:02* shown to be a common restricting HLA allele of the HIV-1 accessory proteins (Altfeld et al., 2001).

Virus from patient 424 had one immune escape mutation in Vif at 18 months, attributed to *HLA-C*03:04* driven pressure which persisted up to the 24 month sample tested. Viral loads increased from 50,000 RNA copies/ml (baseline) to 77,500 RNA copies/ml at 18 months.

Interestingly, patient 722, similar to patient 423, had one mutation in Vif (driven by *HLA-A*03:01* pressure) which was detected in the 12 months sample, reverted to the baseline sequence at 18 months, and then mutated back at 24 months. Viral loads in this patient decreased from 171,000 RNA copies/ml (baseline) to 79,200 RNA copies/ml at 18 months. *HLA-A*03:01* is shown to target three different Vif epitopes according to the Los Alamos Best-defined CTL/CD8+ Epitope list. This was one of two cohort-related HLA alleles

associated with Vif and/or Vpr. Addo and colleagues described three different Vif peptide regions that could be targeted by *HLA-A*03:01* namely ^{28}HMYISKKAK^{36}, ^{17}RIRTWKSLVK^{26} and ^{158}KTKPPLPSVKK^{168} according to the HXB2 reference sequence, but none of these showed any sign of escape in the respective M002 patients (Addo et al., 2002b).

Lastly, in the patient (020) with no detectable HLA-driven escape mutations in Vif, Vpr and Vpu, the viral load remained relatively stable, 10700 RNA copies/ml at baseline, when compared to 9330 RNA copies/ml at 18 months.

It is also important to note that HLA-driven escape is complex and not simply determined by a loss of recognition of epitopes due to mutations within anchor residues alone. Mutations within epitopes but not necessarily in anchor regions may affect how the epitope is processed intracellularly and presented, whilst other mutations may affect other processes independent of epitope presentation such as decreasing the recognition of TCRs for specific epitope-HLA class I complexes (Reviewed in Carlson et al., 2015, Yokomaku et al., 2004, Iglesias et al., 2011) . Mutations flanking important functional regions of a gene may also have a deleterious effect on its functioning (Guarnieri et al., 2006).

In summary, HLA-driven immune pressure in the Vif, Vpr and/or Vpu motifs described here which resulted in amino acid sequence changes (or reversion to baseline sequences) may have contributed to the changes in viral loads (increases or decreases) seen in these patients over time, and likely impacted on disease progression, albeit in combinations with escape mutations in the more highly targeted HIV-1 proteins, such as Gag, Pol and Nef. Future work looking at longitudinal sequence analysis of the entire HIV-1 proteome in these patients will likely reveal the contributing factors leading to immune escape and ultimately impact disease progression to AIDS.

4.1.3 Expression of recombinant Vpu proteins

Based on preliminary data from our laboratory that Vpu is more highly targeted by CD8+ T cells in 14 LTNPs/elite controllers compared to other regulatory regions, and five of the LTNPs/elite controllers studied had NK cell responses to HIV-1 Vpu peptide pools (likely mediated by HIV-specific ADCC antibodies), we cloned and expressed representative HIV-1

subtype C Vpu for the ultimate detection of anti-Vpu antibodies in patient sera from the different cohorts. Overall, three recombinant HIV-1 subtype C Vpu proteins were successfully expressed and partially purified during the course of this study.

The *vpu* sequences used in this study (Cons. C, 052AFV5, 052AFV15) were all obtained from a study by Bell and colleagues (Bell et al., 2007). Two of the sequences (Cons. C, 052AFV5) were typical of HIV-1 subtype C strains with lengths of 86 amino acid residues as compared to other subtype Vpu proteins such as those derived from subtype B, which normally have a length of ~81 amino acids (McCormick-Davis et al., 2000). The 052AFV15 sequences was selected because of the four amino acid deletion in the N-terminus of the protein (82 amino acid residues), thus it is more comparable to an HIV-1 subtype B Vpu. Trafficking of HIV-1 subtype B and C Vpu has been shown to be different, with subtype C Vpu being trafficked more readily to the cellular plasma membrane (Ruiz et al., 2008). Interestingly, this did not appear to affect the expression levels of the three recombinant Vpu proteins, as all seemed to express in similar quantities, albeit in low amounts only detectable by Western blotting.

Low levels of recombinant protein expression can be attributed to various factors. Firstly, *vpu* genes need to be codon optimized in order to increase expression levels, with Nguyen and colleagues showing for the first time the importance of codon optimization of *vpu* (Nguyen et al., 2004). Vpu expression in its natural setting is dependent on HIV-1 regulatory proteins Tat and Rev (Schwartz et al., 1990, Kjems and Askjaer, 2000). When *vpu* mRNA is generated in an autonomous expression system the RNA itself is unstable due to poor cytoplasmic export. The *vpu* genes expressed in this study were codon optimized (humanized) therefore it is highly doubtful that this contributed to the low levels of expression seen during the study.

Secondly, the choice of host cell for protein synthesis is an important consideration. The protein expression and purification protocol for this study was adapted from Lv and colleagues who transiently expressed recombinant his-tagged Vpu proteins in mammalian cells (Lv et al., 2013). Due to Vpu's integration into cellular membranes by way of its transmembrane domain, a prokaryotic system of expression could prove problematic. Additionally, mammalian expression systems were the system of choice in this study because they provide a native cellular environment for Vpu expression, including post-translational modifications, and negate the need for protein folding procedures required for inactive

proteins derived from inclusion bodies expressed in bacterial expression systems (Reviewed in Sahdev et al., 2008). This is particularly relevant, since the ultimate use of the recombinant Vpu is for the detection of anti-Vpu antibodies in HIV-1 infected patient sera, and protein folding and tertiary/quaternary structures are critical for optimal epitope recognition. Nevertheless, bacterial expression systems do have advantages, such as large scale expression with fast cellular growth kinetics, ease of DNA transformation and the relatively inexpensive reagents used for growth media (Reviewed in Rosano and Ceccarelli, 2014). Vpu expression in bacterial systems and purification of the Vpu has been described previously. Ma and colleagues were able to express full length, transmembrane and cytoplasmic sections of recombinant his-tagged Vpu using a bacterial expression system and purification from inclusion bodies (Ma et al., 2002). The proteins were used for Nuclear magnetic resonance (NMR) and Vpu ion channel activity was analysed. Vpu is said to have apparent ion-channel activity due to its structural similarity to influenza virus M2 proteins (Pinto et al., 1992, Park et al., 2003), with the authors confirming functionality of the Vpu proteins based on their ion-channel activity. Thus, it is worthwhile considering bacterial expression in future studies.

A further difficulty that may have compounded the low recombinant protein expression seen during this study is the membrane association of Vpu. Purification of membrane proteins is particularly difficult due to their hydrophobicity, with Vpu itself containing a highly hydrophobic transmembrane domain (Park et al., 2006). Hydrophobic proteins such as Vpu are at risk of precipitating out of solution and this may very well be one of the reasons for the low yields of purified Vpu seen during this study. Free surface area can also be problematic as cell membranes have a limited amount of free surface area that can accommodate Vpu protein, therefore possibly decreasing protein yields. Use of a detergent is essential when purifying a membrane protein in order for extraction and dissolution of the protein to occur, but detergents can be denaturing or lead to protein aggregation (Reviewed in Wiener, 2004). Triton X-100, a nonionic detergent, is said to solubilize membrane proteins in a native state and therefore may not have played a role in the low yields seen during protein purification (Makino et al., 1973, Reviewed in Kalipatnapu and Chattopadhyay, 2005).

Interestingly, the study by Lv and colleagues, from which the Vpu expression and purification protocol was adapted, also faced difficulties with obtaining sufficient recombinant Vpu protein yields (Lv et al., 2013). Vpu has the ability to form oligomers (Maldarelli et al., 1993). Lv and colleagues speculated that due to this oligomer formation,

the his-tag on the Vpu proteins can become embedded within the oligomer, resulting in poor binding to Ni^{2+}-charged agarose beads used in affinity chromatography procedures (Lv et al., 2013). Indeed, in this author's study unknown proteins with sizes greater than 50 kDa were noted throughout the entire purification procedure, indicative of their histidine-rich nature and possible identification as Vpu oligomers. Maldarelli and colleagues noted that aggregating Vpu forms oligomers of ~80 kDa which is comparable to the high kDa protein bands noted throughout this author's study. What is confounding is that untransfected cell lysate did exhibit similar banding patterns leading to the possibility of the unknown proteins being an inherent histadine rich protein in HEK293 cells. There is the caveat though that untransfected cell lysate was not processed through the entire purification procedure for a direct comparison.

Future work needs to focus on optimizing the expression levels of recombinant Vpu, either in a mammalian or bacterial expression system, but more importantly, a purification protocol which will provide sufficient purity of the expressed proteins with consistent results for use in ELISA, Western blots and dot blots is urgently needed.

4.2 Conclusions

This study describes HLA A, B and C-driven immune escape in Vif, Vpr and Vpu epitopes from HIV-1 infected patients in South Africa. Longitudinal plasma samples from eight of 18 patients from the Lung cohort and seven patients from the M002 cohort were successfully RT-PCR amplified and sequenced. HLA-A, B and C alleles were typed and assigned for the M002 cohort individuals (data was available for the Lung cohort). HLA-driven CTL escape mutations in Vif, Vpr and/or Vpu were detected in four (50%) patients from the Lung cohort and six (86%) from the M002 cohort. Additionally, some reversions to the baseline sequences were noted over time for the M002 cohort. Interestingly, none of the identified escape mutations are amongst the best described and most optimal HIV-1 CD8+ CTL epitopes of HIV-1 accessory proteins in the databases. Overall, the HLA-driven immune pressure in the Vif, Vpr and/or Vpu motifs described in this study may have in part contributed to the changes in viral loads (increases and decreases) noted in these patients over time, and likely impacted on disease progression, albeit in combination with escape mutations in the more highly targeted HIV-1 proteins, such as Gag, Pol and Nef.

Three selected *vpu* sequences, cons.C, 05ZAFV05 and 05ZAFV15, were successfully used to express and purify recombinant Vpu proteins in HEK 293T mammalian cell lines. Protocols for expression and purification were established and, as evidenced by SDS-PAGE, Western blot and dot blot analyses, the purification protocol used in this study did not provide sufficient protein yields and purity required for subsequent use. Ongoing work focusing on optimization of Vpu expression and purification will provide the recombinant Vpu necessary to fully elucidate the role of Vpu and anti-Vpu immune responses in control of HIV-1 infection.

5 References

ADDO, M. M., ALTFELD, M., RATHOD, A., YU, M., XU, G. Y., GOULDER, P. J., ROSENBERG, E. S. & WALKER, B. D. 2002a. HIV-1 Vpu represents a minor target for cytotoxic T lymphocytes in HIV-1-infection. *AIDS,* 16**,** 1071-1073.

ADDO, M. M., YU, X. G., ROSENBERG, E. S., WALKER, B. D. & ALTFELD, M. 2002b. Cytotoxic T-Lymphocyte (CTL) Responses Directed against Regulatory and Accessory Proteins in HIV-1 Infection. *DNA and Cell Biology,* 21**,** 671-678.

ALMEIDA, J. R., PRICE, D. A., PAPAGNO, L., ARKOUB, Z. A., SAUCE, D., BORNSTEIN, E., ASHER, T. E., SAMRI, A., SCHNURIGER, A., THEODOROU, I., COSTAGLIOLA, D., ROUZIOUX, C., AGUT, H., MARCELIN, A.-G., DOUEK, D., AUTRAN, B. & APPAY, V. 2007. Superior control of HIV-1 replication by CD8+ T cells is reflected by their avidity, polyfunctionality, and clonal turnover. *The Journal of Experimental Medicine,* 204**,** 2473-2485.

ALTER, G., HECKERMAN, D., SCHNEIDEWIND, A., FADDA, L., KADIE, C. M., CARLSON, J. M., ONIANGUE-NDZA, C., MARTIN, M., LI, B. & KHAKOO, S. I. 2011. HIV-1 adaptation to NK-cell-mediated immune pressure. *Nature,* 476**,** 96-100.

ALTER, G., MARTIN, M. P., TEIGEN, N., CARR, W. H., SUSCOVICH, T. J., SCHNEIDEWIND, A., STREECK, H., WARING, M., MEIER, A., BRANDER, C., LIFSON, J. D., ALLEN, T. M., CARRINGTON, M. & ALTFELD, M. 2007. Differential natural killer cellâ€“mediated inhibition of HIV-1 replication based on distinct KIR/HLA subtypes. *The Journal of Experimental Medicine,* 204**,** 3027-3036.

ALTER, G. & MOODY, M. A. 2010. The humoral response to HIV-1: new insights, renewed focus. *The Journal of Infectious Diseases,* 202 Suppl 2**,** S315-22.

ALTFELD, M., ADDO, M. M., ELDRIDGE, R. L., YU, X. G., THOMAS, S., KHATRI, A., STRICK, D., PHILLIPS, M. N., COHEN, G. B., ISLAM, S. A., KALAMS, S. A., BRANDER, C., GOULDER, P. J. R., ROSENBERG, E. S., WALKER, B. D. & COLLABORATION, T. H. S. 2001. Vpr Is Preferentially Targeted by CTL During HIV-1 Infection. *The Journal of Immunology,* 167**,** 2743-2752.

ALTFELD, M., ADDO, M. M., ROSENBERG, E. S., HECHT, F. M., LEE, P. K., VOGEL, M., YU, X. G., DRAENERT, R., JOHNSTON, M. N., STRICK, D., ALLEN, T. M., FEENEY, M. E., KAHN, J. O., SEKALY, R. P., LEVY, J. A., ROCKSTROH, J. K., GOULDER, P. J. & WALKER, B. D. 2003. Influence of HLA-B57 on clinical presentation and viral control during acute HIV-1 infection. *Aids,* 17**,** 2581-91.

ALTFELD, M., KALIFE, E. T., QI, Y., STREECK, H., LICHTERFELD, M., JOHNSTON, M. N., BURGETT, N., SWARTZ, M. E., YANG, A., ALTER, G., YU, X. G., MEIER, A., ROCKSTROH, J. K., ALLEN, T. M., JESSEN, H., ROSENBERG, E. S., CARRINGTON, M. & WALKER, B. D. 2006. HLA Alleles Associated with Delayed Progression to AIDS Contribute Strongly to the Initial CD8(+) T Cell Response against HIV-1. *PLoS Med,* 3**,** e403.

ALVAREZ, R. A., HAMLIN, R. E., MONROE, A., MOLDT, B., HOTTA, M. T., RODRIGUEZ CAPRIO, G., FIERER, D. S., SIMON, V. & CHEN, B. K. 2014. HIV-1 Vpu Antagonism of Tetherin Inhibits Antibody-Dependent Cellular Cytotoxic Responses by Natural Killer Cells. *Journal of virology,* 88**,** 6031-6046.

ANDERSEN, J. L., DEHART, J. L., ZIMMERMAN, E. S., ARDON, O., KIM, B., JACQUOT, G., BENICHOU, S. & PLANELLES, V. 2006. HIV-1 Vpr-Induced Apoptosis Is Cell Cycle Dependent and Requires Bax but Not ANT. *PLoS Pathog,* 2**,** e127.

ANDREW, A. J., KAO, S. & STREBEL, K. 2011. C-terminal Hydrophobic Region in Human Bone Marrow Stromal Cell Antigen 2 (BST-2)/Tetherin Protein Functions as Second Transmembrane Motif. *Journal of Biological Chemistry,* 286**,** 39967-39981.

ARIAS, J. F., HEYER, L. N., VON BREDOW, B., WEISGRAU, K. L., MOLDT, B., BURTON, D. R., RAKASZ, E. G. & EVANS, D. T. 2014. Tetherin antagonism by Vpu protects HIV-infected cells from antibody-dependent cell-mediated cytotoxicity. *Proceedings of the National Academy of Sciences,* 111**,** 6425-6430.

BACHAND, F., YAO, X. J., HRIMECH, M., ROUGEAU, N. & COHEN, E. A. 1999. Incorporation of Vpr into human immunodeficiency virus type 1 requires a direct interaction with the p6 domain of the p55 gag precursor. *J Biol Chem,* 274**,** 9083-91.

BAGGALEY, R. F., WHITE, R. G. & BOILY, M. C. 2010. HIV transmission risk through anal intercourse: systematic review, meta-analysis and implications for HIV prevention. *International Journal of Epidemiology,* 39**,** 1048-63.

BAR, K. J., LI, H., CHAMBERLAND, A., TREMBLAY, C., ROUTY, J. P., GRAYSON, T., SUN, C., WANG, S., LEARN, G. H. & MORGAN, C. J. 2010. Wide variation in the multiplicity of HIV-1 infection among injection drug users. *Journal of virology,* 84**,** 6241-6247.

BARTEE, E., MCCORMACK, A. & FRUH, K. 2006. Quantitative membrane proteomics reveals new cellular targets of viral immune modulators. *PLoS Pathog,* 2**,** e107.

BAUR, A. S., SAWAI, E. T., DAZIN, P., FANTL, W. J., CHENG-MAYER, C. & MATIJA PETERLIN, B. 1994. HIV-1 nef leads to inhibition or activation of T cells depending on its intracellular localization. *Immunity,* 1**,** 373-384.

BELL, C. M., CONNELL, B. J., CAPOVILLA, A., VENTER, W. D., STEVENS, W. S. & PAPATHANASOPOULOS, M. A. 2007. Molecular characterization of the HIV type 1 subtype C accessory genes vif, vpr, and vpu. *AIDS research and human retroviruses,* 23**,** 322-330.

BERGER, E. A., DOMS, R. W., FENYO, E. M., KORBER, B. T. M., LITTMAN, D. R., MOORE, J. P., SATTENTAU, Q. J., SCHUITEMAKER, H., SODROSKI, J. & WEISS, R. A. 1998. A new classification for HIV-1. *Nature,* 391**,** 240-240.

BERGER, G., LAWRENCE, M., HUÉ, S. & NEIL, S. J. D. 2015. G2/M Cell Cycle Arrest Correlates with Primate Lentiviral Vpr Interaction with the SLX4 Complex. *Journal of Virology,* 89**,** 230-240.

BETTS, M. R., NASON, M. C., WEST, S. M., DE ROSA, S. C., MIGUELES, S. A., ABRAHAM, J., LEDERMAN, M. M., BENITO, J. M., GOEPFERT, P. A., CONNORS, M., ROEDERER, M. & KOUP, R. A. 2006. HIV nonprogressors preferentially maintain highly functional HIV-specific CD8+ T cells. *Blood,* 107**,** 4781-9.

BOILY, M.-C., BAGGALEY, R. F., WANG, L., MASSE, B., WHITE, R. G., HAYES, R. J. & ALARY, M. 2009. Heterosexual risk of HIV-1 infection per sexual act: systematic review and meta-analysis of observational studies. *The Lancet Infectious Diseases,* 9**,** 118-129.

BOLDUAN, S., HUBEL, P., REIF, T., LODERMEYER, V., FRITZ, J. L. V., SAUTER, D., KIRCHHOFF, F., FACKLER, O. T., SCHINDLER, M. & SCHUBERT, U. 2013. HIV-1 Vpu affects the anterograde transport and the glycosylation pattern of NTB-A. *Virology,* 440**,** 190-203.

BORGHANS, J. A. M., MØLGAARD, A., DE BOER, R. J. & KE?MIR, C. 2007. HLA Alleles Associated with Slow Progression to AIDS Truly Prefer to Present HIV-1 p24. *PLoS ONE,* 2**,** e920.

BORTHWICK, N., AHMED, T., ONDONDO, B., HAYES, P., ROSE, A., EBRAHIMSA, U., HAYTON, E.-J., BLACK, A., BRIDGEMAN, A., ROSARIO, M., HILL, A. V. S., BERRIE, E., MOYLE, S., FRAHM, N., COX, J., COLLOCA, S., NICOSIA, A., GILMOUR, J., MCMICHAEL, A. J., DORRELL, L. & HANKE, T. 2014. Vaccine-elicited Human T Cells Recognizing Conserved Protein Regions Inhibit HIV-1. *Molecular Therapy,* 22**,** 464-475.

BOUHAMDAN, M., BENICHOU, S., REY, F., NAVARRO, J. M., AGOSTINI, I., SPIRE, B., CAMONIS, J., SLUPPHAUG, G., VIGNE, R., BENAROUS, R. & SIRE, J. 1996. Human immunodeficiency virus type 1 Vpr protein binds to the uracil DNA glycosylase DNA repair enzyme. *Journal of virology,* 70**,** 697-704.

BOULET, S., KLEYMAN, M., KIM, J. Y., KAMYA, P., SHARAFI, S., SIMIC, N., BRUNEAU, J., ROUTY, J.-P., TSOUKAS, C. M. & BERNARD, N. F. 2008. A combined genotype of KIR3DL1 high expressing alleles and HLA-B* 57 is associated with a reduced risk of HIV infection. *AIDS,* 22**,** 1487-1491.

BOUR, S., PERRIN, C., AKARI, H. & STREBEL, K. 2001. The human immunodeficiency virus type 1 Vpu protein inhibits NF-κB activation by interfering with βTrCP-mediated degradation of IκB. *Journal of Biological Chemistry,* 276**,** 15920-15928.

BOUR, S., SCHUBERT, U. & STREBEL, K. 1995. The human immunodeficiency virus type 1 Vpu protein specifically binds to the cytoplasmic domain of CD4: implications for the mechanism of degradation. *J Virol,* 69**,** 1510-20.

BRIGGS, J. A., SIMON, M. N., GROSS, I., KRAUSSLICH, H. G., FULLER, S. D., VOGT, V. M. & JOHNSON, M. C. 2004. The stoichiometry of Gag protein in HIV-1. *Nature Structural & Molecular Biology,* 11**,** 672-5.

BUTSCH, M. & BORIS-LAWRIE, K. 2002. Destiny of Unspliced Retroviral RNA: Ribosome and/or Virion? *Journal of virology,* 76**,** 3089-3094.

BUTTICAZ, C., MICHIELIN, O., WYNIGER, J., TELENTI, A. & ROTHENBERGER, S. 2007. Silencing of both beta-TrCP1 and HOS (beta-TrCP2) is required to suppress human immunodeficiency virus type 1 Vpu-mediated CD4 down-modulation. *Journal of Virology,* 81**,** 1502-5.

BUZON, V., NATRAJAN, G., SCHIBLI, D., CAMPELO, F., KOZLOV, M. M. & WEISSENHORN, W. 2010. Crystal Structure of HIV-1 gp41 Including Both Fusion Peptide and Membrane Proximal External Regions. *PLoS Pathog,* 6**,** e1000880.

CAMPBELL, E. M., NUNEZ, R. & HOPE, T. J. 2004. Disruption of the Actin Cytoskeleton Can Complement the Ability of Nef To Enhance Human Immunodeficiency Virus Type 1 Infectivity. *Journal of Virology,* 78**,** 5745-5755.

CAMPBELL, K. S. & PURDY, A. K. 2011. Structure/function of human killer cell immunoglobulin-like receptors: lessons from polymorphisms, evolution, crystal structures and mutations. *Immunology,* 132**,** 315-325.

CANDLER, A., FEATHERSTONE, M., ALI, R., MALONEY, L., WATTS, A. & FISCHER, W. B. 2005. Computational analysis of mutations in the transmembrane region of Vpu from HIV-1. *Biochimica et Biophysica Acta (BBA) - Biomembranes,* 1716**,** 1-10.

CARDINAUD, S., BOUZIAT, R., ROHRLICH, P.-S., TOURDOT, S., WEISS, L., LANGLADE-DEMOYEN, P., BURGEVIN, A., FIORENTINO, S., VAN ENDERT, P. & LEMONNIER, F. A. 2009. Design of a HIV-1-derived HLA-B07. 02-restricted polyepitope construct. *AIDS,* 23**,** 1945-1954.

CARLSON, J. M., LE, A. Q., SHAHID, A. & BRUMME, Z. L. 2015. HIV-1 adaptation to HLA: a window into virus-host immune interactions. *Trends in Microbiology,* 23**,** 212-24.

CHAN, D. C., FASS, D., BERGER, J. M. & KIM, P. S. 1997. Core structure of gp41 from the HIV envelope glycoprotein. *Cell,* 89**,** 263-273.

CHEN, R., LE ROUZIC, E., KEARNEY, J. A., MANSKY, L. M. & BENICHOU, S. 2004. Vpr-mediated Incorporation of UNG2 into HIV-1 Particles Is Required to Modulate the Virus Mutation Rate and for Replication in Macrophages. *Journal of Biological Chemistry,* 279**,** 28419-28425.

CHEN, Y.-M., REY, W.-Y., LAN, Y.-C., LAI, S.-F., HUANG, Y.-C., WU, S.-L., LIU, T.-T. & HSIAO, K.-J. 2003. Antibody reactivity to HIV-1 Vpu in HIV-1/AIDS patients on highly active antiretroviral therapy. *Journal of Biomedical Science,* 10**,** 266-275.

COHEN, G. B., GANDHI, R. T., DAVIS, D. M., MANDELBOIM, O., CHEN, B. K., STROMINGER, J. L. & BALTIMORE, D. 1999. The Selective Downregulation of Class I Major Histocompatibility Complex Proteins by HIV-1 Protects HIV-Infected Cells from NK Cells. *Immunity,* 10**,** 661-671.

COLLINS, D. R. & COLLINS, K. L. 2014. HIV-1 accessory proteins adapt cellular adaptors to facilitate immune evasion. *PLoS pathogens,* 10**,** e1003851.

COLLINS, K. L., CHEN, B. K., KALAMS, S. A., WALKER, B. D. & BALTIMORE, D. 1998. HIV-1 Nef protein protects infected primary cells against killing by cytotoxic T lymphocytes. *Nature,* 391**,** 397-401.

COLLINS, K. R., QUIÑONES-MATEU, M. E., WU, M., LUZZE, H., JOHNSON, J. L., HIRSCH, C., TOOSSI, Z. & ARTS, E. J. 2002. Human immunodeficiency virus type 1 (HIV-1) quasispecies at the sites of Mycobacterium tuberculosis infection contribute to systemic HIV-1 heterogeneity. *Journal of virology,* 76**,** 1697-1706.

DANIEL, M. D., KIRCHHOFF, F., CZAJAK, S. C., SEHGAL, P. K. & DESROSIERS, R. C. 1992. Protective effects of a live attenuated SIV vaccine with a deletion in the nef gene. *Science,* 258**,** 1938-41.

DE NORONHA, C. M. C., SHERMAN, M. P., LIN, H. W., CAVROIS, M. V., MOIR, R. D., GOLDMAN, R. D. & GREENE, W. C. 2001. Dynamic Disruptions in Nuclear Envelope Architecture and Integrity Induced by HIV-1 Vpr. *Science,* 294**,** 1105-1108.

DEBAISIEUX, S., RAYNE, F., YEZID, H. & BEAUMELLE, B. 2012. The ins and outs of HIV-1 Tat. *Traffic,* 13**,** 355-63.

DEPIENNE, C., MOUSNIER, A. L., LEH, H., LE ROUZIC, E., DORMONT, D., BENICHOU, S. & DARGEMONT, C. 2001. Characterization of the nuclear import pathway for HIV-1 integrase. *Journal of Biological Chemistry,* 276**,** 18102-18107.

DOHERTY, P. & ZINKERNAGEL, R. 1975. A biological role for the major histocompatibility antigens. *The Lancet,* 305**,** 1406-1409.

DOS SANTOS FRANCISCO, R., BUHLER, S., NUNES, J. M., BITARELLO, B. D., FRANÇA, G. S., MEYER, D. & SANCHEZ-MAZAS, A. 2015. HLA supertype variation across populations: new insights into the role of natural selection in the evolution of HLA-A and HLA-B polymorphisms. *Immunogenetics,* 67**,** 651-663.

DOUGLAS, J. L., VISWANATHAN, K., MCCARROLL, M. N., GUSTIN, J. K., FRÃ¼H, K. & MOSES, A. V. 2009. Vpu Directs the Degradation of the Human Immunodeficiency Virus Restriction Factor BST-2/Tetherin via a Î²TrCP-Dependent Mechanism. *Journal of virology,* 83**,** 7931-7947.

DUBÉ, M., PAQUAY, C., ROY, B. B., BEGO, M. G., MERCIER, J. & COHEN, É. A. 2011. HIV-1 Vpu Antagonizes BST-2 by Interfering Mainly with the Trafficking of Newly Synthesized BST-2 to the Cell Surface. *Traffic,* 12**,** 1714-1729.

EARL, P. L., DOMS, R. W. & MOSS, B. 1990. Oligomeric structure of the human immunodeficiency virus type 1 envelope glycoprotein. *Proceedings of the National Academy of Sciences of the United States of America,* 87**,** 648-652.

ECKSTEIN, D. A., SHERMAN, M. P., PENN, M. L., CHIN, P. S., DE NORONHA, C. M. C., GREENE, W. C. & GOLDSMITH, M. A. 2001. HIV-1 Vpr Enhances Viral Burden by Facilitating Infection of Tissue Macrophages but Not Nondividing CD4+ T Cells. *The Journal of Experimental Medicine,* 194**,** 1407-1419.

ELDIN, P., CHAZAL, N., FENARD, D., BERNARD, E., GUICHOU, J.-F. O. & BRIANT, L. 2013. Vpr expression abolishes the capacity of HIV-1 infected cells to repair uracilated DNA. *Nucleic Acids Research,* 42**,** 1698-1710.

EMU, B., SINCLAIR, E., HATANO, H., FERRE, A., SHACKLETT, B., MARTIN, J. N., MCCUNE, J. M. & DEEKS, S. G. 2008. HLA Class I-Restricted T-Cell Responses May Contribute to the Control of Human Immunodeficiency Virus Infection, but Such Responses Are Not Always Necessary for Long-Term Virus Control. *Journal of virology,* 82**,** 5398-5407.

FARNET, C. M. & HASELTINE, W. A. 1990. Integration of human immunodeficiency virus type 1 DNA in vitro. *Proceedings of the National Academy of Sciences of the United States of America,* 87**,** 4164-8.

FARROW, M. A., SOMASUNDARAN, M., ZHANG, C., GABUZDA, D., SULLIVAN, J. L. & GREENOUGH, T. C. 2005. Nuclear localization of HIV type 1 Vif isolated from a long-term asymptomatic individual and potential role in virus attenuation. *AIDS Research and Human Retroviruses,* 21**,** 565-74.

FENG, Y., WEI, H., HSI, J., XING, H., HE, X., LIAO, L., MA, Y., NING, C., WANG, N. & TAKEBE, Y. 2014. Identification of a novel HIV type 1 circulating recombinant form (CRF65_cpx) composed of CRF01_AE and subtypes B and C in western Yunnan, China. *AIDS research and human retroviruses,* 30**,** 598-602.

FERRE, A. L., HUNT, P. W., CRITCHFIELD, J. W., YOUNG, D. H., MORRIS, M. M., GARCIA, J. C., POLLARD, R. B., YEE, H. F., MARTIN, J. N., DEEKS, S. G. & SHACKLETT, B. L. 2009. Mucosal immune responses to HIV-1 in elite controllers: a potential correlate of immune control. *Blood,* 113**,** 3978-3989.

FISCHER, A., LEJCZAK, C., LAMBERT, C., ROMAN, F., SERVAIS, J., KARITA, E., ALLEN, S., SCHMIT, J. C. & ARENDT, V. 2004. Is the Vpr R77Q mutation associated with long-term non-progression of HIV infection? *AIDS,* 18**,** 1346-7.

GABUZDA, D. H., LAWRENCE, K., LANGHOFF, E., TERWILLIGER, E., DORFMAN, T., HASELTINE, W. A. & SODROSKI, J. 1992. Role of vif in replication of human immunodeficiency virus type 1 in CD4+ T lymphocytes. *Journal of Virology,* 66**,** 6489-95.

GALÃO, R. P., LE TORTOREC, A., PICKERING, S., KUECK, T. & NEIL, S. J. 2012. Innate sensing of HIV-1 assembly by Tetherin induces NFκB-dependent proinflammatory responses. *Cell host & microbe,* 12**,** 633-644.

GELDMACHER, C., CURRIER, J. R., HERRMANN, E., HAULE, A., KUTA, E., MCCUTCHAN, F., NJOVU, L., GEIS, S., HOFFMANN, O., MABOKO, L., WILLIAMSON, C., BIRX, D., MEYERHANS, A., COX, J. & HOELSCHER, M. 2007. CD8 T-Cell Recognition of Multiple Epitopes within Specific Gag Regions Is Associated with Maintenance of a Low Steady-State Viremia in Human Immunodeficiency Virus Type 1-Seropositive Patients. *Journal of virology,* 81**,** 2440-2448.

GINOCCHIO, C. C., WANG, X.-P., KAPLAN, M. H., MULLIGAN, G., WITT, D., ROMANO, J. W., CRONIN, M. & CARROLL, R. 1997. Effects of specimen collection, processing, and storage conditions on stability of human immunodeficiency virus type 1 RNA levels in plasma. *Journal of clinical microbiology,* 35**,** 2886-2893.

GORI, W. C., ROOST, M. E., KMSEV, C. M. & MICHAEL, S. F. 1998. HIV-1 Vpr increases viral expression by manipulation of the cell cycle: a mechanism for selection of Vpr in vivo.

GORRY, P. R. & ANCUTA, P. 2011. Coreceptors and HIV-1 pathogenesis. *Curr HIV/AIDS Rep,* 8**,** 45-53.

GORRY, P. R., DUNFEE, R. L., MEFFORD, M. E., KUNSTMAN, K., MORGAN, T., MOORE, J. P., MASCOLA, J. R., AGOPIAN, K., HOLM, G. H., MEHLE, A., TAYLOR, J., FARZAN, M., WANG, H., ELLERY, P., WILLEY, S. J., CLAPHAM, P. R., WOLINSKY, S. M., CROWE, S. M. & GABUZDA, D. 2007. Changes in the V3 region of gp120 contribute to unusually broad coreceptor usage of an HIV-1 isolate from a CCR5 Delta32 heterozygote. *Virology,* 362**,** 163-78.

GOTTLIEB, M. S., SCHROFF, R., SCHANKER, H. M., WEISMAN, J. D., FAN, P. T., WOLF, R. A. & SAXON, A. 1981. Pneumocystis carinii pneumonia and mucosal candidiasis in previously healthy homosexual men: evidence of a new acquired cellular immunodeficiency. *New England Journal of Medicine,* 305**,** 1425-1431.

GOULDER, P. J., BUNCE, M., KRAUSA, P., MCINTYRE, K., CROWLEY, S., MORGAN, B., EDWARDS, A., GIANGRANDE, P., PHILLIPS, R. E. & MCMICHAEL, A. J. 1996. Novel, cross-restricted,

conserved, and immunodominant cytotoxic T lymphocyte epitopes in slow progressors in HIV type 1 infection. *AIDS Research and Human Retroviruses*. 12**,** 1691-8.

GRAY, C. M., MLOTSHWA, M., RIOU, C., MATHEBULA, T., DE ASSIS ROSA, D., MASHISHI, T., SEOIGHE, C., NGANDU, N., VAN LOGGERENBERG, F. & MORRIS, L. 2009. Human immunodeficiency virus-specific gamma interferon enzyme-linked immunospot assay responses targeting specific regions of the proteome during primary subtype C infection are poor predictors of the course of viremia and set point. *Journal of virology,* 83**,** 470-478.

GUARNIERI, M., KIM, K. H., BANG, G., LI, J., ZHOU, Y., TANG, X., WANDS, J. & TONG, S. 2006. Point mutations upstream of hepatitis B virus core gene affect DNA replication at the step of core protein expression. *Journal of Virology,* 80**,** 587-95.

GUENZEL, C. A., HERATE, C. & BENICHOU, S. 2014. HIV-1 Vpr-a still "enigmatic multitasker". *Front Microbiol,* 5**,** 127.

GUO, T. W., YU, F. H., HUANG, K. J. & WANG, C. T. 2015. p6gag domain confers cis HIV-1 Gag-Pol assembly and release capability. *The Journal of General Virology,* 97(1):209-19.

HA, T. T. T., MALJKOVIC, I., SWARTLING, S., CAM, P. D., CHIODI, F. & LEITNER, T. 2004. HIV-1 CRF01_AE in intravenous drug users in Hanoi, Vietnam. *AIDS research and human retroviruses,* 20**,** 341-345.

HAFFAR, O. K., POPOV, S., DUBROVSKY, L., AGOSTINI, I., TANG, H., PUSHKARSKY, T., NADLER, S. G. & BUKRINSKY, M. 2000. Two nuclear localization signals in the HIV-1 matrix protein regulate nuclear import of the HIV-1 pre-integration complex1. *Journal of Molecular Biology,* 299**,** 359-368.

HALLENBERGER, S., BOSCH, V., ANGLIKER, H., SHAW, E., KLENK, H. D. & GARTEN, W. 1992. Inhibition of furin-mediated cleavage activation of HIV-1 glycoprotein gp160. *Nature,* 360**,** 358-61.

HANSEN, S. G., JR, M. P., VENTURA, A. B., HUGHES, C. M., GILBRIDE, R. M., FORD, J. C., OSWALD, K., SHOEMAKER, R., LI, Y., LEWIS, M. S., GILLIAM, A. N., XU, G., WHIZIN, N., BURWITZ, B. J., PLANER, S. L., TURNER, J. M., LEGASSE, A. W., AXTHELM, M. K., NELSON, J. A., FRUH, K., SACHA, J. B., ESTES, J. D., KEELE, B. F., EDLEFSEN, P. T., LIFSON, J. D. & PICKER, L. J. 2013a. Immune clearance of highly pathogenic SIV infection. *Nature,* 502**,** 100-104.

HANSEN, S. G., SACHA, J. B., HUGHES, C. M., FORD, J. C., BURWITZ, B. J., SCHOLZ, I., GILBRIDE, R. M., LEWIS, M. S., GILLIAM, A. N., VENTURA, A. B., MALOULI, D., XU, G., RICHARDS, R., WHIZIN, N., REED, J. S., HAMMOND, K. B., FISCHER, M., TURNER, J. M., LEGASSE, A. W., AXTHELM, M. K., EDLEFSEN, P. T., NELSON, J. A., LIFSON, J. D., FRUH, K. & PICKER, L. J. 2013b. Cytomegalovirus vectors violate CD8+ T cell epitope recognition paradigms. *Science,* 340**,** 1237874.

HASAN, Z., CARLSON, J. M., GATANAGA, H., LE, A. Q., BRUMME, C. J., OKA, S., BRUMME, Z. L. & UENO, T. 2012. Minor contribution of HLA class I-associated selective pressure to the variability of HIV-1 accessory protein Vpu. *Biochemical and Biophysical Research Communications,* 421**,** 291-295.

HEINZINGER, N. K., BUKINSKY, M. I., HAGGERTY, S. A., RAGLAND, A. M., KEWALRAMANI, V., LEE, M. A., GENDELMAN, H. E., RATNER, L., STEVENSON, M. & EMERMAN, M. 1994. The Vpr protein of human immunodeficiency virus type 1 influences nuclear localization of viral nucleic acids in nondividing host cells. *Proceedings of the National Academy of Sciences,* 91**,** 7311-7315.

HELLMANN, I., LIM, S.-Y., GELMAN, R. S. & LETVIN, N. L. 2012. Association of Activating KIR Copy Number Variation of NK Cells with Containment of SIV Replication in Rhesus Monkeys. *PLoS Pathog,* 7**,** e1002436.

HINZ, A., MIGUET, N., NATRAJAN, G., USAMI, Y., YAMANAKA, H., RENESTO, P., HARTLIEB, B., MCCARTHY, A. A., SIMORRE, J.-P., GÖTTLINGER, H. & WEISSENHORN, W. 2010. Structural Basis of HIV-1 Tethering to Membranes by the BST-2/Tetherin Ectodomain. *Cell Host & Microbe,* 7**,** 314-323.

HISCOTT, J., KWON, H. & GENIN, P. 2001. Hostile takeovers: viral appropriation of the NF-kappaB pathway. *The Journal of Clinical Investigation,* 107**,** 143-51.

HO, D. D., NEUMANN, A. U., PERELSON, A. S., CHEN, W., LEONARD, J. M. & MARKOWITZ, M. 1995. Rapid turnover of plasma virions and CD4 lymphocytes in HIV-1 infection. *Nature,* 373**,** 123-126.

HÖLZEMER , A., THOBAKGALE, C. F., JIMENEZ CRUZ, C. A., GARCIA-BELTRAN, W. F., CARLSON, J. M., VAN TEIJLINGEN, N. H., MANN, J. K., JAGGERNATH, M., KANG, S.-G., CHUNG, A. W., SCHAFER, J. L., EVANS, D. T., ALTER, G., WALKER, B. D., GOULDER, P. J., CARRINGTON, M., HARTMANN, P., PERTEL, T., ZHOU, R. & ALTFELD, M. 2015. Selection of an HLA-C*03:04-

Restricted HIV-1 p24 Gag Sequence Variant Is Associated with Viral Escape from KIR2DL3+ Natural Killer Cells: Data from an Observational Cohort in South Africa. *PLoS Med,* 12**,** e1001900.

HONEYBORNE, I., PRENDERGAST, A., PEREYRA, F., LESLIE, A., CRAWFORD, H., PAYNE, R., REDDY, S., BISHOP, K., MOODLEY, E., NAIR, K., VAN DER STOK, M., MCCARTHY, N., ROUSSEAU, C. M., ADDO, M., MULLINS, J. I., BRANDER, C., KIEPIELA, P., WALKER, B. D. & GOULDER, P. J. 2007. Control of human immunodeficiency virus type 1 is associated with HLA-B*13 and targeting of multiple gag-specific CD8+ T-cell epitopes. *Journal of Virology,* 81**,** 3667-72.

HUTTER, G., NOWAK, D., MOSSNER, M., GANEPOLA, S., MUSSIG, A., ALLERS, K., SCHNEIDER, T., HOFMANN, J., KUCHERER, C., BLAU, O., BLAU, I. W., HOFMANN, W. K. & THIEL, E. 2009. Long-term control of HIV by CCR5 Delta32/Delta32 stem-cell transplantation. *New England Journal of Medicine,* 360**,** 692-8.

IGLESIAS, M. C., ALMEIDA, J. R., FASTENACKELS, S., VAN BOCKEL, D. J., HASHIMOTO, M., VENTURI, V., GOSTICK, E., URRUTIA, A., WOOLDRIDGE, L., CLEMENT, M., GRAS, S., WILMANN, P. G., AUTRAN, B., MORIS, A., ROSSJOHN, J., DAVENPORT, M. P., TAKIGUCHI, M., BRANDER, C., DOUEK, D. C., KELLEHER, A. D., PRICE, D. A. & APPAY, V. 2011. Escape from highly effective public CD8(+) T-cell clonotypes by HIV. *Blood,* 118**,** 2138-2149.

ISHIKAWA, J., KAISHO, T., TOMIZAWA, H., LEE, B. O., KOBUNE, Y., INAZAWA, J., ORITANI, K., ITOH, M., OCHI, T., ISHIHARA, K. & HIRANO, T. 1995. Molecular cloning and chromosomal mapping of a bone marrow stromal cell surface gene, BST2, that may be involved in pre-B-cell growth. *Genomics,* 26**,** 527-534.

IWABU, Y., FUJITA, H., KINOMOTO, M., KANEKO, K., ISHIZAKA, Y., TANAKA, Y., SATA, T. & TOKUNAGA, K. 2009. HIV-1 Accessory Protein Vpu Internalizes Cell-surface BST-2/Tetherin through Transmembrane Interactions Leading to Lysosomes. *Journal of Biological Chemistry,* 284**,** 35060-35072.

JACOTOT, E., FERRI, K. F., EL HAMEL, C., BRENNER, C., DRUILLENNEC, S., HOEBEKE, J., RUSTIN, P., METIVIER, D., LENOIR, C., GEUSKENS, M., VIEIRA, H. L., LOEFFLER, M., BELZACQ, A. S., BRIAND, J. P., ZAMZAMI, N., EDELMAN, L., XIE, Z. H., REED, J. C., ROQUES, B. P. & KROEMER, G. 2001. Control of mitochondrial membrane permeabilization by adenine nucleotide translocator interacting with HIV-1 viral protein rR and Bcl-2. *The Journal of Experimental Medicine,* 193**,** 509-19.

JAGER, S., KIM, D. Y., HULTQUIST, J. F., SHINDO, K., LARUE, R. S., KWON, E., LI, M., ANDERSON, B. D., YEN, L. & STANLEY, D. 2012. Vif hijacks CBF-[bgr] to degrade APOBEC3G and promote HIV-1 infection. *Nature,* 481**,** 371-375.

KALIPATNAPU, S. & CHATTOPADHYAY, A. 2005. Membrane protein solubilization: recent advances and challenges in solubilization of serotonin1A receptors. *IUBMB life,* 57**,** 505-512.

KAMATA, M. & AIDA, Y. 2000. Two putative alpha-helical domains of human immunodeficiency virus type 1 Vpr mediate nuclear localization by at least two mechanisms. *Journal of Virology,* 74.

KAMATA, M., WATANABE, N., NAGAOKA, Y. & CHEN, I. S. 2008. Human immunodeficiency virus type 1 Vpr binds to the N lobe of the Wee1 kinase domain and enhances kinase activity for CDC2. *Journal of Virology,* 82**,** 5672-82.

KAO, S., KHAN, M. A., MIYAGI, E., PLISHKA, R., BUCKLER-WHITE, A. & STREBEL, K. 2003. The human immunodeficiency virus type 1 Vif protein reduces intracellular expression and inhibits packaging of APOBEC3G (CEM15), a cellular inhibitor of virus infectivity. *Journal of Virology,* 77**,** 11398-407.

KASLOW, R., CARRINGTON, M., APPLE, R., PARK, L., MUNOZ, A., SAAH, A., GOEDERT, J., WINKLER, C., O'BRIEN, S. & RINALDO, C. 1996. Influence of combinations of human major histocompatibility complex genes on the course of HIVâ€“1 infection. *Nature medicine,* 2**,** 405-411.

KEELE, B. F. & ESTES, J. D. 2011. Barriers to mucosal transmission of immunodeficiency viruses. *Blood,* 118**,** 839-846.

KEELE, B. F., GIORGI, E. E., SALAZAR-GONZALEZ, J. F., DECKER, J. M., PHAM, K. T., SALAZAR, M. G., SUN, C., GRAYSON, T., WANG, S. & LI, H. 2008. Identification and characterization of transmitted and early founder virus envelopes in primary HIV-1 infection. *Proceedings of the National Academy of Sciences,* 105**,** 7552-7557.

KEELE, B. F., VAN HEUVERSWYN, F., LI, Y., BAILES, E., TAKEHISA, J., SANTIAGO, M. L., BIBOLLET-RUCHE, F., CHEN, Y., WAIN, L. V. & LIEGEOIS, F. 2006. Chimpanzee reservoirs of pandemic and nonpandemic HIV-1. *Science,* 313**,** 523-526.

KIEPIELA, P., LESLIE, A. J., HONEYBORNE, I., RAMDUTH, D., THOBAKGALE, C., CHETTY, S., RATHNAVALU, P., MOORE, C., PFAFFEROTT, K. J., HILTON, L., ZIMBWA, P., MOORE, S., ALLEN, T., BRANDER, C., ADDO, M. M., ALTFELD, M., JAMES, I., MALLAL, S., BUNCE, M., BARBER, L. D., SZINGER, J., DAY, C., KLENERMAN, P., MULLINS, J., KORBER, B.,

COOVADIA, H. M., WALKER, B. D. & GOULDER, P. J. 2004. Dominant influence of HLA-B in mediating the potential co-evolution of HIV and HLA. *Nature,* 432**,** 769-75.

KIEPIELA, P., NGUMBELA, K., THOBAKGALE, C., RAMDUTH, D., HONEYBORNE, I., MOODLEY, E., REDDY, S., DE PIERRES, C., MNCUBE, Z. & MKHWANAZI, N. 2007. CD8+ T-cell responses to different HIV proteins have discordant associations with viral load. *Nature medicine,* 13**,** 46-53.

KINO, T., GRAGEROV, A., VALENTIN, A., TSOPANOMIHALOU, M., ILYINA-GRAGEROVA, G., ERWIN-COHEN, R., CHROUSOS, G. P. & PAVLAKIS, G. N. 2005. Vpr Protein of Human Immunodeficiency Virus Type 1 Binds to 14-3-3 Proteins and Facilitates Complex Formation with Cdc25C: Implications for Cell Cycle Arrest. *Journal of Virology,* 79**,** 2780-2787.

KIRCHHOFF, F., GREENOUGH, T. C., BRETTLER, D. B., SULLIVAN, J. L. & DESROSIERS, R. C. 1995. Brief report: absence of intact nef sequences in a long-term survivor with nonprogressive HIV-1 infection. *New England Journal of Medicine,* 332**,** 228-32.

KJEMS, J. & ASKJAER, P. 2000. Rev protein and its cellular partners. *Adv Pharmacol,* 48**,** 251-98.

KLARMANN, G. J., SCHAUBER, C. A. & PRESTON, B. D. 1993. Template-directed pausing of DNA synthesis by HIV-1 reverse transcriptase during polymerization of HIV-1 sequences in vitro. *Journal of Biological Chemistry,* 268**,** 9793-802.

KLATZMANN, D. & GLUCKMAN, J. 1986. HIV infection: facts and hypotheses. *Immunology today,* 7**,** 291-296.

KLIMKAIT, T., STREBEL, K., HOGGAN, M. D., MARTIN, M. A. & ORENSTEIN, J. M. 1990. The human immunodeficiency virus type 1-specific protein vpu is required for efficient virus maturation and release. *Journal of Virology,* 64**,** 621-9.

KLOVERPRIS, H. N., ADLAND, E., KOYANAGI, M., STRYHN, A., HARNDAHL, M., MATTHEWS, P. C., SHAPIRO, R., WALKER, B. D., NDUNG'U, T., BRANDER, C., TAKIGUCHI, M., BUUS, S. R. & GOULDER, P. 2014. HIV Subtype Influences HLA-B*07:02-Associated HIV Disease Outcome. *AIDS research and human retroviruses,* 30**,** 468-475.

KLØVERPRIS, H. N., COLE, D. K., FULLER, A., CARLSON, J., BECK, K., SCHAUENBURG, A. J., RIZKALLAH, P. J., BUUS, S., SEWELL, A. K. & GOULDER, P. 2015. A molecular switch in immunodominant HIV-1-specific CD8 T-cell epitopes shapes differential HLA-restricted escape. *Retrovirology,* 12**,** 1.

KLOVERPRIS, H. N., PAYNE, R. P., SACHA, J. B., RASAIYAAH, J. T., CHEN, F., TAKIGUCHI, M., YANG, O. O., TOWERS, G. J., GOULDER, P. & PRADO, J. G. 2013. Early antigen presentation of protective HIV-1 KF11Gag and KK10Gag epitopes from incoming viral particles facilitates rapid recognition of infected cells by specific CD8+ T cells. *Journal of Virology,* 87**,** 2628-38.

KUPZIG, S., KOROLCHUK, V., ROLLASON, R., SUGDEN, A., WILDE, A. & BANTING, G. 2003. Bst-2/HM1.24 Is a Raft-Associated Apical Membrane Protein with an Unusual Topology. *Traffic,* 4**,** 694-709.

KWONG, P. D., WYATT, R., ROBINSON, J., SWEET, R. W., SODROSKI, J. & HENDRICKSON, W. A. 1998. Structure of an HIV gp120 envelope glycoprotein in complex with the CD4 receptor and a neutralizing human antibody. *Nature,* 393**,** 648-659.

LADINSKY, M. S., KIEFFER, C., OLSON, G., DERUAZ, M., VRBANAC, V., TAGER, A. M., KWON, D. S. & BJORKMAN, P. J. 2014. Electron tomography of HIV-1 infection in gut-associated lymphoid tissue. *PLoS Pathog,* 10**,** e1003899.

LAGUETTE, N., BRÉGNARD, C., HUE, P., BASBOUS, J., YATIM, A., LARROQUE, M., KIRCHHOFF, F., CONSTANTINOU, A., SOBHIAN, B. & BENKIRANE, M. 2014. Premature activation of the SLX4 complex by Vpr promotes G2/M arrest and escape from innate immune sensing. *Cell,* 156**,** 134-145.

LAMA, J., MANGASARIAN, A. & TRONO, D. 1999. Cell-surface expression of CD4 reduces HIV-1 infectivity by blocking Env incorporation in a Nef- and Vpu-inhibitable manner. *Curr Biol,* 9**,** 622-31.

LAMBOTTE, O., FERRARI, G., MOOG, C., YATES, N. L., LIAO, H.-X., PARKS, R. J., HICKS, C. B., OWZAR, K., TOMARAS, G. D. & MONTEFIORI, D. C. 2009. Heterogeneous neutralizing antibody and antibody-dependent cell cytotoxicity responses in HIV-1 elite controllers. *AIDS (London, England),* 23**,** 897.

LANZAVECCHIA, A., ROOSNEK, E., GREGORY, T., BERMAN, P. & ABRIGNANI, S. 1988. T cells can present antigens such as HIV gp120 targeted to their own surface molecules. *Nature,* 334**,** 530-2.

LE ROUZIC, E., BELAÏDOUNI, N., ESTRABAUD, E., MOREL, M., RAIN, J.-C., TRANSY, C. & MARGOTTIN-GOGUET, F. 2007. HIV1 Vpr arrests the cell cycle by recruiting DCAF1/VprBP, a receptor of the Cul4-DDB1 ubiquitin ligase. *Cell cycle,* 6**,** 182-188.

Full Length Vpu from HIV-1: Combining Molecular Dynamics Simulations with NMR Spectroscopy, 2006. doi: 10.1080/07391102.2006.10507074. Directed by LEMAITRE, V., WILLBOLD, D., WATTS, A. & FISCHER, W. B.: Taylor & Francis.

LESLIE, A., MATTHEWS, P. C., LISTGARTEN, J., CARLSON, J. M., KADIE, C., NDUNG'U, T., BRANDER, C., COOVADIA, H., WALKER, B. D. & HECKERMAN, D. 2010. Additive contribution of HLA class I alleles in the immune control of HIV-1 infection. *Journal of virology,* 84**,** 9879-9888.

LESLIE, A., PFAFFEROTT, K., CHETTY, P., DRAENERT, R., ADDO, M., FEENEY, M., TANG, Y., HOLMES, E., ALLEN, T. & PRADO, J. 2004. HIV evolution: CTL escape mutation and reversion after transmission. *Nature medicine,* 10**,** 282-289.

LEVESQUE, K., ZHAO, Y. S. & COHEN, E. A. 2003. Vpu exerts a positive effect on HIV-1 infectivity by down-modulating CD4 receptor molecules at the surface of HIV-1-producing cells. *Journal of Biological Chemistry,* 278**,** 28346-53.

LEWINSKI, M. K., JAFARI, M., ZHANG, H., OPELLA, S. J. & GUATELLI, J. 2015. Membrane Anchoring by a C-terminal Tryptophan Enables HIV-1 Vpu to Displace BST2 from Sites of Viral Assembly. *Journal of Biological Chemistry*.

LIN, M.-H., APOLLONI, A., CUTILLAS, V., SIVAKUMARAN, H., MARTIN, S., LI, D., WEI, T., WANG, R., JIN, H., SPANN, K. & HARRICH, D. 2015. A Mutant Tat Protein Inhibits HIV-1 Reverse Transcription by Targeting the Reverse Transcription Complex. *Journal of Virology,* 89**,** 4827-4836.

LLANO, A., WILLIAMS, A., OLVERA, A., SILVA-ARRIETA, S. & BRANDER, C. 2013. Best-characterized HIV-1 CTL epitopes: the 2013 update. *HIV molecular immunology,* 2013**,** 3-25.

LOSALAMOSNATIONALLABORATORY. 2016. *HIV Circulating Recombinant Forms (CRFs)* [Online]. Available: http://www.hiv.lanl.gov/content/sequence/HIV/CRFs/CRFs.html 2016].

LUM, J. J., COHEN, O. J., NIE, Z., WEAVER, J. G., GOMEZ, T. S., YAO, X.-J., LYNCH, D., PILON, A., HAWLEY, N., KIM, J. E., CHEN, Z., MONTPETIT, M., SANCHEZ-DARDON, J., COHEN, E. A. & BADLEY, A. D. 2003. Vpr R77Q is associated with long-term nonprogressive HIV infection and impaired induction of apoptosis. *Journal of Clinical Investigation,* 111**,** 1547-1554.

LUO, W. & PETERLIN, B. M. 1997. Activation of the T-cell receptor signaling pathway by Nef from an aggressive strain of simian immunodeficiency virus. *Journal of virology,* 71**,** 9531-9537.

LV, M., ZHU, Y., WANG, J., ZHANG, H., WANG, X., ZUO, T., LIU, D., ZHANG, J., WU, J., KONG, W. & YU, X. 2013. Purification of eukaryotic tetherin/Vpu proteins and detection of their interaction by ELISA. *Protein Expression and Purification,* 91**,** 112-118.

MA, C., MARASSI, F. M., JONES, D. H., STRAUS, S. K., BOUR, S., STREBEL, K., SCHUBERT, U., OBLATT-MONTAL, M., MONTAL, M. & OPELLA, S. J. 2002. Expression, purification, and activities of full-length and truncated versions of the integral membrane protein Vpu from HIV-1. *Protein Sci,* 11**,** 546-57.

MACREADIE, I. G., ARUNAGIRI, C. K., HEWISH, D. R., WHITE, J. F. & AZAD, A. A. 1996. Extracellular addition of a domain of HIVâ€□1 Vpr containing the amino acid sequence motif H (S/F) RIG causes cell membrane permeabilization and death. *Molecular microbiology,* 19**,** 1185-1192.

MAGADAN, J. G. & BONIFACINO, J. S. 2012. Transmembrane domain determinants of CD4 Downregulation by HIV-1 Vpu. *Journal of Virology,* 86**,** 757-72.

MAGADÁN, J. G., FJ, P.-V., SOUGRAT, R., YE, Y., STREBEL, K. & BONIFACINO, J. S. 2010. Multilayered Mechanism of CD4 Downregulation by HIV-1 Vpu Involving Distinct ER Retention and ERAD Targeting Steps. *PLoS Pathog,* 6**,** e1000869.

MAKINO, S., REYNOLDS, J. A. & TANFORD, C. 1973. The binding of deoxycholate and Triton X-100 to proteins. *Journal of Biological Chemistry,* 248**,** 4926-4932.

MALDARELLI, F., CHEN, M. Y., WILLEY, R. L. & STREBEL, K. 1993. Human immunodeficiency virus type 1 Vpu protein is an oligomeric type I integral membrane protein. *Journal of Virology,* 67**,** 5056-61.

MALIM, M. H., HAUBER, J., LE, S.-Y., MAIZEL, J. V. & CULLEN, B. R. 1989. The HIV-1 rev trans-activator acts through a structured target sequence to activate nuclear export of unspliced viral mRNA. *Nature,* 338**,** 254-257.

MANGASARIAN, A., FOTI, M., AIKEN, C., CHIN, D., CARPENTIER, J.-L. & TRONO, D. 1997. The HIV-1 Nef Protein Acts as a Connector with Sorting Pathways in the Golgi and at the Plasma Membrane. *Immunity,* 6**,** 67-77.

MANGEAT, B., GERS-HUBER, G., LEHMANN, M., ZUFFEREY, M., LUBAN, J. & PIGUET, V. 2009. HIV-1 Vpu Neutralizes the Antiviral Factor Tetherin/BST-2 by Binding It and Directing Its Beta-TrCP2-Dependent Degradation. *PLoS Pathog,* 5**,** e1000574.

MANGEAT, B., TURELLI, P., CARON, G., FRIEDLI, M., PERRIN, L. & TRONO, D. 2003. Broad antiretroviral defence by human APOBEC3G through lethal editing of nascent reverse transcripts. *Nature,* 424**,** 99-103.

MANSKY, L. M., PREVERAL, S., SELIG, L., BENAROUS, R. & BENICHOU, S. 2000. The Interaction of Vpr with Uracil DNA Glycosylase Modulates the Human Immunodeficiency Virus Type 1 In Vivo Mutation Rate. *Journal of virology,* 74**,** 7039-7047.

MARGOTTIN, F., BENICHOU, S., DURAND, H., RICHARD, V., LIU, L. X., GOMAS, E. & BENAROUS, R. 1996. Interaction between the Cytoplasmic Domains of HIV-1 Vpu and CD4: Role of Vpu Residues Involved in CD4 Interaction andin VitroCD4 Degradation. *Virology,* 223**,** 381-386.

MARGOTTIN, F., BOUR, S. P., DURAND, H., SELIG, L., BENICHOU, S., RICHARD, V., THOMAS, D., STREBEL, K. & BENAROUS, R. 1998. A Novel Human WD Protein, h-Î²TrCP, that Interacts with HIV-1 Vpu Connects CD4 to the ER Degradation Pathway through an F-Box Motif. *Molecular Cell,* 1**,** 565-574.

MARSH, S. G., PARHAM, P., DUPONT, B., GERAGHTY, D. E., TROWSDALE, J., MIDDLETON, D., VILCHES, C., CARRINGTON, M., WITT, C., GUETHLEIN, L. A., SHILLING, H., GARCIA, C. A., HSU, K. C. & WAIN, H. 2003. Killer-cell immunoglobulin-like receptor (KIR) nomenclature report, 2002. *Immunogenetics,* 55**,** 220-6.

MARTIN, E., CARLSON, J. M., LE, A. Q., CHOPERA, D. R., MCGOVERN, R., RAHMAN, M. A., NG, C., JESSEN, H., KELLEHER, A. D., MARKOWITZ, M., ALLEN, T. M., MILLOY, M.-J., CARRINGTON, M., WAINBERG, M. A. & BRUMME, Z. L. 2014. Early immune adaptation in HIV-1 revealed by population-level approaches. *Retrovirology,* 11**,** 1-16.

MARTIN, M. P., GAO, X., LEE, J.-H., NELSON, G. W., DETELS, R., GOEDERT, J. J., BUCHBINDER, S., HOOTS, K., VLAHOV, D., TROWSDALE, J., WILSON, M., O'BRIEN, S. J. & CARRINGTON, M. 2002. Epistatic interaction between KIR3DS1 and HLA-B delays the progression to AIDS. *Nature Genetics,* 31**,** 429-434.

MARTIN, M. P., QI, Y., GAO, X., YAMADA, E., MARTIN, J. N., PEREYRA, F., COLOMBO, S., BROWN, E. E., SHUPERT, W. L., PHAIR, J., GOEDERT, J. J., BUCHBINDER, S., KIRK, G. D., TELENTI, A., CONNORS, M., O'BRIEN, S. J., WALKER, B. D., PARHAM, P., DEEKS, S. G., MCVICAR, D. W. & CARRINGTON, M. 2007. Innate partnership of HLA-B and KIR3DL1 subtypes against HIV-1. *Nature Genetics,* 39**,** 733-740.

MARTINEZ-PICADO, J., PRADO, J. G., FRY, E. E., PFAFFEROTT, K., LESLIE, A., CHETTY, S., THOBAKGALE, C., HONEYBORNE, I., CRAWFORD, H., MATTHEWS, P., PILLAY, T., ROUSSEAU, C., MULLINS, J. I., BRANDER, C., WALKER, B. D., STUART, D. I., KIEPIELA, P. & GOULDER, P. 2006. Fitness Cost of Escape Mutations in p24 Gag in Association with Control of Human Immunodeficiency Virus Type 1. *Journal of Virology,* 80**,** 3617-3623.

MCCORMICK-DAVIS, C., DALTON, S. B., SINGH, D. K. & STEPHENS, E. B. 2000. Comparison of Vpu sequences from diverse geographical isolates of HIV type 1 identifies the presence of highly variable domains, additional invariant amino acids, and a signature sequence motif common to subtype C isolates. *AIDS Research and Human Retroviruses,* 16**,** 1089-95.

MCNATT, M. W., ZANG, T. & BIENIASZ, P. D. 2013. Vpu Binds Directly to Tetherin and Displaces It from Nascent Virions. *PLoS Pathog,* 9**,** e1003299.

MEDZHITOV, R. & JANEWAY, C. A. 2002. Decoding the patterns of self and nonself by the innate immune system. *Science,* 296**,** 298-300.

MEHLE, A., GONCALVES, J., SANTA-MARTA, M., MCPIKE, M. & GABUZDA, D. 2004. Phosphorylation of a novel SOCS-box regulates assembly of the HIV-1 Vif-Cul5 complex that promotes APOBEC3G degradation. *Genes and Development,* 18**,** 2861-6.

MEHLE, A., THOMAS, E. R., RAJENDRAN, K. S. & GABUZDA, D. 2006. A zinc-binding region in Vif binds Cul5 and determines cullin selection. *Journal of Biological Chemistry,* 281**,** 17259-65.

MEHLE, A., WILSON, H., ZHANG, C., BRAZIER, A. J., MCPIKE, M., PERY, E. & GABUZDA, D. 2007. Identification of an APOBEC3G Binding Site in Human Immunodeficiency Virus Type 1 Vif and Inhibitors of Vif-APOBEC3G Binding. *Journal of Virology,* 81**,** 13235-13241.

METKAR, S. S., WANG, B., AGUILAR-SANTELISES, M., RAJA, S. M., UHLIN-HANSEN, L., PODACK, E., TRAPANI, J. A. & FROELICH, C. J. 2002. Cytotoxic cell granule-mediated apoptosis: Perforin delivers granzyme b-serglycin complexes into target cells without plasma membrane pore formation. *Immunity,* 16**,** 417-428.

MIGUELES, S. A., LABORICO, A. C., IMAMICHI, H., SHUPERT, W. L., ROYCE, C., MCLAUGHLIN, M., EHLER, L., METCALF, J., LIU, S., HALLAHAN, C. W. & CONNORS, M. 2003. The Differential Ability of HLA B*5701+ Long-Term Nonprogressors and Progressors To Restrict Human Immunodeficiency Virus Replication Is Not Caused by Loss of Recognition of Autologous Viral gag Sequences. *Journal of virology,* 77**,** 6889-6898.

MIGUELES, S. A., SABBAGHIAN, M. S., SHUPERT, W. L., BETTINOTTI, M. P., MARINCOLA, F. M., MARTINO, L., HALLAHAN, C. W., SELIG, S. M., SCHWARTZ, D., SULLIVAN, J. & CONNORS,

M. 2000. HLA B*5701 is highly associated with restriction of virus replication in a subgroup of HIV-infected long term nonprogressors. *Proceedings of the National Academy of Sciences,* 97**,** 2709-2714.
MILLER, J., PRESNYAK, V. & SMITH, H. 2007. The dimerization domain of HIV-1 viral infectivity factor Vif is required to block virion incorporation of APOBEC3G. *Retrovirology,* 4**,** 81.
MILLER, M. D., FARNET, C. M. & BUSHMAN, F. D. 1997. Human immunodeficiency virus type 1 preintegration complexes: studies of organization and composition. *Journal of virology,* 71**,** 5382-90.
MILLER, R. J., CAIRNS, J. S., BRIDGES, S. & SARVER, N. 2000. Human Immunodeficiency Virus and AIDS: Insights from Animal Lentiviruses. *Journal of virology,* 74**,** 7187-7195.
MOLL, M., ANDERSSON, S. K., SMED-SÖRENSEN, A. & SANDBERG, J. K. 2010. Inhibition of lipid antigen presentation in dendritic cells by HIV-1 Vpu interference with CD1d recycling from endosomal compartments. *Blood,* 116**,** 1876-1884.
MOODY, D. B. 2006. The surprising diversity of lipid antigens for CD1-restricted T cells. *Advances in Immunology,* 89**,** 87-139.
MOORE, C. B., JOHN, M., JAMES, I. R., CHRISTIANSEN, F. T., WITT, C. S. & MALLAL, S. A. 2002. Evidence of HIV-1 Adaptation to HLA-Restricted Immune Responses at a Population Level. *Science,* 296**,** 1439-1443.
MORITA, E., SANDRIN, V., MCCULLOUGH, J., KATSUYAMA, A., HAMILTON, I. B. & SUNDQUIST, W. I. 2011. ESCRT-III Protein Requirements for HIV-1 Budding. *Cell host & microbe,* 9**,** 235-242.
MURRAY, J. M., KELLEHER, A. D. & COOPER, D. A. 2011. Timing of the Components of the HIV Life Cycle in Productively Infected CD4+ T Cells in a Population of HIV-Infected Individuals. *Journal of Virology,* 85**,** 10798-10805.
NEIL, S. J., SANDRIN, V., SUNDQUIST, W. I. & BIENIASZ, P. D. 2007. An interferon-alpha-induced tethering mechanism inhibits HIV-1 and Ebola virus particle release but is counteracted by the HIV-1 Vpu protein. *Cell Host Microbe,* 2**,** 193-203.
NEIL, S. J. D., EASTMAN, S. W., JOUVENET, N. & BIENIASZ, P. D. 2006. HIV-1 Vpu Promotes Release and Prevents Endocytosis of Nascent Retrovirus Particles from the Plasma Membrane. *PLoS Pathog,* 2**,** e39.
NEIL, S. J. D., ZANG, T. & BIENIASZ, P. D. 2008. Tetherin inhibits retrovirus release and is antagonized by HIV-1 Vpu. *Nature,* 451**,** 425-430.
NGUMBELA, K. C., DAY, C. L., MNCUBE, Z., NAIR, K., RAMDUTH, D., THOBAKGALE, C., MOODLEY, E., REDDY, S., DE PIERRES, C., MKHWANAZI, N., BISHOP, K., VAN DER STOK, M., ISMAIL, N., HONEYBORNE, I., CRAWFORD, H., KAVANAGH, D. G., ROUSSEAU, C., NICKLE, D., MULLINS, J., HECKERMAN, D., KORBER, B., COOVADIA, H., KIEPIELA, P., GOULDER, P. J. & WALKER, B. D. 2008. Targeting of a CD8 T cell env epitope presented by HLA-B*5802 is associated with markers of HIV disease progression and lack of selection pressure. *AIDS Research and Human Retroviruses,* 24**,** 72-82.
NGUYEN, K.-L., LLANO, M., AKARI, H., MIYAGI, E., POESCHLA, E. M., STREBEL, K. & BOUR, S. 2004. Codon optimization of the HIV-1 vpu and vif genes stabilizes their mRNA and allows for highly efficient Rev-independent expression. *Virology,* 319**,** 163-175.
NITAHARA-KASAHARA, Y., KAMATA, M., YAMAMOTO, T., ZHANG, X., MIYAMOTO, Y., MUNETA, K., IIJIMA, S., YONEDA, Y., TSUNETSUGU-YOKOTA, Y. & AIDA, Y. 2007. Novel Nuclear Import of Vpr Promoted by Importin Î± Is Crucial for Human Immunodeficiency Virus Type 1 Replication in Macrophages. *Journal of virology,* 81**,** 5284-5293.
O'NEIL, P. K., SUN, G., YU, H., RON, Y., DOUGHERTY, J. P. & PRESTON, B. D. 2002. Mutational analysis of HIV-1 long terminal repeats to explore the relative contribution of reverse transcriptase and RNA polymerase II to viral mutagenesis. *Journal of Biological Chemistry,* 277**,** 38053-38061.
OGAWA, S., HACHIYA, A., HOSAKA, M., MATSUDA, M., ODE, H., SHIGEMI, U., OKAZAKI, R., SADAMASU, K., NAGASHIMA, M. & TOYOKAWA, T. 2015. A Novel Drug-Resistant HIV-1 Circulating Recombinant Form CRF76_01B Identified by Near Full-Length Genome Analysis. *AIDS research and human retroviruses*.
PACYNIAK, E., GOMEZ, M. L., GOMEZ, L. M., MULCAHY, E. R., JACKSON, M., HOUT, D. R., WISDOM, B. J. & STEPHENS, E. B. 2005. Identification of a region within the cytoplasmic domain of the subtype B Vpu protein of human immunodeficiency virus type 1 (HIV-1) that is responsible for retention in the golgi complex and its absence in the Vpu protein from a subtype C HIV-1. *AIDS Research & Human Retroviruses,* 21**,** 379-394.
PARK, S. H., DE ANGELIS, A. A., NEVZOROV, A. A., WU, C. H. & OPELLA, S. J. 2006. Three-Dimensional Structure of the Transmembrane Domain of Vpu from HIV-1 in Aligned Phospholipid Bicelles. *Biophysical Journal,* 91**,** 3032-3042.

PARK, S. H., MRSE, A. A., NEVZOROV, A. A., MESLEH, M. F., OBLATT-MONTAL, M., MONTAL, M. & OPELLA, S. J. 2003. Three-dimensional Structure of the Channel-forming Trans-membrane Domain of Virus Protein â€œuâ€ (Vpu) from HIV-1. *Journal of Molecular Biology,* 333**,** 409-424.

PAXIMADIS, M., MATHEBULA, T. Y., GENTLE, N. L., VARDAS, E., COLVIN, M., GRAY, C. M., TIEMESSEN, C. T. & PUREN, A. 2011. Human leukocyte antigen class I (A, B, C) and II (DRB1) diversity in the black and Caucasian South African population. *Human immunology,* 73**,** 80-92.

PELAK, K., NEED, A. C., FELLAY, J., SHIANNA, K. V., FENG, S., URBAN, T. J., GE, D., DE LUCA, A., MARTINEZ-PICADO, J., WOLINSKY, S. M., MARTINSON, J. J., JAMIESON, B. D., BREAM, J. H., MARTIN, M. P., BORROW, P., LETVIN, N. L., MCMICHAEL, A. J., HAYNES, B. F., TELENTI, A., CARRINGTON, M., GOLDSTEIN, D. B., ALTER, G. & ON BEHALF OF, N. C. F. H. I. V. A. V. I. 2011. Copy Number Variation of KIR Genes Influences HIV-1 Control. *PLoS Biol,* 9**,** e1001208.

PEREZ-CABALLERO, D., ZANG, T., EBRAHIMI, A., MCNATT, M. W., GREGORY, D. A., JOHNSON, M. C. & BIENIASZ, P. D. 2009. Tetherin Inhibits HIV-1 Release by Directly Tethering Virions to Cells. *Cell,* 139**,** 499-511.

PETTIT, S. C., LINDQUIST, J. N., KAPLAN, A. H. & SWANSTROM, R. 2005. Processing sites in the human immunodeficiency virus type 1 (HIV-1) Gag-Pro-Pol precursor are cleaved by the viral protease at different rates. *Retrovirology,* 2**,** 66.

PINTO, L. H., HOLSINGER, L. J. & LAMB, R. A. 1992. Influenza virus M2 protein has ion channel activity. *Cell,* 69**,** 517-28.

PLANTIER, J. C., LEOZ, M., DICKERSON, J. E., DE OLIVEIRA, F., CORDONNIER, F., LEMEE, V., DAMOND, F., ROBERTSON, D. L. & SIMON, F. 2009. A new human immunodeficiency virus derived from gorillas. *Nature Medicine,* 15**,** 871-2.

POPOV, S., REXACH, M., RATNER, L., BLOBEL, G. N. & BUKRINSKY, M. 1998. Viral Protein R Regulates Docking of the HIV-1 Preintegration Complex to the Nuclear Pore Complex. *Journal of Biological Chemistry,* 273**,** 13347-13352.

POPOVIC, M., SARNGADHARAN, M. G., READ, E. & GALLO, R. C. 1984. Detection, isolation, and continuous production of cytopathic retroviruses (HTLV-III) from patients with AIDS and pre-AIDS. *Science,* 224**,** 497-500.

POSS, M., MARTIN, H. L., KREISS, J. K., GRANVILLE, L., CHOHAN, B., NYANGE, P., MANDALIYA, K. & OVERBAUGH, J. 1995. Diversity in virus populations from genital secretions and peripheral blood from women recently infected with human immunodeficiency virus type 1. *Journal of virology,* 69**,** 8118-8122.

PRESTON, B., POIESZ, B. & LOEB, L. 1988. Fidelity of HIV-1 reverse transcriptase. *Science,* 242**,** 1168-1171.

RACHINGER, A., NAVIS, M., VAN ASSEN, S., GROENEVELD, P. H. P. & SCHUITEMAKER, H. 2008. Recovery of Viremic Control after Superinfection with Pathogenic HIV Type 1 in a Long-Term Elite Controller of HIV Type 1 Infection. *Clinical Infectious Diseases,* 47**,** e86-e89.

RAMIREZ, P. W., DEPAULA-SILVA, A. B., SZANIAWSKI, M., BARKER, E., BOSQUE, A. & PLANELLES, V. 2015. HIV-1 Vpu utilizes both cullin-RING ligase (CRL) dependent and independent mechanisms to downmodulate host proteins. *Retrovirology,* 12**,** 65.

RAUSCH, J. & LE GRICE, S. F. 2015. HIV Rev Assembly on the Rev Response Element (RRE): A Structural Perspective. *Viruses,* 7**,** 3053-3075.

RE, F., BRAATEN, D., FRANKE, E. K. & LUBAN, J. 1995. Human immunodeficiency virus type 1 Vpr arrests the cell cycle in G2 by inhibiting the activation of p34cdc2-cyclin B. *Journal of Virology,* 69**,** 6859-64.

REISS, P., LANGE, J. M., DE RONDE, A., DE WOLF, F., DEKKER, J., DEBOUCK, C. & GOUDSMIT, J. 1990a. Speed of progression to AIDS and degree of antibody response to accessory gene products of HIV-1. *Journal of Medical Virology,* 30**,** 163-8.

REISS, P., LANGE, J. M., RONDE, A., DE WOLF, F., DEKKER, J., DANNER, S. A., DEBOUCK, C. & GOUDSMIT, J. 1990b. Antibody response to viral proteins U (vpu) and R (vpr) in HIV-1-infected individuals. *JAIDS Journal of Acquired Immune Deficiency Syndromes,* 3**,** 115-122.

RERKS-NGARM, S., PITISUTTITHUM, P., NITAYAPHAN, S., KAEWKUNGWAL, J., CHIU, J., PARIS, R., PREMSRI, N., NAMWAT, C., DE SOUZA, M., ADAMS, E., BENENSON, M., GURUNATHAN, S., TARTAGLIA, J., MCNEIL, J. G., FRANCIS, D. P., STABLEIN, D., BIRX, D. L., CHUNSUTTIWAT, S., KHAMBOONRUANG, C., THONGCHAROEN, P., ROBB, M. L., MICHAEL, N. L., KUNASOL, P. & KIM, J. H. 2009. Vaccination with ALVAC and AIDSVAX to Prevent HIV-1 Infection in Thailand. *New England Journal of Medicine,* 361**,** 2209-2220.

ROLLAND, M., HECKERMAN, D., DENG, W., ROUSSEAU, C. M., COOVADIA, H., BISHOP, K., GOULDER, P. J. R., WALKER, B. D., BRANDER, C. & MULLINS, J. I. 2008. Broad and Gag-Biased HIV-1 Epitope Repertoires Are Associated with Lower Viral Loads. *PLoS ONE,* 3**,** e1424.

ROSANO, G. N. L. & CECCARELLI, E. A. 2014. Recombinant protein expression in Escherichia coli: advances and challenges. *Frontiers in microbiology,* 5**,** 172.

ROSHAL, M., KIM, B., ZHU, Y., NGHIEM, P. & PLANELLES, V. 2003. Activation of the ATR-mediated DNA Damage Response by the HIV-1 Viral Protein R. *Journal of Biological Chemistry,* 278**,** 25879-25886.

ROWLAND-JONES, S. L., DONG, T., FOWKE, K. R., KIMANI, J., KRAUSA, P., NEWELL, H., BLANCHARD, T., ARIYOSHI, K., OYUGI, J., NGUGI, E., BWAYO, J., MACDONALD, K. S., MCMICHAEL, A. J. & PLUMMER, F. A. 1998. Cytotoxic T cell responses to multiple conserved HIV epitopes in HIV-resistant prostitutes in Nairobi. *Journal of Clinical Investigation,* 102**,** 1758-65.

RUIZ, A., HILL, M. S., SCHMITT, K., GUATELLI, J. & STEPHENS, E. B. 2008. Requirements of the membrane proximal tyrosine and dileucine-based sorting signals for efficient transport of the subtype C Vpu protein to the plasma membrane and in virus release. *Virology,* 378**,** 58-68.

SABBAJ, S., BANSAL, A., RITTER, G. D., PERKINS, C., EDWARDS, B. H., GOUGH, E., TANG, J., SZINGER, J. J., KORBER, B. & WILSON, C. M. 2003. Cross-Reactive CD8+ T Cell Epitopes Identified in US Adolescent Minorities. *JAIDS-HAGERSTOWN MD-,* 33**,** 426-438.

SADLER, H. A., STENGLEIN, M. D., HARRIS, R. S. & MANSKY, L. M. 2010. APOBEC3G contributes to HIV-1 variation through sublethal mutagenesis. *Journal of virology,* 84**,** 7396-7404.

SAHDEV, S., KHATTAR, S. K. & SAINI, K. S. 2008. Production of active eukaryotic proteins through bacterial expression systems: a review of the existing biotechnology strategies. *Molecular and cellular biochemistry,* 307**,** 249-264.

SALAZAR-GONZALEZ, J. F., SALAZAR, M. G., KEELE, B. F., LEARN, G. H., GIORGI, E. E., LI, H., DECKER, J. M., WANG, S., BAALWA, J. & KRAUS, M. H. 2009. Genetic identity, biological phenotype, and evolutionary pathways of transmitted/founder viruses in acute and early HIV-1 infection. *The Journal of Experimental Medicine,* 206**,** 1273-1289.

SAMSON, M., LIBERT, F., DORANZ, B. J., RUCKER, J., LIESNARD, C., FARBER, C. M., SARAGOSTI, S., LAPOUMEROULIE, C., COGNAUX, J., FORCEILLE, C., MUYLDERMANS, G., VERHOFSTEDE, C., BURTONBOY, G., GEORGES, M., IMAI, T., RANA, S., YI, Y., SMYTH, R. J., COLLMAN, R. G., DOMS, R. W., VASSART, G. & PARMENTIER, M. 1996. Resistance to HIV-1 infection in caucasian individuals bearing mutant alleles of the CCR-5 chemokine receptor gene. *Nature,* 382**,** 722-5.

SCHMIDT, S., FRITZ, J. V., BITZEGEIO, J., FACKLER, O. T. & KEPPLER, O. T. 2011. HIV-1 Vpu blocks recycling and biosynthetic transport of the intrinsic immunity factor CD317/tetherin to overcome the virion release restriction. *MBio,* 2**,** e00036-11.

SCHRODER, A. R., SHINN, P., CHEN, H., BERRY, C., ECKER, J. R. & BUSHMAN, F. 2002. HIV-1 integration in the human genome favors active genes and local hotspots. *Cell,* 110**,** 521-9.

SCHRÖFELBAUER, B., HAKATA, Y. & LANDAU, N. R. 2007. HIV-1 Vpr function is mediated by interaction with the damage-specific DNA-binding protein DDB1. *Proceedings of the National Academy of Sciences,* 104**,** 4130-4135.

SCHROFELBAUER, B., YU, Q., ZEITLIN, S. G. & LANDAU, N. R. 2005. Human immunodeficiency virus type 1 Vpr induces the degradation of the UNG and SMUG uracil-DNA glycosylases. *Journal of Virology,* 79**,** 10978-87.

SCHUBERT, U., HENKLEIN, P., BOLDYREFF, B., WINGENDER, E., STREBEL, K. & PORSTMANN, T. 1994. The human immunodeficiency virus type 1 encoded Vpu protein is phosphorylated by casein kinase-2 (CK-2) at positions Ser52 and Ser56 within a predicted alpha-helix-turn-alpha-helix-motif. *Journal of Molecular Biology,* 236**,** 16-25.

SCHWARTZ, S., FELBER, B. K., FENYO, E. M. & PAVLAKIS, G. N. 1990. Env and Vpu proteins of human immunodeficiency virus type 1 are produced from multiple bicistronic mRNAs. *Journal of Virology,* 64**,** 5448-56.

SELIG, L., PAGES, J. C., TANCHOU, V., PREVERAL, S., BERLIOZ-TORRENT, C., LIU, L. X., ERDTMANN, L., DARLIX, J., BENAROUS, R. & BENICHOU, S. 1999. Interaction with the p6 domain of the gag precursor mediates incorporation into virions of Vpr and Vpx proteins from primate lentiviruses. *Journal of Virology,* 73**,** 592-600.

SHAH, A. H., SOWRIRAJAN, B., DAVIS, Z. B., WARD, J. P., CAMPBELL, E. M., PLANELLES, V. & BARKER, E. 2010. Degranulation of Natural Killer Cells Following Interaction with HIV-1-Infected Cells Is Hindered by Downmodulation of NTB-A by Vpu. *Cell host & microbe,* 8**,** 397-409.

SHARP, P. M. & HAHN, B. H. 2011. Origins of HIV and the AIDS pandemic. *Cold Spring Harb Perspect Med,* 1**,** a006841.

SHEEHY, A. M., GADDIS, N. C., CHOI, J. D. & MALIM, M. H. 2002. Isolation of a human gene that inhibits HIV-1 infection and is suppressed by the viral Vif protein. *Nature,* 418**,** 646-50.

SIMON, J. H. & MALIM, M. H. 1996. The human immunodeficiency virus type 1 Vif protein modulates the postpenetration stability of viral nucleoprotein complexes. *Journal of Virology,* 70**,** 5297-305.

SIMON, V., ZENNOU, V., MURRAY, D., HUANG, Y., HO, D. D. & BIENIASZ, P. D. 2005. Natural variation in Vif: differential impact on APOBEC3G/3F and a potential role in HIV-1 diversification. *PLoS Pathog,* 1**,** e6.

SINGH, S. K., MÖCKEL, L., THIAGARAJAN-ROSENKRANZ, P., WITTLICH, M., WILLBOLD, D. & KOENIG, B. W. 2012. Mapping the interaction between the cytoplasmic domains of HIV-1 viral protein U and human CD4 with NMR spectroscopy. *FEBS Journal,* 279**,** 3705-3714.

SKASKO, M., TOKAREV, A., CHEN, C.-C., FISCHER, W. B., PILLAI, S. K. & GUATELLI, J. 2011. BST-2 is rapidly down-regulated from the cell surface by the HIV-1 protein Vpu: evidence for a post-ER mechanism of Vpu-action. *Virology,* 411**,** 65-77.

SQUIRES, K., MONAJEMI, M., WOODWORTH, C. F., GRANT, M. D. & LARIJANI, M. 2015. Impact of APOBEC mutations on CD8+ T cell recognition of HIV epitopes varies depending on the restricting HLA. *JAIDS Journal of Acquired Immune Deficiency Syndromes*.

STANLEY, B. J., EHRLICH, E. S., SHORT, L., YU, Y., XIAO, Z., YU, X.-F. & XIONG, Y. 2008. Structural Insight into the Human Immunodeficiency Virus Vif SOCS Box and Its Role in Human E3 Ubiquitin Ligase Assembly. *Journal of Virology,* 82**,** 8656-8663.

STRATOV, I., CHUNG, A. & KENT, S. J. 2008. Robust NK cell-mediated human immunodeficiency virus (HIV)-specific antibody-dependent responses in HIV-infected subjects. *Journal of Virology,* 82**,** 5450-9.

STREECK, H., JOLIN, J. S., QI, Y., YASSINE-DIAB, B., JOHNSON, R. C., KWON, D. S., ADDO, M. M., BRUMME, C., ROUTY, J.-P., LITTLE, S., JESSEN, H. K., KELLEHER, A. D., HECHT, F. M., SEKALY, R.-P., ROSENBERG, E. S., WALKER, B. D., CARRINGTON, M. & ALTFELD, M. 2009. Human Immunodeficiency Virus Type 1-Specific CD8+ T-Cell Responses during Primary Infection Are Major Determinants of the Viral Set Point and Loss of CD4+ T Cells. *Journal of Virology,* 83**,** 7641-7648.

SUH, W. K., COHEN-DOYLE, M. F., FRUH, K., WANG, K., PETERSON, P. A. & WILLIAMS, D. B. 1994. Interaction of MHC class I molecules with the transporter associated with antigen processing. *Science,* 264**,** 1322-6.

TAMAMIS, P. & FLOUDAS, C. A. 2014. Molecular recognition of CCR5 by an HIV-1 gp120 V3 loop. *PLoS One,* 9**,** e95767.

TANG, J., TANG, S., LOBASHEVSKY, E., MYRACLE, A. D., FIDELI, U., ALDROVANDI, G., ALLEN, S., MUSONDA, R. & KASLOW, R. A. 2002. Favorable and unfavorable HLA class I alleles and haplotypes in Zambians predominantly infected with clade C human immunodeficiency virus type 1. *Journal of Virology,* 76**,** 8276-84.

TAYLOR, B. S., SOBIESZCZYK, M. E., MCCUTCHAN, F. E. & HAMMER, S. M. 2008. The Challenge of HIV-1 Subtype Diversity. *New England Journal of Medicine,* 358**,** 1590-1602.

TECHTMANN, S. M., GHIRLANDO, R., KAO, S., STREBEL, K. & MAYNARD, E. L. 2012. Hydrodynamic and Functional Analysis of HIV-1 Vif Oligomerization. *Biochemistry,* 51**,** 2078-2086.

TEMIN, H. M. 1982. Function of the retrovirus long terminal repeat. *Cell,* 28**,** 3-5.

THOBAKGALE, C. F., FADDA, L., LANE, K., TOTH, I., PEREYRA, F., BAZNER, S., NDUNG'U, T., WALKER, B. D., ROSENBERG, E. S. & ALTER, G. 2012. Frequent and strong antibody-mediated natural killer cell activation in response to HIV-1 Env in individuals with chronic HIV-1 infection. *Journal of virology,* 86**,** 6986-6993.

TIAN, C., YU, X., ZHANG, W., WANG, T., XU, R. & YU, X. F. 2006. Differential requirement for conserved tryptophans in human immunodeficiency virus type 1 Vif for the selective suppression of APOBEC3G and APOBEC3F. *Journal of Virology,* 80**,** 3112-5.

TIEMESSEN, C. T., PAXIMADIS, M., MINEVICH, G., WINCHESTER, R., SHALEKOFF, S., GRAY, G. E., SHERMAN, G. G., COOVADIA, A. H. & KUHN, L. 2011. Natural killer cell responses to HIV-1 peptides are associated with more activating KIR genes and HLA-C genes of the C1 allotype. *Journal of acquired immune deficiency syndromes (1999),* 57**,** 181.

TIGANOS, E., FRIBORG, J., ALLAIN, B., DANIEL, N. G., YAO, X.-J. & COHEN, É. A. 1998. Structural and Functional Analysis of the Membrane-Spanning Domain of the Human Immunodeficiency Virus Type 1 Vpu Protein. *Virology,* 251**,** 96-107.

TOKAREV, A., SUAREZ, M., KWAN, W., FITZPATRICK, K., SINGH, R. & GUATELLI, J. 2013. Stimulation of NF-Î°B Activity by the HIV Restriction Factor BST2. *Journal of virology,* 87**,** 2046-2057.

UNAIDS 2014. Global Reports-UNAIDS report on the global AIDS epidemic 2014. Geneva.

VAN DAMME, N., GOFF, D., KATSURA, C., JORGENSON, R. L., MITCHELL, R., JOHNSON, M. C., STEPHENS, E. B. & GUATELLI, J. 2008. The interferon-induced protein BST-2 restricts HIV-1 release and is downregulated from the cell surface by the viral Vpu protein. *Cell Host Microbe,* 3**,** 245-52.

VAN DEUTEKOM, H. W. M. & KEŞMIR, C. 2015. Zooming into the binding groove of HLA molecules: which positions and which substitutions change peptide binding most? *Immunogenetics,* 67**,** 425-436.

VAN HARMELEN, J. H., VAN DER RYST, E., LOUBSER, A. S., YORK, D., MADURAI, S., LYONS, S., WOOD, R. & WILLIAMSON, C. 1999. A predominantly HIV type 1 subtype C-restricted epidemic in South African urban populations. *AIDS Research and Human Retroviruses,* 15**,** 395-8.

VENKATESH, S. & BIENIASZ, P. D. 2013. Mechanism of HIV-1 Virion Entrapment by Tetherin. *PLoS Pathog,* 9**,** e1003483.

VIDAL, N., PEETERS, M., MULANGA-KABEYA, C., NZILAMBI, N., ROBERTSON, D., ILUNGA, W., SEMA, H., TSHIMANGA, K., BONGO, B. & DELAPORTE, E. 2000. Unprecedented Degree of Human Immunodeficiency Virus Type 1 (HIV-1) Group M Genetic Diversity in the Democratic Republic of Congo Suggests that the HIV-1 Pandemic Originated in Central Africa. *Journal of Virology,* 74**,** 10498-10507.

VIDER-SHALIT, T., ALMANI, M., SARID, R. & LOUZOUN, Y. 2009. The HIV hide and seek game: an immunogenomic analysis of the HIV epitope repertoire. *AIDS,* 23**,** 1311-8.

VODICKA, M. A., KOEPP, D. M., SILVER, P. A. & EMERMAN, M. 1998. HIV-1 Vpr interacts with the nuclear transport pathway to promote macrophage infection. *Genes and Development,* 12**,** 175-185.

WANG, Y., JACOBS, C., HOOK, K. E., DUAN, H., BOOHER, R. N. & SUN, Y. 2000. Binding of 14-3-3beta to the carboxyl terminus of Wee1 increases Wee1 stability, kinase activity, and G2-M cell population. *Cell growth & differentiation: the molecular biology journal of the American Association for Cancer Research,* 11**,** 211-219.

WATTS, J. M., DANG, K. K., GORELICK, R. J., LEONARD, C. W., BESS JR, J. W., SWANSTROM, R., BURCH, C. L. & WEEKS, K. M. 2009. Architecture and secondary structure of an entire HIV-1 RNA genome. *Nature,* 460**,** 711-716.

WEIL, A. F., GHOSH, D., ZHOU, Y., SEIPLE, L., MCMAHON, M. A., SPIVAK, A. M., SILICIANO, R. F. & STIVERS, J. T. 2013. Uracil DNA glycosylase initiates degradation of HIV-1 cDNA containing misincorporated dUTP and prevents viral integration. *Proceedings of the National Academy of Sciences,* 110**,** E448-E457.

WEN, X., DUUS, K. M., FRIEDRICH, T. D. & DE NORONHA, C. M. C. 2007. The HIV1 Protein Vpr Acts to Promote G2 Cell Cycle Arrest by Engaging a DDB1 and Cullin4A-containing Ubiquitin Ligase Complex Using VprBP/DCAF1 as an Adaptor. *Journal of Biological Chemistry,* 282**,** 27046-27057.

WIENER, M. C. 2004. A pedestrian guide to membrane protein crystallization. *Methods,* 34**,** 364-72.

WILLEY, R. L., MALDARELLI, F., MARTIN, M. A. & STREBEL, K. 1992. Human immunodeficiency virus type 1 Vpu protein induces rapid degradation of CD4. *Journal of virology,* 66**,** 7193-7200.

WOLFS, T. F., ZWART, G. L., BAKKER, M. & GOUDSMIT, J. 1992. HIV-1 genomic RNA diversification following sexual and parenteral virus transmission. *Virology,* 189**,** 103-110.

WRAY, V., FEDERAU, T., HENKLEIN, P., KLABUNDE, S., KUNERT, O., SCHOMBURG, D. & SCHUBERT, U. 1995. Solution structure of the hydrophilic region of HIV-1 encoded virus protein U (Vpu) by CD and 1H NMR spectroscopy. *International Journal of Peptide and Protein Research,* 45**,** 35-43.

WREN, L. H., CHUNG, A. W., ISITMAN, G., KELLEHER, A. D., PARSONS, M. S., AMIN, J., COOPER, D. A., STRATOV, I., NAVIS, M. & KENT, S. J. 2013. Specific antibody dependent cellular cytotoxicity responses associated with slow progression of HIV infection. *Immunology,* 138**,** 116-123.

WRIGHT, J. K., NAIDOO, V. L., BRUMME, Z. L., PRINCE, J. L., CLAIBORNE, D. T., GOULDER, P. J. R., BROCKMAN, M. A., HUNTER, E. & NDUNG'U, T. 2012. Impact of HLA-B*81-Associated Mutations in HIV-1 Gag on Viral Replication Capacity. *Journal of virology,* 86**,** 3193-3199.

YAN, N., O'DAY, E., WHEELER, L. A., ENGELMAN, A. & LIEBERMAN, J. 2011. HIV DNA is heavily uracilated, which protects it from autointegration. *Proceedings of the National Academy of Sciences,* 108**,** 9244-9249.

YAN, N., REGALADO-MAGDOS, A. D., STIGGELBOUT, B., LEE-KIRSCH, M. A. & LIEBERMAN, J. 2010. The cytosolic exonuclease TREX1 inhibits the innate immune response to HIV-1. *Nature immunology,* 11**,** 1005-1013.

YOKOMAKU, Y., MIURA, H., TOMIYAMA, H., KAWANA-TACHIKAWA, A., TAKIGUCHI, M., KOJIMA, A., NAGAI, Y., IWAMOTO, A., MATSUDA, Z. & ARIYOSHI, K. 2004. Impaired processing and presentation of cytotoxic-T-lymphocyte (CTL) epitopes are major escape mechanisms from CTL immune pressure in human immunodeficiency virus type 1 infection. *Journal of Virology,* 78**,** 1324-32.

YU, X., YU, Y., LIU, B., LUO, K., KONG, W., MAO, P. & YU, X. F. 2003. Induction of APOBEC3G ubiquitination and degradation by an HIV-1 Vif-Cul5-SCF complex. *Science,* 302**,** 1056-60.

YUSIM, K., HONEYBORNE, I., CALEF, C., GOULDER, P. & KORBER, B. 2003. Enhanced motif scan: A tool to scan for HLA anchor residues in proteins. *HIV Immunology and HIV/SIV Vaccine Databases***,** 25-36.

YUSIM, K., KESMIR, C., GASCHEN, B., ADDO, M. M., ALTFELD, M., BRUNAK, S., CHIGAEV, A., DETOURS, V. & KORBER, B. T. 2002. Clustering Patterns of Cytotoxic T-Lymphocyte Epitopes in Human Immunodeficiency Virus Type 1 (HIV-1) Proteins Reveal Imprints of Immune Evasion on HIV-1 Global Variation. *Journal of Virology,* 76**,** 8757-8768.

ZHANG, H., LIN, E. C., DAS, B. B., TIAN, Y. & OPELLA, S. J. 2015. Structural determination of virus protein U from HIV-1 by NMR in membrane environments. *Biochim Biophys Acta,* 1848**,** 3007-18.

ZHANG, H., YANG, B., POMERANTZ, R. J., ZHANG, C., ARUNACHALAM, S. C. & GAO, L. 2003. The cytidine deaminase CEM15 induces hypermutation in newly synthesized HIV-1 DNA. *Nature,* 424**,** 94-8.

ZHU, K., DOBARD, C. & CHOW, S. A. 2004. Requirement for integrase during reverse transcription of human immunodeficiency virus type 1 and the effect of cysteine mutations of integrase on its interactions with reverse transcriptase. *Journal of Virology,* 78**,** 5045-55.

ZHU, P., LIU, J., BESS JR, J., CHERTOVA, E., LIFSON, J. D., GRISÉ, H., OFEK, G. A., TAYLOR, K. A. & ROUX, K. H. 2006. Distribution and three-dimensional structure of AIDS virus envelope spikes. *Nature,* 441**,** 847-852.

ZHU, P., WINKLER, H., CHERTOVA, E., TAYLOR, K. A. & ROUX, K. H. 2008. Cryoelectron tomography of HIV-1 envelope spikes: further evidence for tripod-like legs. *PLoS Pathog,* 4**,** e1000203.

ZIMMERMAN, E. S., CHEN, J., ANDERSEN, J. L., ARDON, O., DEHART, J. L., BLACKETT, J., CHOUDHARY, S. K., CAMERINI, D., NGHIEM, P. & PLANELLES, V. 2004. Human Immunodeficiency Virus Type 1 Vpr-Mediated G2 Arrest Requires Rad17 and Hus1 and Induces Nuclear BRCA1 and γ-H2AX Focus Formation. *Molecular and Cellular Biology,* 24**,** 9286-9294.

Appendix A: Bacterial and DNA Work

LB medium (1 L)

- Measure out 10 g tryptone, 10 g yeast extract and 5 g NaCl and add all ingredients into a beaker, add 1L of dH_2O, autoclave and store at room temperature.

Ampiclin 1000× stock (10 ml)

- Dissolve 1 g of ampicilin in 3 ml of Sabax water by vortexing. Top up with 100% ethanol.

Transformation buffer (100 ml)

- Measure out 1.47 g $CaCl_2.H_2O$ and 0.3024 g PIPES. Top up with ddH_2O to 80 ml.

Add 15 ml Glycerol, pH to 7.0 with NaOH and top up to 100 ml with ddH_2O. Autoclave and store at 4°C.

LB Agar (200 ml)

- Measure out 7 g of Nutrient Agar (Sigma Aldrich, USA) and top up with 200 ml of ddH_2O. Autoclave and store at room temperature.

Competent bacterial cells

- Prepare 10 ml LB medium cultures with bacterial cells diluted 1/10. Culture cells overnight at 37°C in shaking incubator. Do not add antibiotic.
- Dilute 1 ml of overnight culture in 40 ml of sterile LB medium.
- Grow culture in shake incubator at 37°C until an A600 of 0,4 is reached.
- Pellet cells by centrifugation at 1500 RPM for 10 min.
- Add 10 ml of transformation buffer to pelleted cells
- Incubate on ice for 20 min.
- Centrifuge again at 1500 RPM for 10 min.
- Resuspend in 1 ml of transformation buffer.
- Make 100 ul aliquots and store in freezer at -80°C.

50×TAE buffer (1 L)

- Weigh out 242 g tris base. Add 57.1 mL glacial acetic acid and 100 mL 0.5 EDTA. Add 800 mL of distilled water. Adjust pH to 8.0 with HCl. Top up to 1L with dH_2O. Store at room temperature.

EDTA 0.5 M (500 ml)

- Measure out 93.05 g of $Na_2EDTA.H_2O$ and dissolve in 350 ml of dH_2O. pH to 8.0 with 10 M NaOH. Top up to 500 ml with dH_2O and autoclave. Store at room temperature.

1% Agarose gel (200 ml)

- Add 2 g of agarose to 200 ml of 1 × TAE buffer.

Appendix B: Recombinant Protein Work

SDS-PAGE

Monomer solution (30% Acrylamide/ 0.8% Bisacrylamide, 100 ml)

- Measure and add together 30 g of acrylamide and 0.8 g of N, N'-methylenebisacrylamide. Top up to 100 ml with dH_2O.

4 × Tris-Cl, pH 6.8 (Stacking buffer, 100 ml)

- Measure out 6.05 g of Tris and add to 40 ml of dH_2O. pH to 6.8 with HCl. Top up to 100 ml with dH_2O and store at 4°C.

4 × Tris-Cl, pH 8.8 (Running buffer, 500 ml)

- Measure out 91 g of Tris and add to 300 ml of dH_2O. pH to 8.8 with HCl. Top up to 100 ml with dH_2O and store at 4°C.

10% SDS (100 ml)

- Measure out 10 g of SDS and top up to 100 ml with dH_2O.

10% Ammonium Persulphate (1 ml)

- Measure out 0.1 g of ammonium persulphate and top up to 1 ml with dH_2O.

2 × Sample Buffer (10 ml)

- Measure out and add together 2.5 ml of 4 × stacking buffer, 4 ml of 10% SDS, 2 ml glycerol, 0.2 ml of β-Mercaptoethanol, and 2 mg of bromophenol blue. Top up to 10 ml with dH_2O. Make 1 ml aliquots and store at – 20°C.

10 × Electrophoresis buffer (1 L)

- Measure out and add together 30.28 g Tris, 144.13 g glycine and 10 g of SDS. Top up to 1 L with dH_2O and store at room temperature.

Gel staining and Western blotting

Transfer buffer (1 L)

- Add 200 ml of methanol in 800 ml of 1 × Electrophoresis buffer.

Coomassie Blue (1 L)

- Add 500 ml methanol and 100 ml acetic acid into 400 ml of dH_2O. Dissolve in 0.25g Coomassie R250. Store at room temperature.

Destain (1 L)

- Add 50 ml ethanol and 70ml acetic acid into 850ml of dH_2O. Store at room temperature.

10 × TBS (1 L)

- Measure out and add together 10 g NaCl, 30 g Tris and 2.0 g of KCl. Dissolve into 950 mL of dH_2O. Adjust pH to 7.4 with HCl. Make up to 1 L with dH_2O. Store at 4^oC.

T-TBS (1 L)

- Add 500 µL of Tween into 1L of 1 × TBS. Dissolve. Store at 4^oC.

Milk blocking solution

- Mix 2.5 mg of fat-free milk powder per 25ml of 1 × T-TBS.

Protein purification

Lysis buffer

- Add together 150 mM NaCl, 50 mM Tris–HCl, 0.5% Triton X-100 (Sigma-Aldrich, USA), 5% glycerol and cOmplete Protease Inhibitor (Roche, Switzerland). Adjust pH to 7,4 with HCl.

Wash buffer (0 mM imidazole)

- Add together 150 mM NaCl, 50 mM Tris–HCl, 5% glycerol. Adjust pH to 7,4 with HCl.

Elution buffer (500 mM imidazole)

- Add together 150 mM NaCl, 50 mM Tris–HCl, 5% glycerol and 500 mM imidazole. Adjust pH to 7,4 with HCl.

Wash buffers (10 mM, 20 mM, 50 mM imidazole)

- Utilize 0 mM and 500 mM imidazole buffers to make desired imidazole concentrations of wash buffers.

Appendix C: Manufacturer's protocols

Plasmid Extraction/Midi Prep (Qiagen, USA)

- Pick a bacterial colony from a freshly grown bacterial plate and inoculate a starter culture of 5 ml LB medium containing selective antibiotic. Incubate overnight at 37°C on shaking platform.
- Dilute the starter culture 1 / 500 in 25 ml selective LB medium and incubate overnight at 37°C on shaking platform.
- Harvest bacterial cells by centrifugation at 6000 x g for 15 min at 4°C.
- Resuspend pellet in 4 ml of Buffer P1 thoroughly until no clumps remain.
- Add 4 ml of Buffer P2 and mix thoroughly to remove any clumping. Incubate at room temperature for 5 min.
- Add 4 ml of pre-chilled Buffer P3 and mix by inverting vessel 4-6 times. Incubate on ice for 15 min.
- Centrifuge at 20 000 x g for 30 min at 4°C. Supernatant containing plasmid DNA should then be removed swiftly.
- Re-centrifuge the supernatant at 20 000 x g for 15 min at 4°C. Supernatant containing plasmid DNA should then be removed swiftly.
- Equilibrate a QIAGEN-tip 100 by adding 4 ml of Buffer QBT, and allow the column to empty.
- Add plasmid-containing supernatant to column and allow to enter resin by gravity.
- Wash the QIAGEN-tip with two 10 ml washes with Buffer QC.
- Elute DNA with 5 ml of Buffer QF.
- Precipitate the DNA by adding 3.5 ml of room-temperature isopropanol and centrifuge immediately at ≥15,000 x g for 30 min at 4°C and carefully remove the supernatant.
- Wash the DNA pellet with 2 ml of room-temperature 70% ethanol and centrifuge at 15 000 x g for 10 min. Remove supernatant without disturbing the DNA pellet.
- Air-dry the pellet for 10 min and then redissolve the DNA in high quality sterile water or any other suitable buffer.
- Quantify by spectrophotometry and store at -20°C until required.

GeneJet PCR Purification Kit (Thermo Fisher Scientific, USA)

- To PCR products, add 1:1 volume of Binding Buffer and mix until entire mixture turns yellow.
- Transfer mixture to GeneJet purification columns and centrifuge at >12000 × g for 60s. Discard flow through.
- Add 700 µl of Wash Buffer to the purification column and centrifuge at >12000 × g for 60s. Discard flow through.
- Centrifuge a further 60 s at >12000 × g to remove residual buffer in column.
- Add GeneJet purification column to a 1,5 ml microcentrifuge tube and add 50 µL of Elution Buffer. Centrifuge at >12000 × g for 60s.
- Discard the column and store microcentrifuge tube containing the purified DNA at -20°C until required.

Agencourt AMPure XP - PCR Purification 96 well plate (Beckman Coulter, USA)

- Determine whether PCR products require transfer from plates to larger welled plate (transfer only if the PCR reaction volume multiplied by 2.8 exceeds the volume of the PCR plate).
- Shake the Agencourt AMPure XP bottle and add to PCR sample reactions according to the following equation (Volume of Agencourt AMPure XP per reaction) = 1.8 x (Reaction Volume). Mix until homogenous by pipetting.
- Allow to sit for 5 min at room temperature.
- Place plate onto Agencourt SPRIPlate 96 Super Magnet Plate for 2 minutes to separate beads from the solution, solution should become clear before proceeding.
- Remove the cleared liquid on top from the concentrated beads (do this while plate is still on magnetic plate). Make sure to leave around 5 µl of liquid so as not to disturb beads.
- While still on magnetic plate, add 200 µl of 70% ethanol to each well and incubate for 30 s at room temperature. Do not disturb beads. Remove ethanol following incubation and discard. Repeat twice.
- Remove plate PCR reaction plate from amgentic plate and add 40 µl of elution buffer to each well and pipette mix thoroughly. Incubate for 2 min.
- Place PCR reaction plate back onto magnetic plate and allow separation of beads for 1 min and then transfer eluate to a new plate

Appendix D: Ethics Approval

R14/49 Mr Roberto Pereira

HUMAN RESEARCH ETHICS COMMITTEE (MEDICAL)

CLEARANCE CERTIFICATE NO. M160151

NAME: (Principal Investigator)	Mr Roberto Pereira
DEPARTMENT:	School of Pathology Molecular Medicine and Haematology
PROJECT TITLE:	Immune Escape in HIV-1 Subtype C Accessory Proteins Vif, vpr and Vpu
DATE CONSIDERED:	Adhoc
DECISION:	Approved unconditionally
CONDITIONS:	Substudy Prof Caroline Tiemessen- M140926 and M140989
SUPERVISOR:	Prof Maria Papathanasopoulos
APPROVED BY:	Professor P Cleaton-Jones, Chairperson, HREC (Medical)
DATE OF APPROVAL:	27/01/2016

This clearance certificate is valid for 5 years from date of approval. Extension may be applied for.

DECLARATION OF INVESTIGATORS

To be completed in duplicate and **ONE COPY** returned to the Research Office Secretary in Room 10004, 10th floor, Senate House/2nd Floor, Phillip Tobias Building, Parktown, University of the Witwatersrand. I/we fully understand the conditions under which I am/we are authorized to carry out the above-mentioned research and I/we undertake to ensure compliance with these conditions. Should any departure be contemplated, from the research protocol as approved, I/we undertake to resubmit the application to the Committee. **I agree to submit a yearly progress report**.

Principal Investigator Signature Date

PLEASE QUOTE THE PROTOCOL NUMBER IN ALL ENQUIRIES